JHR 75: 1–13 (2020)
doi: 10.3897/jhr.75.46867
http://jhr.pensoft.net

RESEARCH ARTICLE

JOURNAL OF Hymenoptera RESEARCH
A peer-reviewed open-access journal
The International Society of Hymenopterists

Four new species of the genus *Rodrigama* Gauld, 1991 (Hymenoptera, Ichneumonidae, Poemeniinae) from South Korea

Jin-Kyung Choi[1], Jong-Wook Lee[2]

1 *Department of Science Education, Daegu National University of Education, Daegu, 42411, South Korea*
2 *Department of Life Sciences, Yeungnam University, Gyeongsan, 38543, South Korea*

Corresponding author: Jong-Wook Lee (jwlee1@ynu.ac.kr)

Academic editor: Gavin Broad | Received 26 September 2019 | Accepted 16 January 2020 | Published 27 February 2020

http://zoobank.org/F63A0FF3-AFD8-48EF-BF27-CF84D2EF26D1

Citation: Choi J-K, Lee J-W (2020) Four new species of the genus *Rodrigama* Gauld, 1991 (Hymenoptera, Ichneumonidae, Poemeniinae) from South Korea. Journal of Hymenoptera Research 75: 1–13. https://doi.org/10.3897/jhr.75.46867

Abstract

Four new species of the genus *Rodrigama* Gauld are described: *R. sobaekensis* **sp. nov.**, *R. koreana* **sp. nov.**, *R. wooki* **sp. nov.** and *R. unmunensis* **sp. nov.**, all from South Korea. The 11 species of *Rodrigama* are distributed across Central America and Asia, comprising seven previously recorded species and the four new species presented here. An illustrated key to South Korean species of *Rodrigama* is provided.

Keywords

Old World, *R. koreana* sp. nov., *R. sobaekensis* sp. nov., *R. unmunensis* sp. nov., *R. wooki* sp. nov., taxonomy

Introduction

The genus *Rodrigama* is a unique ichneumonid with oblique grooves delimiting a central rhombic area on the second tergite (Wahl and Gauld 1998). According to Wahl and Gauld (1998), *Rodrigama* occupies a basal position in the Poemeniinae. Therefore this genus was bestowed the tribal status 'Rodrigamini'. *Rodrigama* has a disjunct distribution, it is found in Central America, Japan, Taiwan, the Far East of China, Israel, and now in South Korea. It is strongly supported that the distribution pattern of this genus is a relic from a more widely distributed basal lineage of Pimpliformes in the Old World (Wahl and Gauld 1998; Matsumoto and Broad 2011; Broad and Kuslitzky 2019).

Rodrigama is a small genus in the tribe Rodrigamini of the subfamily Poemeniinae, consisting of five species (Yu et al. 2016). This genus was reported from a single Costa Rican species, and two species have been reported from Japan and Taiwan. Recently, one species, *R. maculata* (Sheng and Sun 2010), was transferred from *Pimplaetus* by Sheng et al. in 2014. Also, Broad and Kuslitzky (2019) described one new species, *R. freidbergi* from Israel, and proposed a new combination, *Rodrigama taishanense* (He, 1996) from *Pimplaetus*. Thus, a total of seven species of *Rodrigama* are distributed across Central America and Asia.

In this study, four new species, *R. sobaekensis* sp. nov., *R. koreana* sp. nov., *R. wooki* sp. nov. and *R. unmunensis* sp. nov., from South Korea are described. Photographs, comparative illustrations and an identification key to South Korean species are also provided.

Materials and methods

Type specimens of the four new species are preserved in the Daegu National University of Education (DNUE, Daegu, Korea). Specimens used in this study were collected by sweeping, Malaise trapping and rearing. Paratypes of *R. gauldi*, *R. takakuwai*, and *R. gamezi* in the Natural History Museum, London (BMNH) were examined for comparison with the four new species. Images of specimens of the new species were taken using an AxioCam MRc5 camera attached to a stereo microscope (Zeiss SteREO Discovery. V20; Carl Zeiss, Göttingen, Germany), processed using AxioVision SE64 software (Carl Zeiss), and optimized with a Delta imaging system (i-solution, IMT i-Solution Inc. Vancouver, Canada). Morphological terminology follows that of Gauld (1991). Abbreviations are as follows: CB, Cungcheongbuk-do; GB, Gyeongsangbuk-do; GG, Gyeonggi-do; GW, Gangwon-do.

Taxonomy

Family Ichneumonidae Latreille, 1802
Subfamily Poemeniinae Narayanan & Lal, 1953
Tribe Rodrigamini Wahl & Gauld, 1998

Genus *Rodrigama* Gauld, 1991

Rodrigama Gauld, 1991: 536. Type species: *Rodrigama gamezi* Gauld, by original designation.

Diagnosis. Genus *Rodrigama* can be distinguished from all other poemeniines by the following characteristics: paired antero-lateral and postero-lateral oblique grooves delimiting a central rhombic area on the second tergite; fused tergite and sternite of the first tergite (Wahl and Gauld 1998; Matsumoto and Broad 2011).

Key to the species of South Korean *Rodrigama*

1 Body largely reddish yellow to brown (Fig. 1A); frons and vertex reddish brown (Fig. 2C). Pronotum black, upper margin of pronotum and antero-ventral part yellow (Fig. 2A). Scutellum and postscutellum yellow. Second metasomal tergite long, 1.85–2.10 times as long as wide, with dense and fine punctures (Fig. 2F). Body length longer than 25–27 mm ..... ***R. sobaekensis* Choi & Lee**

– Body largely reddish brown to black (Figs 1B–D); frons black and vertex dark reddish black or both entirely black (Figs 3C, 4C and 5C). Pronotum without yellow spot. Scutellum black. Second metasomal tergite less than 1.70 times as long as wide, with rugose punctures. Body length shorter than 20 mm..... **2**

2 Length of second and third metasomal tergites equal to or shorter than width (Fig. 5F). First tergite less than 2.0 times as long as wide. First metasomal sternite extending to before spiracle (Fig. 5E). Epicnemial carina absent..... ***R. unmunensis* Choi & Lee**

– Length of second and third metasomal tergites greater than width. First metasomal tergite more than 2.3 times as long as wide. First metasomal sternite extending behind spiracle. Epicnemial carina present ventrally **3**

3 Second to fourth hind tarsomeres whitish. Body length 0.80–0.83 times as long as ovipositor length. First metasomal tergite more than 3.0 times as long as wide (Fig. 4G). Pronotum entirely black (Fig. 4A). Fore tibia with four stout spines on dorsal surface and two stout spines on distal end ..... ***R. wooki* Choi**

– Second to fourth hind tarsomeres yellow. Body length 0.63–0.77 times as long as ovipositor length. First metasomal tergite less than 2.5 times as long as wide (Fig. 3G). Pronotum black with reddish spot antero-ventrally (Fig. 3A). Fore tibia with 14 stout spines on dorsal surface and three stout spines on distal end ..... ***R. koreana* Choi & Lee**

***Rodrigama sobaekensis* Choi & Lee, sp. nov.**
http://zoobank.org/5377FE10-44F2-473D-86D1-3C56867DFC68
Figs 1A, 2A–H

Type. ***Holotype*** ♀, 19–30.iv.2007 (Malaise trap), Cheongdong valley (36°57'N, 128°26'E), Sobaeksan National Park, Cheondong-ri, Danyang-eup, Danyang-gun, CB, South Korea (J.W. Lee) [DNUE].

Paratypes. **[South Korea]** 1♀, 1–26.v.2009, Mt. Homyeongsan, Goseong-ri, Cheongpyeong-myeon, Gapyeong-gun, Alt. 220 m (37°43'16.3"N, 127°29'23.4"E), GG, (J.O. Lim); 1♀, 18–31.iv.2009, Mt. Homyeongsan, Goseong-ri, Cheongpyeong-myeon, Gapyeong-gun, Alt. 168 m (37°43'15.0"N, 127°29'18.9"E), GG, (J.O. Lim)

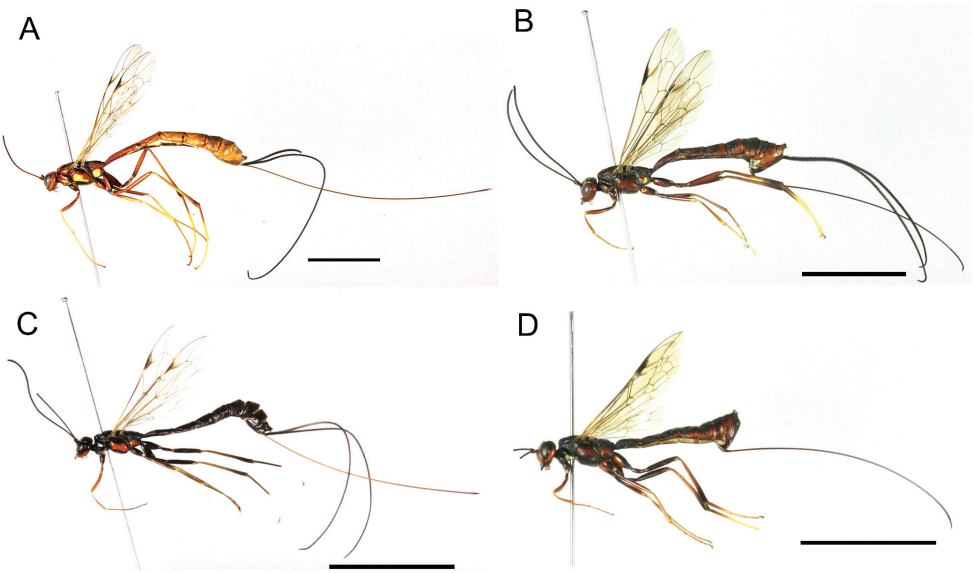

Figure 1. *Rodrigama* spp., habitus in lateral view (type specimens). **A** *R. sobaekensis* sp. nov. **B** *R. koreana* sp. nov. **C** *R. wooki* sp. nov. **D** *R. unmunensis* sp. nov. Scale bars: 10 mm).

Description. Female. Length of fore wing 18–19 mm; body 26–28 mm; ovipositor 35–36 mm. Malar space about 0.45 times as long as basal width of mandible. Inner orbits slightly converging ventrally (Fig. 2B). Occipital carina interrupted medially. Apical flagellomeres tapered and distal end truncate narrowly. Antenna with 33 flagellomeres. Pronotum with strongly impressed and transversely striate groove from epomia to ventroposterior corner; area dorsal to this groove rather strongly and densely punctate, slightly rugose. Mesoscutum in front of scuto-scutellar groove 1.4 times as long as wide in dorsal view (Fig. 2C). Mesopleuron moderately punctate, rather densely covered with pubescence (Fig. 2A); epicnemial carina present ventrally; mesopleural suture transversely striate. Propodeum rugosely punctate, transversely striate dorsomedially, without lateromedian longitudinal carina; posterior transverse carinae very weak and incomplete (Fig. 2D). Hind wing with eleven distal hamuli. Fore tibia with 10 stout spines on dorsal surface and two stout spines on distal end. Hind coxa elongate, 3.1 times as long as maximum width. First metasomal tergite broadened posteriorly in dorsal aspect, 4.1 times as long as posteriorly broad; slightly narrowed a little posterior to spiracle (Fig. 2G); first metasomal tergite with spiracle at anterior 0.41. Posterior end of first metasomal sternite at posterior 0.44 between spiracle and posterior end of first metasomal tergite (Fig. 2E). Second to fourth tergites sparsely covered with fine punctures.

Coloration. Body largely reddish yellow to brown. Face with narrow yellow stripe, extending along inner orbit to top of eye (Fig. 2B). Clypeus yellowish brown. Apical half of mandible black. Frons with black spots behind antennal sockets (Fig. 2C). Vertex with black line from ocelli area to occipital carina. Temple reddish brown (Fig. 2A). Pronotum reddish brown with black elongate markings next to antero-lateral and pos-

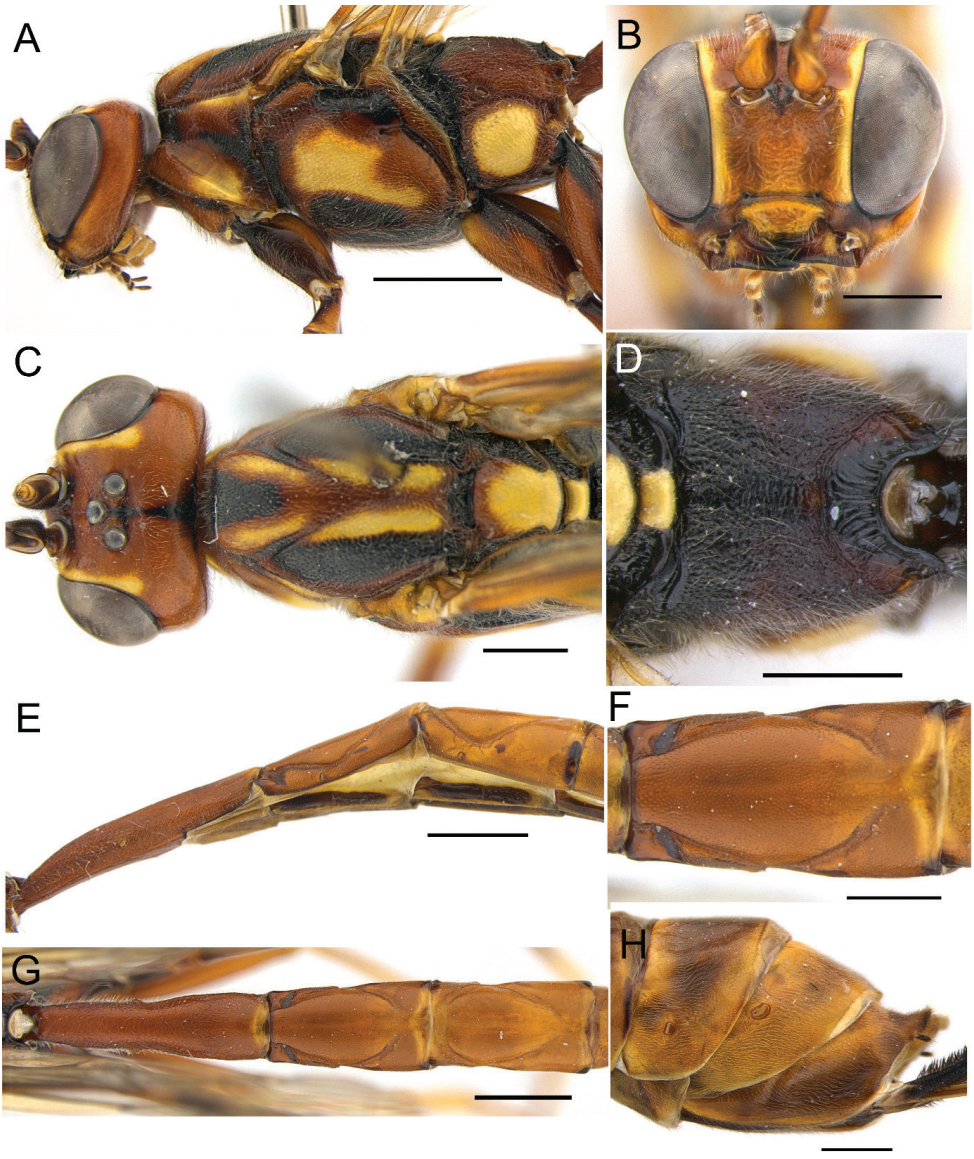

Figure 2. *R. sobaekensis* sp. nov. (holotype). **A** habitus in lateral view **B** head in frontal view **C** Frons and mesoscutum in dorsal view **D** propodeum **E** first to third tergites in lateral view **F** second tergite in dorsal view **G** first to third tergites in dorsal view **H** posterior end of metasoma. Scale bars: 2 mm (**A, E, G**); 1 mm (**B–D, F, H**).

tero-lateral margins, with upper margin yellow posteriorly. Mesoscutum reddish brown with pairs of longitudinal yellow and black spots; median lobe of mesoscutum reddish brown with black spot and yellow longitudinal spots (Fig. 2C). Mesopleuron reddish brown with large yellow spot, upper part of speculum black (Fig. 2A). Mesosternum black. Scutellum and postscutellum yellow (Fig. 2C). Propodeum reddish brown with

black spots anteriorly. Metapleuron reddish brown with anterior margin blackish, with yellow spot below pleural carina. Legs reddish brown. Tibia and tarsus paler. Fore coxa with darkened spots ventrally. Mid and hind coxae with darkened spots dorsally. Wings hyaline, slightly tinged with brown; pterostigma brown, without faint brownish spots around junction of cu-a and Cu1, and on Rs+2r below pterostigma. Metasomal tergites brown to reddish brown. Ovipositor dark brown, sheath black.

Male. Unknown.

Distribution. South Korea.

Region. Eastern Palaearctic.

Etymology. The species is named after Mt. Sobaek National Park, where the holotype specimen was collected.

Remarks. This new species is similar to *R. maculata* (Sheng and Sun 2010), but can be distinguished from by the meso- and metapleuron reddish brown with large yellow spots (evenly reddish brown without yellow spots in *R. maculata*); upper part of speculum and mesosternum black (evenly reddish brown in *R. maculata*); second metasomal tergite about 1.85 times as long as its apical width (about 2.6 times as long as apical width in *R. maculata*); first metasomal tergite short, 1.5 times as long as second tergite (first metasomal tergite 2.0 times as long as second tergite in *R. maculata*).

***Rodrigama koreana* Choi & Lee sp. nov.**

http://zoobank.org/3DAE4674-C8D8-4216-BD5A-A5CFEDFA05AB

Figs 1B, 3A–H

Type. ***Holotype*** ♀, 18–31.iv.2009 (Malaise trap), Mt. Ungilsan Alt. 99 m (37°34'43.2"N, 127°18'40.1"E), Songchon-ri, Choan-myeon, Namyangju-si, GG, South Korea (J.O. Lim) [DNUE].

Paratypes. [South Korea] 1♀, 8.vi.1996, Hwaechon, Maeji-ri, Heungeup-myeon, Wonju-si, GW, (H.Y. Han & H.W. Byun); 1♀, 25.v.2000, Yonsei Univ, Campus, Maeji-ri, Wonju-si, GW, (B.S. Kang & S.H. Kong); 1♀, 19.iv–23.v.2005, Mt. Cheongmoksan, Mitan-myeon, Pyeongchang-gun, GW, (J.W. Lee); 1♀, 18–31.iv.2009, Mt. Homyeongsan, Goseong-ri, Cheongpyeong-myeon, Gapyeong-gun, Alt. 168 m (37°43'15.0"N, 127°29'18.9"E), GG, (J.O. Lim); 1♀, Mt. Yongmunsan, Yeonsu-ri, Yongmun-myeon, Yangpyeong-gun, Alt. 324 m (37°31'48.9"N, 127°34'23.8"E), GG, (J.O. Lim).

Description. Female. Length of fore wing 13–14 mm; body 17–20 mm; ovipositor 22–24 mm. Head and mesosoma with long and dense setae. Malar space about 0.42 times as long as basal width of mandible. Inner orbits slightly converging ventrally (Fig. 3B). Occipital carina interrupted medially. Apical flagellomeres tapered and distal end truncate narrowly. Antenna with 32–35 flagellomeres. Pronotum with strongly impressed and transversely striate groove from epomia to ventroposterior corner; area dorsal to this groove rather strongly and densely punctate, slightly rugose (Fig. 3A). Mesoscutum in front of scuto-scutellar groove 1.3 times as long as wide in

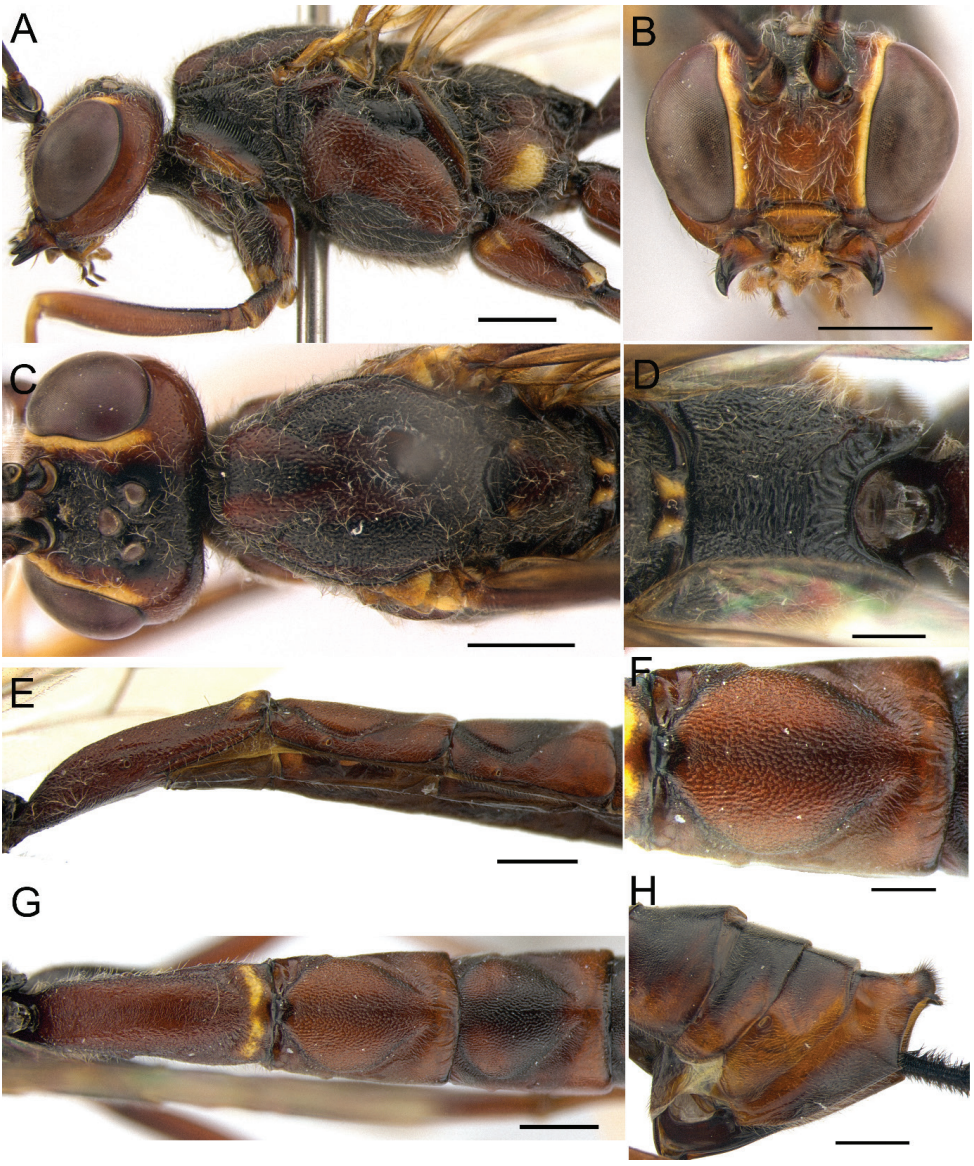

Figure 3. *R. koreana* sp. nov. (holotype). **A** habitus in lateral view **B** head in frontal view **C** Frons and mesoscutum in dorsal view **D** propodeum **E** first to third tergites in lateral view **F** second tergite in dorsal view **G** first to third tergites in dorsal view **H** posterior end of metasoma. Scale bars: 1 mm (**A–C, E, G–H**); 0.5 mm (**D, F**).

dorsal view (Fig. 3C). Mesopleuron densely punctate, rather densely covered with pubescence (Fig. 3A); epicnemial carina present ventrally; mesopleural suture transversely striate. Propodeum rugosely punctate, transversely striate dorsomedially, without lateromedian longitudinal carina; posterior transverse carinae weak and incomplete (Fig. 3D). Hind wing with 10 distal hamuli. Fore tibia with 14 stout spines on dorsal

surface and three stout spines on distal end. Hind coxa elongate, 2.8 times as long as maximum width. First metasomal tergite broadened posteriorly in dorsal aspect, 3.6 times as long as posteriorly broad (Fig. 3G); posterior end of first metasomal sternite at posterior 0.33 between spiracle and posterior end of first metasomal tergite; second to fourth tergites densely covered with strongly fine punctures and minute pubescence.

Coloration. Body largely reddish brown to black. Face with narrow yellow stripe, extending along inner orbit to top of eye (Fig. 3B). Clypeus yellowish brown. Apical half of mandible black. Middle parts on behind of antennal sockets to vertex black in dorsal view (Fig. 3C). Temple reddish brown (Fig. 3A). Pronotum black and reddish brown, antero-lateral margin reddish brown (Fig. 3A). Mesoscutum reddish brown with pairs of longitudinal black spots; median lobe of mesoscutum reddish brown with longitudinal black spots (Fig. 3C). Mesopleuron reddish brown with black spots on margin of mesopleuron; speculum black; mesosternum black; mesepimeron reddish brown; scutellum dark reddish brown to black; postscutellum yellow, with black spot in the middle. Propodeum black; metapleuron reddish brown, with yellow spot below pleural carina. Legs reddish brown to yellowish brown. Tibia and tarsus paler. Fore coxa with darkened spots ventrally. Mid and hind coxae with darkened spots dorsally. All tarsi yellow except for half of hind basitarsus dark brown. Wings hyaline, slightly tinged with brown; pterostigma black, with faint brownish spots around junction of vein R and pterostigma. Metasomal tergites reddish brown to black. Ovipositor dark brown, sheath black.

Male. Unknown.

Distribution. South Korea.

Region. Eastern Palaearctic.

Etymology. The species name is derived from South Korea, the country of the type specimens.

Remarks. This new species is similar to *R. wooki* Choi sp. nov., but can be distinguished from by the second to fourth hind tarsomeres yellow (whitish in *R. wooki*); fore tibia with 14 stout spines on dorsal surface and three stout spines on distal end (fore tibia with four stout spines on dorsal surface and two stout spines on distal end in *R. wooki*); median lobe of mesoscutum reddish brown with longitudinal black spots, scutellum dark reddish brown to black, postscutellum yellow, with black spot in the middle (mesoscutum entirely black, scutellum and postscutellum black in *R. wooki*).

Rodrigama wooki **Choi, sp. nov.**
http://zoobank.org/30B1E9C9-36B2-4426-8033-FE3D121D8C67
Figs 1C, 4A–H

Type. ***Holotype*** ♀, 12–26.iv.2008 (Malaise trap), Mt. Unmunsan site 1 (35°38'45"N, 128°57'33"E), Unmun-myeon, Cheongdo-gun, GB, South Korea (J.W. Lee) [DNUE].

Paratypes. [South Korea] 1♀, 17.v.1997, Mt. Dobongsan, Dobong-gu, Seoul, (H.Y. Lim); 1♀, 15.iv.1989, Mt. Suraksan, Nowon-gu, Seoul, (H.I. Jeong); 1♀,

8.v.2010, Mt. Oseosan; 1♀, 13.v.1994, Mt. Sobaeksan, Chungdong, (Y.S. Kim); 1♀, 26.v.1996, Haeyang-ri, Gyesan-gun, CB, (J.I. Kim); 1♀, 5.v.2001, from Eungoksa to 612.8 m peak, Mt. Taehwasan, Docheok-myeon, Gwangju-si, GG, (S.K. Kim & O.Y. Lim); 1♀, 7.vi.1995, Pyochungsa, Milyang-si, GN, (C.S. Park); 1♀, 7.vi.1986, Yonsei Univ. Maeji-ri, Wonju-si, GW, (T.J. Yoon); 1♀, 25.iv.2005, Yonsei Univ. Campus, Maeji-ri, Heungeup-myeon, Wonju-si, GW, (K.W. Oh, M.S. Kim & K.C. Shin); 1♀, 29.v.2004, Ugye-ri, Cheongha-myeon, Pohang-si, GB, (I.R. Shin).

Description. Female. Length of fore wing 10.5–15 mm; body 15–20 mm; ovipositor 18–29 mm. Head and mesosoma with long and dense setae. Malar space about 0.24 times as long as basal width of mandible. Occipital carina interrupted medially. Apical flagellomeres tapered and distal end truncate narrowly. Antenna with 31–32 flagellomeres. Pronotum with strongly impressed and transversely striate groove weakly from epomia to ventroposterior corner; area dorsal to this groove rather strongly and densely punctate, slightly rugose (Fig. 4A). Mesoscutum in front of scuto-scutellar groove 1.4 times as long as wide in dorsal view (Fig. 4C); mesopleuron moderately punctate anteriorly, rather sparsely punctated posteriorly, rather densely covered with pubescence; epicnemial carina present ventrally; mesopleural suture transversely striate. Propodeum rugosely punctate, transversely striate dorsomedially, without lateromedian longitudinal carina; posterior transverse carinae strong but incomplete (Fig. 4D). Hind wing with eight distal hamuli. Fore tibia with four stout spines on dorsal surface and two stout spines on distal end. Hind coxa elongate, 2.8 times as long as maximum width. First metasomal tergite broadened posteriorly in dorsal aspect, 3.1 times as long as posteriorly broad, slightly narrowed a little posterior to spiracle (Fig. 4G); posterior end of first metasomal sternite at posterior 0.47 between spiracle and posterior end of first metasomal tergite; second to fourth tergites closely covered with weak fine punctures and minute pubescence.

Coloration. Body largely reddish brown to black. Face with narrow yellow stripe, extending along inner orbit to top of eye (Fig. 4B). Clypeus yellowish brown. Apical half of mandible black. Frons and vertex black in dorsal view (Fig. 4C). Upper part of temple black, half of lower part yellowish brown in lateral view (Fig. 4A). Pronotum and mesoscutum entirely black, without pairs of black longitudinal spots (Fig. 4A). Mesopleuron black with large reddish brown spot centrally; speculum black (Fig. 4A); mesosternum black; mesepimeron reddish brown; scutellum and postscutellum black. Propodeum black; metapleuron black, with reddish brown spot below pleural carina. Legs brown to black. Tibia and tarsus paler. Hind coxa to femur black; hind tibia to basitarsus blackish brown; second to fourth hind tarsomeres whitish; fifth tarsomere blackish brown.

Wings hyaline, slightly tinged with brown; pterostigma dark brown, with very weak faint brownish spots around junction of vein R and pterostigma.

Metasomal tergites black. Ovipositor dark brown, sheath black.

Male. Unknown.

Distribution. South Korea.

Region. Eastern Palaearctic.

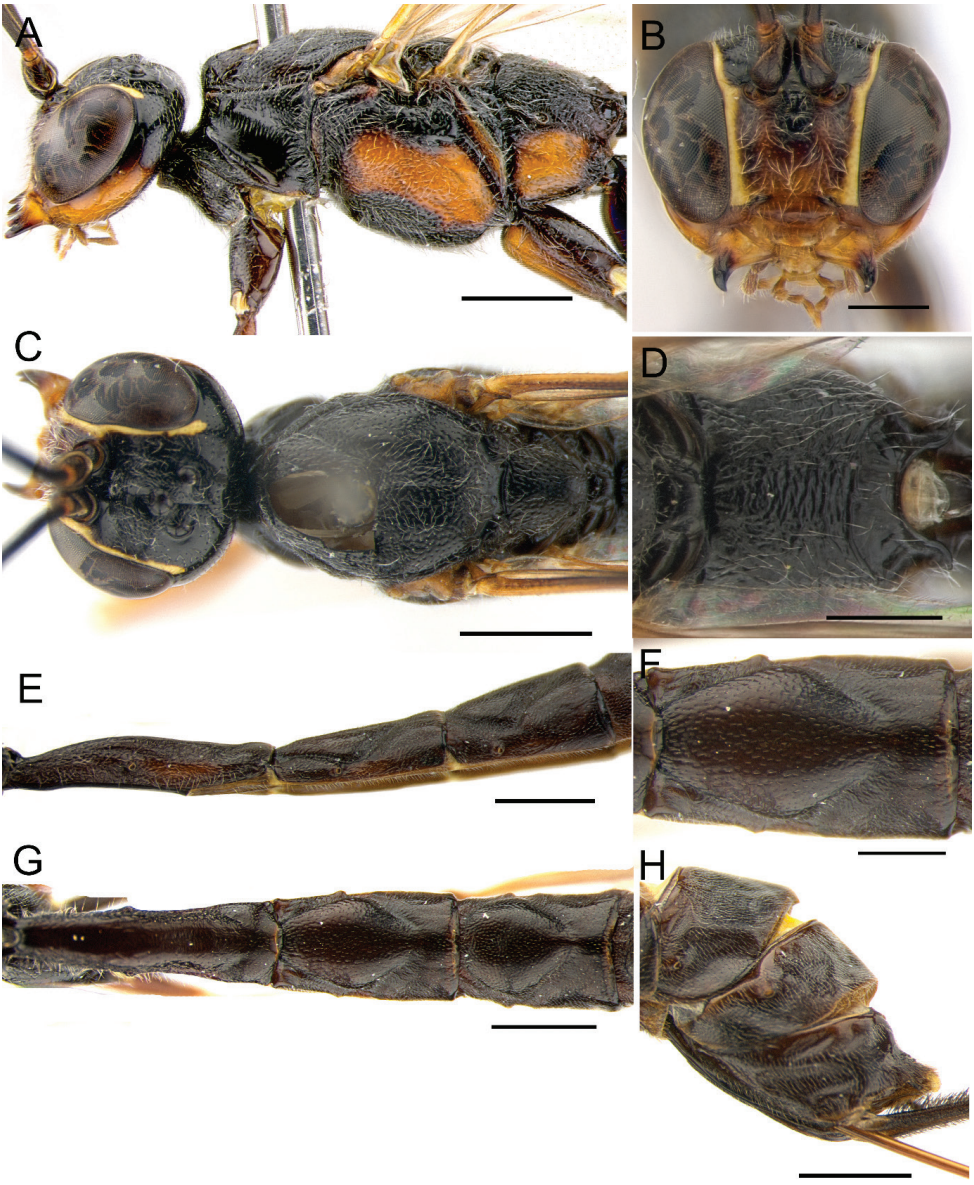

Figure 4. *R. wooki* sp. nov. (holotype). **A** habitus in lateral view **B** head in frontal view **C** Frons and mesoscutum in dorsal view **D** propodeum **E** first to third tergites in lateral view **F** second tergite in dorsal view **G** first to third tergites in dorsal view **H** posterior end of metasoma. Scale bars: 1 mm (**A, C, E, G–H**); 0.5 mm (**B, D, F**).

Etymology. The species is named after Prof. Jong-Wook Lee who collected the holotype specimen and whose collecting efforts have made a great contribution to research into Korean Ichneumonidae.

Remarks. This new species is similar to *R. longissima* (Sheng and Sun 2010), but can be distinguished by the hind coxa to femur black (hind coxa to femur reddish brown in *R. longissima*); hind tibia to basitarsus blackish brown; second to fourth hind tarsomeres whitish (yellow in *R. longissima*); second metasomal tergite about 1.75 times as long as its apical width (about 3.8 times as long as its apical width in *R. longissima*); first metasomal tergite 1.4 times as long as second tergite (first metasomal tergite long, 1.5 times as long as second tergite in *R. longissima*).

***Rodrigama unmunensis* Choi & Lee, sp. nov.**
http://zoobank.org/BA6B8734-C8F2-4117-B4A5-8AA86E655D43
Figs 1D, 5A–H

Type. ***Holotype*** ♀, 30.v.2009, Mt. Unmunsan site 2 (35°38'50"N, 128°58'19"E), Unmun-myeon, Cheongdo-gun, GB, South Korea (G.I. Park) [DNUE].

Description. Female. Length of fore wing 11.5 mm; body 15 mm; ovipositor 20 mm. Head and mesosoma with sparse setae. Malar space about 0.31 times as long as basal width of mandible. Occipital carina interrupted medially. Antennal flagellomeres missing. Pronotum with strongly impressed and transversely striate groove from epomia to ventroposterior corner; area dorsal to this groove rather strongly and densely punctate, slightly rugose; lower part of pronotum glabrous (Fig. 5A). Mesoscutum in front of scuto-scutellar groove 1.2 times as long as in dorsal view (Fig. 5C); mesopleuron densely punctate, rather densely covered with pubescence (Fig. 5A); epicnemial carina absent; mesopleural suture transversely striate. Propodeum rugosely punctate, transversely striate dorsomedially, without lateromedian longitudinal carina; posterior transverse carinae very weak and incomplete (Fig. 5D). Hind wing with 8 distal hamuli. Fore tibia with nine stout spines on dorsal surface and three stout spines on distal end. Hind coxa 2.1 times as long as maximum width. First metasomal tergite broadened posteriorly in dorsal aspect, 1.9 times as long as posteriorly broad (Fig. 5G); second to fourth tergites densely covered with strong punctures and minute pubescence.

Coloration. Body largely reddish brown to black. Face with narrow yellow stripe, extending along inner orbit to top of eye (Fig. 5B). Clypeus reddish brown. Apical half of mandible black. Frons and vertex black in dorsal view (Fig. 5C). Upper part of temple black, lower part reddish brown in lateral view (Fig. 5A). Pronotum and mesoscutum entirely black, without pairs of black longitudinal spots (Fig. 5A). Mesopleuron black with large reddish brown spot centrally; speculum black (Fig. 5A); mesosternum black; mesepimeron reddish brown; scutellum and postscutellum black. Propodeum black; metapleuron black, with reddish brown spot below pleural carina. Legs reddish brown to black. Tibia and tarsus paler. Fore coxa reddish brown with black spot in ventral view. Posterior part of mid coxa and trochanter darkened. Hind coxa with black spot dorsally; hind tibia reddish brown, darkened apically; hind tarsus yellow, basitarsus darker proximally. Wings hyaline, slightly tinged with brown; pterostigma

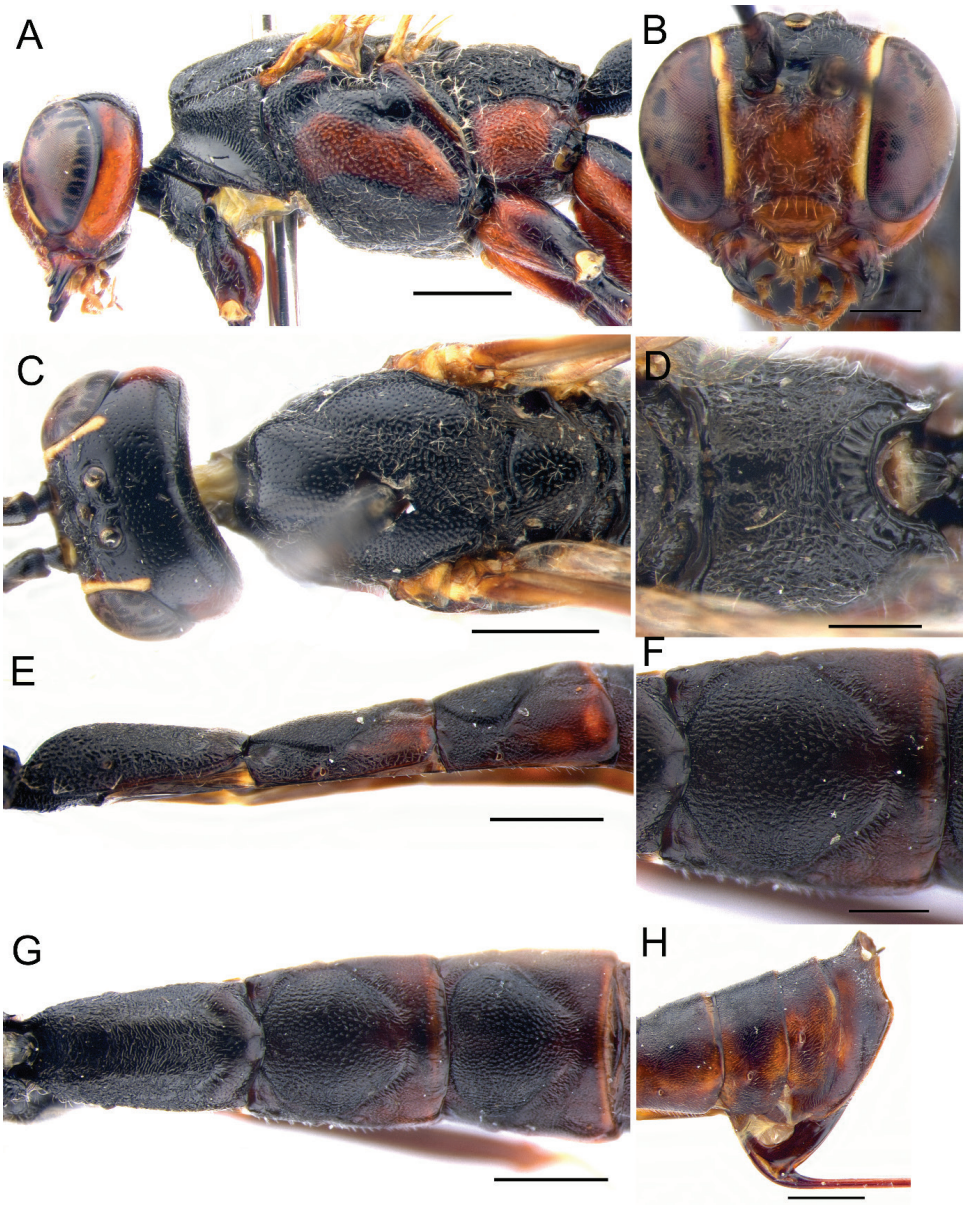

Figure 5. *R. unmunensis* sp. nov. (holotype). **A** habitus in lateral view **B** head in frontal view **C** Frons and mesoscutum in dorsal view **D** propodeum **E** first to third tergites in lateral view **F** second tergite in dorsal view **G** first to third tergites in dorsal view **H** posterior end of metasoma. Scale bars: 1 mm (**A, C, E, G–H**); 0.5 mm (**B, D, F**).

black, with very weak faint brownish spots around junction of vein R and pterostigma. Metasomal tergites reddish brown to black. Ovipositor dark brown.

Male. Unknown.

Distribution. South Korea.

Region. Eastern Palaearctic.

Etymology. The species is named after Mt. Unmun where the holotype specimen was collected.

Remarks. This new species is similar to *R. taishanense*, but can be distinguished from by the ventral half of the hind coxa reddish brown and its dorsal half black (hind coxa black in *R. taishanense*); posterior parts of metasomal tergites with weak brown lines and metasomal tergites reddish brown to black in lateral view (metasomal tergites black in *R. taishanense*); epicnemial carina absent (*R. taishanense* has the ventral section of the epicnemial carina); the first metasomal tergite of *R. taishanense* is much longer than in the new species.

Acknowledgements

We are deeply grateful to the reviewers and the subject editor Gavin Broad for reviewing this manuscript and constructive criticism that improved this paper. This work was supported by a grant from the National Institute of Biological Resources (NIBR), funded by the Ministry of Environment (MOE) of the Republic of Korea (NIBR201902205).

References

Broad GR, Kuslitzky WS (2019) A new species of *Rodrigama* Gauld (Hymenoptera: Ichneumonidae: Poemeniinae) from Israel: a significant range extension. Zootaxa 4567(1): 193–200. https://doi.org/10.11646/zootaxa.4567.1.12

Gauld ID (1991) The Ichneumonidae of Costa Rica, 1. Introduction, keys to subfamilies, and keys to the species of the lower Pimpliform subfamilies Rhyssinae, Poemeniinae, Acaenitinae and Cylloceriinae. Memoirs of the American Entomological Institute No. 47: 589 pp.

Matsumoto R, Broad GR (2011) Discovery of *Rodrigama* Gauld in the Old World, with description of two new species (Hymenoptera, Ichneumonidae, Poemeniinae). Journal of Hymenoptera Research 20: 65–75. https://doi.org/10.3897/jhr.29.872

Sheng ML, Sun SP (2010) Parasitic ichneumonids on woodborers in China (Hymenoptera: Ichneumonidae). Science Press, Beijing, 338 pp. [in Chinese with English summary]

Sheng ML, Sun SP, Ding DS, Luo JG (2013) Ichneumonid Fauna of Jiangxi. Science Press, Beijing, 569 pp.

Sheng ML, Sun SP (2014) Ichneumonid Fauna of Liaoning. (in Chinese with English abstract) Science Press. Beijing, 464 pp.

Wahl DB, Gauld ID (1998) The cladistics and higher classification of the Pimpliformes (Hymenoptera: Ichneumonidae). Systematic Entomology 23: 265–298. https://doi.org/10.1046/j.1365-3113.1998.00057.x

Yu DS, van Achterberg C, Horstmann K (2016) Taxapad 2016, Ichneumonoidea 2015. Database on flash-drive. Nepean, Ontario. www.taxapad.com [Accessed 1 January 2016]

JHR 75: 15–65 (2020)
doi: 10.3897/jhr.75.47006
http://jhr.pensoft.net

REVIEW ARTICLE

JOURNAL OF Hymenoptera RESEARCH
A peer-reviewed open-access journal
The International Society of Hymenopterists

A review of the genus *Orthocentrus* Gravenhorst (Hymenoptera, Ichneumonidae, Orthocentrinae) from South Korea

Andrei E. Humala[1], Jong-Wook Lee[2], Jin-Kyung Choi[3]

1 *Forest Research Institute, Karelian Research Centre, Russian Academy of Sciences, 185910, Petrozavodsk, Russia* **2** *Department of Sciences, Yeungnam University, Gyeongsan, 38541, South Korea* **3** *Department of Science Education, Daegu National University of Education, Daegu, 42411, South Korea*

Corresponding author: Jin-Kyung Choi (jkchoi624@dnue.ac.kr)

Academic editor: G. Broad | Received 2 October 2019 | Accepted 16 December 2019 | Published 27 February 2020

http://zoobank.org/69D2154C-21AC-463D-A0B4-A56ACAF37FE3

Citation: Humala AE, Lee J-W, Choi J-K (2020) A review of the genus *Orthocentrus* Gravenhorst (Hymenoptera, Ichneumonidae, Orthocentrinae) from South Korea. Journal of Hymenoptera Research 75: 15–65. https://doi.org/10.3897/jhr.75.47006

Abstract

Twenty six species of the genus *Orthocentrus* Gravenhorst occurring in South Korea are reviewed. This is the first record of the genus from South Korea. Fifteen species, *O. brachycerus* **sp. nov.**, *O. caudalis* **sp. nov.**, *O. consobrinus* **sp. nov.**, *O. flavescens* **sp. nov.**, *O. koreanus* **sp. nov.**, *O. leei* **sp. nov.**, *O. leucostomus* **sp. nov.**, *O. orientalis* **sp. nov.**, *O. pacificus* **sp. nov.**, *O. parvus* **sp. nov.**, *O. pulchellus* **sp. nov.**, *O. setosus* **sp. nov.**, *O. tenuiventris* **sp. nov.**, *O. trichophthalmus* **sp. nov.** and *O. trichoptilus* **sp. nov.**, are described as new, and ten more species are recorded from South Korea for the first time. *Orthocentrus consobrinus* **sp. nov.** is also reported from Russia, *O. caudalis* **sp. nov.** from China, and *O. winnertzii* from Japan. A key to *Orthocentrus* species occurring in South Korea is provided. The status of *O. stigmaticus* Holmgren, 1858 as a valid species is resurrected (**stat. rev.**).

Keywords

Fauna, key, Korea, new species, Palaearctic region, parasitoids, taxonomy

Introduction

Orthocentrinae is a moderately large cosmopolitan subfamily of about 500 described species (Yu et al. 2016). Most orthocentrines are known to be koinobiont endoparasitoids of primitive dipteran hosts of the superfamily Sciaroidea. Only the Western Palaearctic fauna of this subfamily has been studied relatively well, although some genera should be revised even for Europe. The Eastern Palaearctic fauna has been poorly studied, only twelve species of orthocentrines from six genera are known in China and 17 species from 14 genera in Japan (Humala 2007, Yu et al. 2016, Watanabe 2016, 2018, 2019a, b). In the catalogue of Ichneumonidae of the Russian Far East (Kasparyan et al. 2012) there are 28 genera and 110 species of Orthocentrinae s. l. (including Microleptinae, Cylloceriinae and Diacritinae). The genera most rich in species in Russian Far East are *Eusterinx* Förster (13 species known), *Megastylus* Schiødte (8 species), *Orthocentrus* Gravenhorst, 1829 (4 species), *Stenomacrus* Förster, 1869 (2 species), *Plectiscidea* Viereck, 1914 (9 species), and *Proclitus* Förster, 1869 (9 species), but many genera need to be revised and these number are a poor reflection of actual diversity. South Korean orthocentrines are poorly known (Humala et al. 2016). Eighteen Orthocentrinae genera have been found to occur in South Korea: *Batakomacrus* Kolarov, 1986, *Neurateles* Ratzeburg, 1848, *Orthocentrus* Gravenhorst, *Picrostigeus* Förster, 1869, *Stenomacrus* Förster, *Plectiscus* Gravenhorst, 1829, *Aperileptus* Förster, 1869, *Apoclima* Förster, 1869, *Dialipsis* Förster, 1869, *Entypoma* Förster, 1869, *Eusterinx* Förster, 1869, *Gnathochorisis* Förster, 1869, *Helictes* Haliday, 1837, *Megastylus* Schiødte, 1838, *Pantisartrus* Förster, 1871, *Plectiscidea* Viereck, *Proclitus* Förster, and *Symplecis* Förster, 1869. All these genera are entirely or predominantly Holarctic, and many of them are abundant and species-rich genera. Recently the Korean species from the genera *Gnathochorisis* (5 species), *Symplecis* (2 species) and *Eusterinx* (9 species) were reviewed (Humala et al. 2016, 2018), and a review of the genera *Megastylus* and *Helictes* is in process (Choi et al. in prep.). However, the majority of Orthocentrinae genera have not been taxonomically treated yet, including *Stenomacrus* and *Plectiscus*, rich in species in the local fauna.

Orthocentrus is a large and worldwide genus comprising 95 extant described species (Yu et al. 2016), with the majority of species in the Palaearctic and Neotropical regions. The European fauna of *Orthocentrus* was revised by Aubert (1978), however his revision cannot be considered exhaustive, since it is based only on his own material from the Mediterranean area and Holmgren and Thomson collections. The Eastern Palaearctic fauna of the genus is poorly studied – only eleven species have been recognized there: among them, four species were reported from the Russian Far East, two species from China and one species from Japan, the remaining species were reported from Iran (Yu et al. 2016). The genus *Orthocentrus* was not recorded from South Korea hitherto.

The aim of this work is to review the Korean species of the genus *Orthocentrus*, describe new taxa and provide an identification key to species occurring there.

Materials and methods

A large quantity of material of Korean Orthocentrinae from the Animal Systematic Laboratory of the Yeungnam University (Gyeongsan, South Korea), collected by sweep-netting and Malaise traps, was examined. Additional specimens were borrowed from the National Institute of Agricultural Sciences. Colour photographs were taken with an AxioCam MRc5 camera attached to a stereo microscope Zeiss SteREO Discovery V20. Images were combined from stacks of photographs using AxioVision SE64 software (Carl Zeiss), and optimized with a Delta imaging system (i-solution, IMTi-Solution Inc.).

The morphological terminology generally follows Gauld (1991), except for the terms 'temple' for the upper part of the gena, between the eye and the occipital carina, 'nervellus' for the combined hind wing veins Cu and cu-a, and postocellar line (**POL**) – the shortest distance between the lateral ocelli. Descriptions of sculpture are based on Eady (1968).

The material used in this study, including the holotype specimens, is deposited mostly in the Department of Science Education, Daegu National University of Education, Daegu, South Korea. Some paratype specimens will be deposited in the Zoological Institute, Russian Academy of Sciences, St Petersburg, Russia.

In 'Distribution' sections the new records are marked by an asterisk (*) and all scale bars are 1 mm.

Abbreviations are used as follows:

CB Chungcheongbuk-do;
CN Chungcheonnam-do;
GB Gyeongsangbuk-do;
GN Gyeongsangnam-do;
GG Gyeonggi-do;
GW Gangwon-do;
JB Jeollabuk-do;
JJ Jeju-do;
JN Jellanam-do;
MT Malaise trap;
DNUE Daegu National University of Education, Science Education, Daegu, South Korea;
NIAS National Institute of Agricultural Sciences, South Korea;
ZIN Zoological Institute, Russian Academy of Sciences, St. Petersburg, Russia.

Taxonomy

Family Ichneumonidae Latreille, 1802
Subfamily Orthocentrinae Förster, 1869

Genus *Orthocentrus* Gravenhorst, 1829

Orthocentrus Gravenhorst, 1829: 1–1097. Type species: *Orthocentrus anomalus* Gravenhorst, 1829.

Diagnosis. Clypeus fused with face, forming uniformly convex surface; lower edge of clypeus usually convex or truncate; labrum hidden. Antennal scape unusually long, subcylindrical. Mandibles narrowed apically, not overlapping when closed; lower tooth much shorter than upper tooth, or sometimes completely reduced. Malar space with or without subocular sulcus. Fore wing with pentagonal areolet or without areolet. Hind wing with abscissa of vein Cu present or absent; nervellus reclivous, inclivous or vertical. Ovipositor straight or upcurved, with or without dorsal subapical notch, short, as a rule not longer than apical height of metasoma; ovipositor sheaths with setae along most of the length, except at the very base. Legs generally robust.

Remarks. Twenty five species of the genus *Orthocentrus* have been recognized in South Korea, of them fifteen species are new to science. The genus is characterized by significant sexual dimorphism, which often leads to the inability to confidently establish that males and females belong to the same species.

Key to *Orthocentrus* species occurring in South Korea
(Females only)

1 Face and frons yellow except for interocellar area (Fig. 13C). Median part of mesoscutum with yellow bars along notauli (Fig. 13E). Fore wing without areolet (Fig. 13F)..... **18. *O. pulchellus* sp. nov.**
– Face and frons both never entirely yellow. Mesoscutum fuscous or with light bars along notauli. Fore wing with or without areolet.....**22**
2 Eyes densely setose (Figs 6B, 15F, 17B, 18B).....**3**
– Eyes without conspicuous setae.....**6**
3 Antenna with 45 flagellomeres, first flagellomere 2.3 times as long as wide (Fig. 17A). Larger species (fore wing about 4.0 mm)....**24. *O. trichophthalmus* sp. nov.**
– Antenna with 24–38 flagellomeres, first flagellomere 0.8–1.2 times as long as wide. Smaller species (fore wing 2.0–3.0 mm).....**4**
4 Antenna longer than fore wing, with 37–38 flagellomeres, first flagellomere elongate.....**8. *O. hirsutor* Aubert**
– Antenna shorter than fore wing, with 24–26 flagellomeres.....**5**
5 Face, mesoscutum, propleuron and mesopleuron fuscous (Fig. 18A, B, D, E); vertex dark brown (Fig. 18C); second tergite with weak shallow transverse depression in apical half (Fig. 18G). Fore wing with vein cu-a slightly distad of Rs&M; pterostigma nearly symmetrical; (Fig. 18F). Antennae short, flagellum serrate (Fig. 18A) .....**25. *O. trichoptilus* sp. nov.**
– Face, mesoscutum, propleuron and mesopleuron yellowish (Fig. 15A, B, E); vertex brown with large creamy orbital marks (Fig. 15F); second tergite with strong transverse furrow in apical half (Fig. 15D). Fore wing with vein cu-a oblique, well distad of Rs&M; pterostigma strongly asymmetrical (Fig. 15C).....
.....**20. *O. setosus* sp. nov.**

6 Ovipositor 2.6 times as long as hind basitarsus and as long as hind femur (Fig. 3A, E) ..... **4. *O. caudalis* sp. nov.**
– Ovipositor at most as long as hind basitarsus, does not exceed apical height of metasoma..... **7**
7 Second tergite 2.0–2.9 times as long as posteriorly wide (Fig. 16G). Metasoma long and slender, about 2.0 times as long as head and mesosoma together (Fig. 16A) ..... **23. *O. tenuiventris* sp. nov.**
– Second tergite at most 1.8 times as long as posteriorly wide. Metasoma not longer than 1.8 times as long as head and mesosoma together **8**
8 Metasomal tergites 2–3 with strong transverse-diagonal furrows separating creamy latero-posterior corners (Fig. 5G) **9**
– Metasomal tergites 2–3 without strong transverse-diagonal furrows, if such furrows present on tergite 2, there is no colour difference between latero-posterior corners and anterior part of tergite **10**
9 Areolet absent (Fig. 5F); antenna with 20 flagellomeres; mesosoma mostly light-brown (Fig. 5D, E) ..... **6. *O. flavescens* sp. nov.**
– Areolet present; antenna with 27–29 flagellomeres; mesosoma mostly dark-brown (Fig. 1C) ..... **3. *O. castellanus* Ceballos**
10 Head lenticular in lateral view (Figs 4D, 7D); face flattened **11**
– Head not lenticular in lateral view; face convex..... **14**
11 Areolet present (Figs 4F, 7F); flagellum with more than 20 flagellomeres **12**
– Areolet absent (Figs 2A, 8F); flagellum with 19–20 flagellomeres..... **13**
12 First tergite 1.5 times as long as posteriorly wide (Fig. 4G). Flagellum short, with 21 flagellomeres; temple 0.18 times as wide as eye (Fig. 4C); face brown (Fig. 4B)..... **5. *O. consobrinus* sp. nov.**
– First tergite 2.1 times as long as posteriorly wide (Fig. 7G). Flagellum longer, with 26–27 flagellomeres; temple 0.3 times as wide as eye (Fig. 7C); face yellowish (Fig. 7B) ..... **9. *O. koreanus* sp. nov.**
13 Face and frontal orbits mostly yellow up to level of lateral ocelli (Fig. 2B); POL 1.8 times as long as diameter of lateral ocellus (Fig. 2D) .... **2. *O. brachycerus* sp. nov.**
– Face fuscous, frontal orbits with yellowish marks only close to antennal sockets (Fig. 8B); POL 1.1 times as long as diameter of lateral ocellus (Fig. 8C) .... **10. *O. leei* sp. nov.**
14 Inner orbits yellowish up to level of lateral ocelli (Fig. 9C); face fuscous, malar space creamy (Fig. 9D)..... **11. *O. leucostomus* sp. nov.**
– Inner orbits fuscous, at most with yellowish marks not reaching level of front ocellus; if face fuscous, malar space fuscous..... **15**
15 First flagellomere distinctly elongate, 1.8–2.5 times as long as wide; nervellus intercepted in the middle or below middle..... **16**
– First flagellomere from transverse to slightly elongate, 0.9–1.3 times as long as wide; nervellus intercepted below middle or not intercepted..... **18**

16 Second tergite 1.3 times as long as posteriorly wide; first tergite 1.8 times as long as posteriorly wide, with lateromedian longitudinal carinae subparallel .... **12. *O. marginatus* Holmgren**

– Second tergite 1.8 times as long as posteriorly wide; first tergite 2.0–2.1 times as long as posteriorly wide, with lateromedian longitudinal carinae somewhat convergent posteriorly **17**

17 Face smooth (Fig. 10B). Antenna with 22–24 flagellomeres; fore wing with areolet narrowly sessile (Fig. 10F); nervellus intercepted in lower 0.4..... ..... **13. *O. orientalis* sp. nov.**

– Face granulate (Fig. 6F). Antenna with 30 flagellomeres; areolet large, widely sessile, pentagonal (Fig. 6E); hind wing with nervellus intercepted in the middle.... ..... **16. *O. patulus* Holmgren**

18 Frontal orbits above antennal sockets with large yellow marks (Figs 1B, 14D) **19**

– Frontal orbits above antennal sockets at most with indistinct small yellowish spots close to antennal sockets **20**

19 Face granulate (Fig. 1B); antenna with 25–28 subquadrate flagellomeres, first flagellomere as long as wide; areolet narrowly sessile; nervellus not intercepted; legs entirely rufous (Fig. 1A); second tergite without polished posterior corners separated by a transverse-diagonal groove..... **1. *O. asper* Gravenhorst**

– Face nearly smooth, finely transversely striate (Fig. 14D); antenna with 20–24 flagellomeres, first flagellomere distinctly elongate; areolet narrow or sometimes open; nervellus intercepted in lower third; hind coxa infuscate (Fig. 14E); second tergite with polished posterior corners separated by a transverse-diagonal groove ..... **19. *O. sannio* Holmgren**

20 Face finely punctate (Figs 11B, 12B); fore wing with areolet **21**

– Face granulate (Figs 10B, 14B, 19B); fore wing with or without areolet..... **24**

21 Temples about 0.25 times of eye width (Fig. 12D); occipital carina absent. Smaller species, fore wing length 1.7 mm ..... **15. *O. parvus* sp. nov.**

– Temples wider (Fig. 11C); occipital carina present or absent. Larger species, fore wing length at least 2.2 mm **22**

22 Hind legs partly fuscous, hind coxa brown to black (Fig. 14E). Head almost cubic, subocular sulcus not developed; occipital carina absent; notauli not developed. Face fuscous (Fig. 14F) ..... **21. *O. spurius* Gravenhorst**

– All legs entirely red; subocular sulcus distinct; occipital carina present, often reduced dorsally; mesoscutum anteriorly with distinct notauli (Fig. 11A, E). Face yellowish or infuscate **23**

23 Antenna with 25–29 flagellomeres; second tergite as long as posteriorly wide or transverse, polished with distinct longitudinal striae; vein Rs+2r meeting pterostigma at proximal 0.4 (Fig. 1E). Larger species, fore wing 3.4–4.0 mm..... ..... **7. *O. fulvipes* Gravenhorst**

– Antenna with 24–25 flagellomeres; second tergite 1.2 times as long as posteriorly wide, coriaceous, without striae (Fig. 11G); vein Rs+2r meeting middle of pterostigma (Fig. 11F). Smaller species, fore wing 2.2–2.5 mm..... **14. *O. pacificus* sp. nov.**

24 Second tergite 1.0–1.3 times as long as posteriorly wide; face granulate; areolet present; vertex prominent (Fig. 14B).....**17. *O. protervus* Holmgren**
– Second tergite 1.6–1.8 times as long as posteriorly wide; face convex, more finely sculptured (Fig. 19B); areolet present or absent; vertex not particularly prominent **25**
25 Areolet absent (Fig. 19C); first tergite without lateromedian longitudinal carinae .....**26. *O. winnertzii* Förster**
– Areolet present (Fig. 19A); first tergite with lateromedian longitudinal carinae ... .**22. *O. stigmaticus* Holmgren**

1. *Orthocentrus asper* Gravenhorst, 1829
Figs 1A, B

Biology. Parasitoid of *Sciophila lutea* Macquart (Diptera, Mycetophilidae).

Material examined. South Korea, 1♀, **JN**: Jirisan National Park, Sunduryu, 24.X.1989, J.G. Kim leg. (NIBR–0147); **GB:** 1♀, Uljin-gun, Mt. Baekamsan, 14.V–19.VI.1999, D.S. Ku leg. (NIAS); 1♂, Cheongdo-gun, Mt. Unmunsan, 28.VI.1984, J.G. Kim leg. (DNUE– 0477); **GW**: 1♂, Chuncheon-si, Dong-myeon Iinae-ri, 1–8. VIII.2005, S.J. Jang leg. (DNUE–0122).

Distribution. Holarctic; *South Korea (GB, GW, JN).

2. *Orthocentrus brachycerus* Humala & Lee, sp. nov.
http://zoobank.org/194E053E-96AB-4B55-9A82-8328ACE150AE
Fig. 2

Description. Female. Fore wing length 3.0–3.5 mm.

Face at level of antennal sockets 1.4 times as wide as high; face smooth, polished, sparsely and slightly punctate; eyes not setose; dorsal ridge of face in between antennal sockets with a median blunt low prominence; face profile straight except dorsally very slightly impressed; inner eye orbits slightly divergent ventrally; edge of clypeus straight; antennal sockets not on a distinct high shelf; subocular sulcus distinct, sharp, slightly bent towards occiput; maxillary palp reaching fore coxa. In dorsal view, head posteriorly concave, temples short; lateral ocellus separated from eye by its maximum diameter; POL 1.8 times as long as diameter of lateral ocellus; ocellar-ocular grooves present. Minimum distance between antennal sockets about 0.4× diameter of socket; antenna very short, with 19 flagellomeres (n = 15) gradually shortening towards apex of antenna; basal flagellomere 1.5 times as long as wide and about 0.4× of length of scape; scape slightly convex on inner surface, slightly concave on outer surface.

Mesosoma polished; mesoscutum anteriorly with distinct notauli; in profile, scutellum weakly convex, metapleuron slightly convex; propodeum with posterior

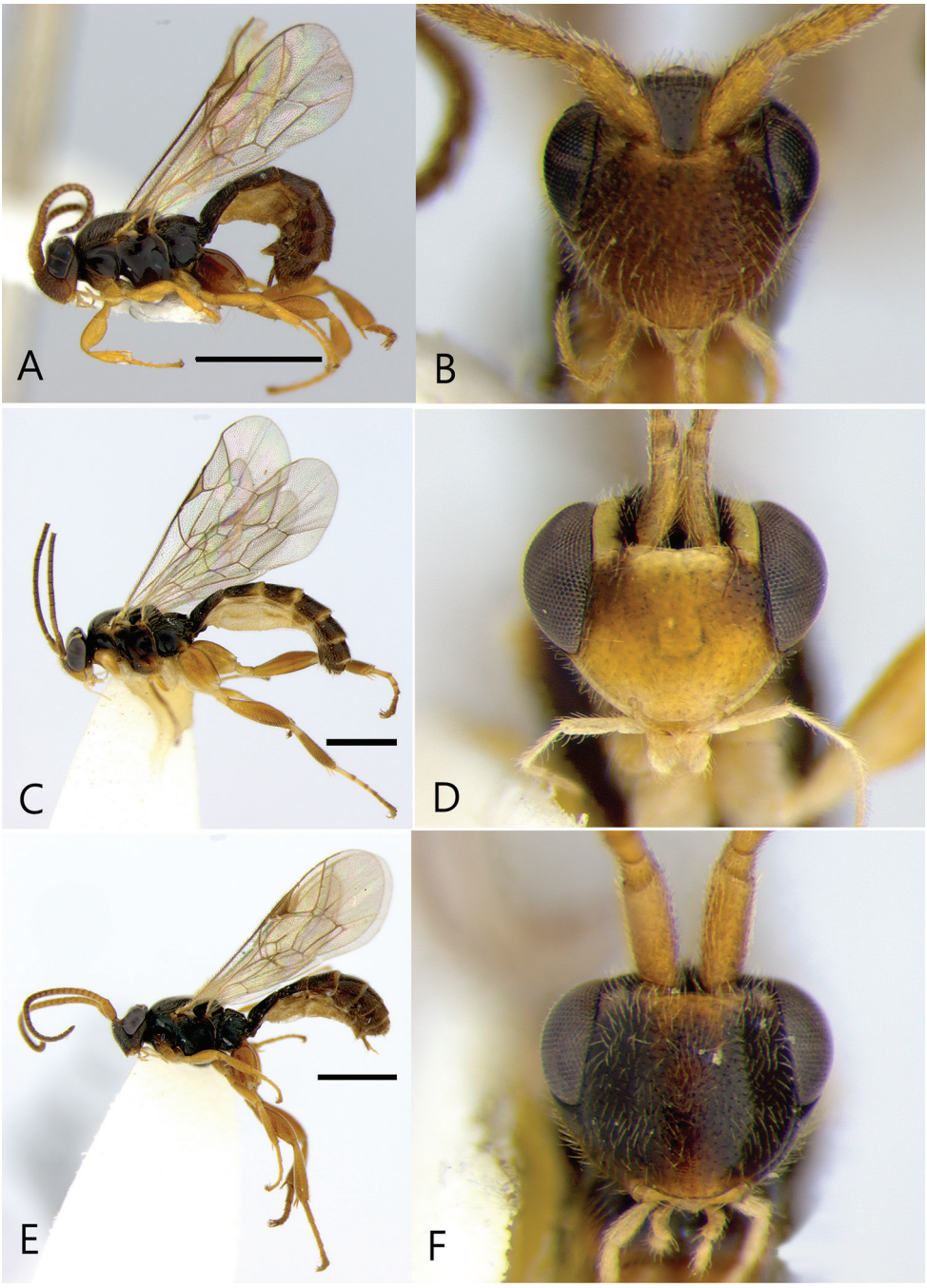

Figure 1. *Orthocentrus* spp. **A** Habitus in lateral view of *O. asper* **B** head in frontal view of *O. asper* **C** habitus in lateral view of *O. castellanus* **D** head in frontal view of *O. castellanus* **E** habitus in lateral view of *O. fulvipes* **F** head in frontal view of *O. fulvipes*.

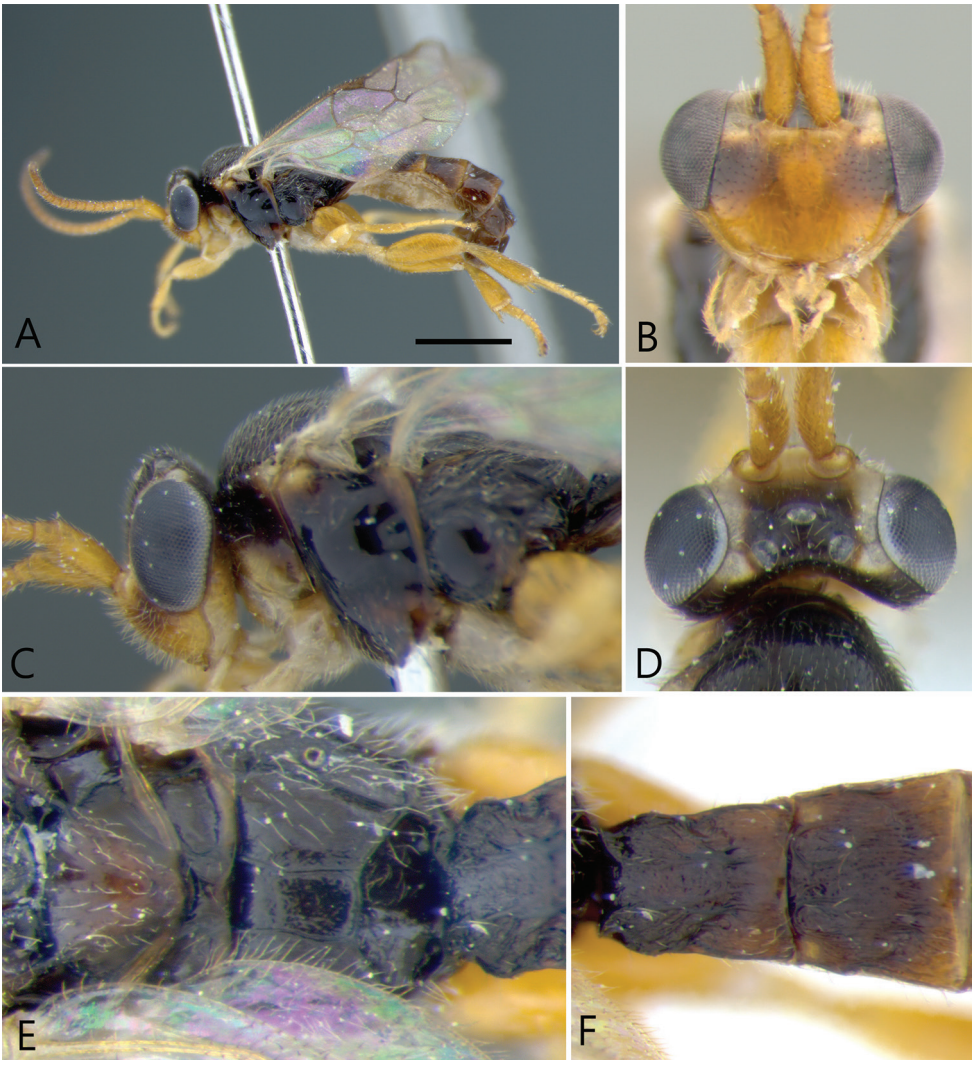

Figure 2. *Orthocentrus brachycerus* sp. nov. Holotype. **A** Habitus in lateral view **B** head in frontal view **C** head and mesosoma in lateral view **D** head in dorsal view **E** scutellum and propodeum in dorsal view **F** first and second tergites in dorsal view.

transverse carina complete, strong and raised between lateral longitudinal carinae, lateromedian longitudinal carinae complete, lateral longitudinal carinae distinct, propodeal spiracle small.

Legs robust; coxae polished, femora with coriaceous microsculpture, tibiae and tarsi coriaceous-granulate; hind femur 3.0 times as long as high, hind tibia 4.0 times as long as apically wide, with spine-like setae.

Wings not particularly narrow; fore wing without areolet; vein Rs nearly straight; vein Rs+2r meeting pterostigma at basal 0.45; vein cu-a opposite Rs&M; nervellus intercepted in lower third.

First tergite slightly widening posteriorly, 1.2 times as long as apically wide; coriaceous, with two distinct lateromedian longitudinal carinae and indistinct longitudinal striae, with transverse impressions originating at about middle of tergite, sloping posteriorly, meeting centrally.

Second tergite 0.9 times as long as posteriorly wide; coriaceous and longitudinally striate, sometimes with lateromedian longitudinal carinae in anterior half, anterior corners impressed and transverse groove near posterior margin bending anteriorly near lateral margins, forming a somewhat uplifted area medially with longitudinal striae; thyridia rounded. Third tergite with coriaceous microsculpture anteriorly; remainder of metasoma unsculptured, polished. Ovipositor thin, slightly upcurved, without subapical dorsal notch; ovipositor sheath narrow, with sparse setae.

Body setose except eyes, pronotum, mesopleuron and metapleuron; setae scattered on metasoma and posterior sides of coxae.

Blackish brown; face yellow, sometimes laterally infuscate; inner orbits broadly whitish-yellow up to occiput; antenna orange; malar area yellow posterior to malar sulcus and up to level of lower third of eye; mouthparts, fore and mid coxae, all trochanters and trochantelli yellowish creamy, remainder of fore and mid legs yellow; hind legs orange, posterior margins of tergites 1–4 brown. Sometimes lower mesopleuron and scutellum reddish-brown.

Male. Flagellum with 21 flagellomeres; face and frontal orbits yellow. Otherwise as in female.

Biology. Hosts unknown.

Etymology. Named from the Greek *βραχύς* (short) and *κέρας* (horn) after the short antenna.

Comparison. Compared with the other species that have lenticular head, flattened and smooth face, short temples, and eyes glabrous, the fore wing areolet is absent and the flagellum with fewer than 20 flagellomeres, unlike in *O. koreanus* and *O. consobrinus*. From the allied *O. leei* it differs in the yellow face and frontal orbits up to the level of the lateral ocelli; the POL 1.8 times as long as diameter of an ocellus.

Material examined. ***Holotype:*** female; South Korea, **GB**: Daegu-si, Dalseo-gu, Daegok-dong, Daegusumogwon, 35°48'3.26"N,128°31'15.3"E, 27.VII–8.VIII.2011, J.W. Lee leg. (DNUE-0496).

Paratypes: South Korea, **GB**: 1♀, Daegu-si, Dalseo-gu, Daegok-dong, Daegu Arboretum, 88 m, 35°47'38.6"N, 128°31'33.5"E, 4–18.IV.2012, S.G. Kang leg. (DNUE-0120); 1 ♂, Bongjeongsa 10–11.VII.1998, J.W. Lee leg. (DNUE-0135); **GG**: 3 ♀, Pocheon-si, Soheul-eup, Jikdong-ri, Korean National Arboretum, Gwangeung Forest, MTII, 123 m, 37°45'22"N, 127°9'48.9"E, MT, 15.VII–2.VIII.2013, S.Y. Park, J.O. Lim & J.S. Lim leg. (DNUE); 1♀, Pocheon-si, Soheul-eup, Jikdong-ri, Korean National Arboretum, Gwangeung Forest, MTII, 120 m, 37°45'22"N, 127°9'48.9"E, MT, 28.VI–15.VII.2013, S.Y. Park, J.O. Lim & J.S. Lim leg. (ZIN); 1♂, Schihung-si, Mt. Chongsu, 22.VIII.1988 J.W. Lee leg. (DNUE-0481); **GN**: 1♀,

Dapcheon-ri, Ibanseong-myeon, Jinju-si, MTIII, 27.VI–4.VII.2005, B.K. Ahn leg. (ZIN-0376); **GW**: 2♀, Chuncheon-si, Sanong-dong, Gwangwon Provincial Arboretum, 30.VIII–17.IX.2013, I.G. Kim leg. (DNUE); 2♀, Chuncheon-si, Sanong-dong, Gwangwon Provincial Arboretum, 17.VII–1.VIII-2013, I.G. Kim leg. (DNUE); 1♀, Heungeop-myeon, Maeji-ri, Yeosedae gyonae ungoleong yeop, 37°16'53"N, 127°54'02"E, MT, 19.V–6.VI.2011, J.W. Lee leg. (DNUE–0243); **JB**: 2♀, Wanju-gun, Dongsang-myeon, Daea-ri, San1-2, Daea, 35°58'24.24"N, 127°18'13.53"E, MT, 16–31.VIII.2013, J.M. Park leg (DNUE); 1♀, Iksansi Sinyongdong, Wongwang University, 35°57'N, 126°57'E, MT, 21.VII–17.VIII.2006, J.W. Lee leg. (ZIN-0253); **JN**: 1♀, Kwangju-si Buk-gu, Geumgok-dong, Mudeungsan National Park, Wonhyosa, 35°57'N, 126°57'E, MT, 26.VI–27.VII.2013, J.K. Choi leg. (ZIN-0108).

Distribution. South Korea (GB, GG, GN, GW, JB, JN).

3. *Orthocentrus castellanus* Ceballos, 1963

Figs 1C, D

Biology. Hosts unknown.

Material examined. South Korea, **GB**: 1 ♀, Namsa-ri, Hyeongok-myeon, Kyeongju-si, MTII, 28.VII–11.VIII.2005, J.T. Mun leg. (DNUE); **GG**: 1 ♀, Pocheon-si, Soheur-eup, Jikdong-ri, 51-7, Korean National Arboretum, Saengtae tower, 37°44'56"N, 127°08'54.5"E, 31.V–14.VI.2013, I.G. Kim leg. (DNUE); **GN:** 1 ♂, Sancheong-gun, Mt. Soeui, 31.VII–1.VIII.1998 J.C. Ieong leg. (NIBR–0133).

Distribution. Palaearctic [Spain, Iran, Bulgaria]; *South Korea (GB, GG, GN).

4. *Orthocentrus caudalis* Humala & Lee, sp. nov.

http://zoobank.org/47B8B539-5A41-4AA4-A487-7A50E49A04AA

Fig. 3

Description. Female. Fore wing length 3.0 mm.

Face at level of antennal sockets as wide as high; head smooth and polished, face with punctures; eyes not setose; dorsal ridge of face in between antennal sockets without a median prominence; face in profile straight, except just before antennal sockets impressed; edge of clypeus straight, antennal sockets on a shelf; malar space with distinct subocular sulcus which is bent towards occiput; maxillary palp reaching to beyond fore coxa. In dorsal view, head posteriorly concave; temples short; lateral ocellus separated from eye by a distance 1.3 times longer than its maximum diameter; POL 1.3 times as long as diameter of lateral ocellus, lacking ocellar-ocular grooves. Minimum distance between antennal sockets about 0.7× diameter of socket; antenna comparatively short and thick, with 24 flagellomeres (25 in paratype) which gradually shortening apically; first flagellomere 1.5 times as long as wide and about 0.4 times as long as scape; scape nearly parallel-sided.

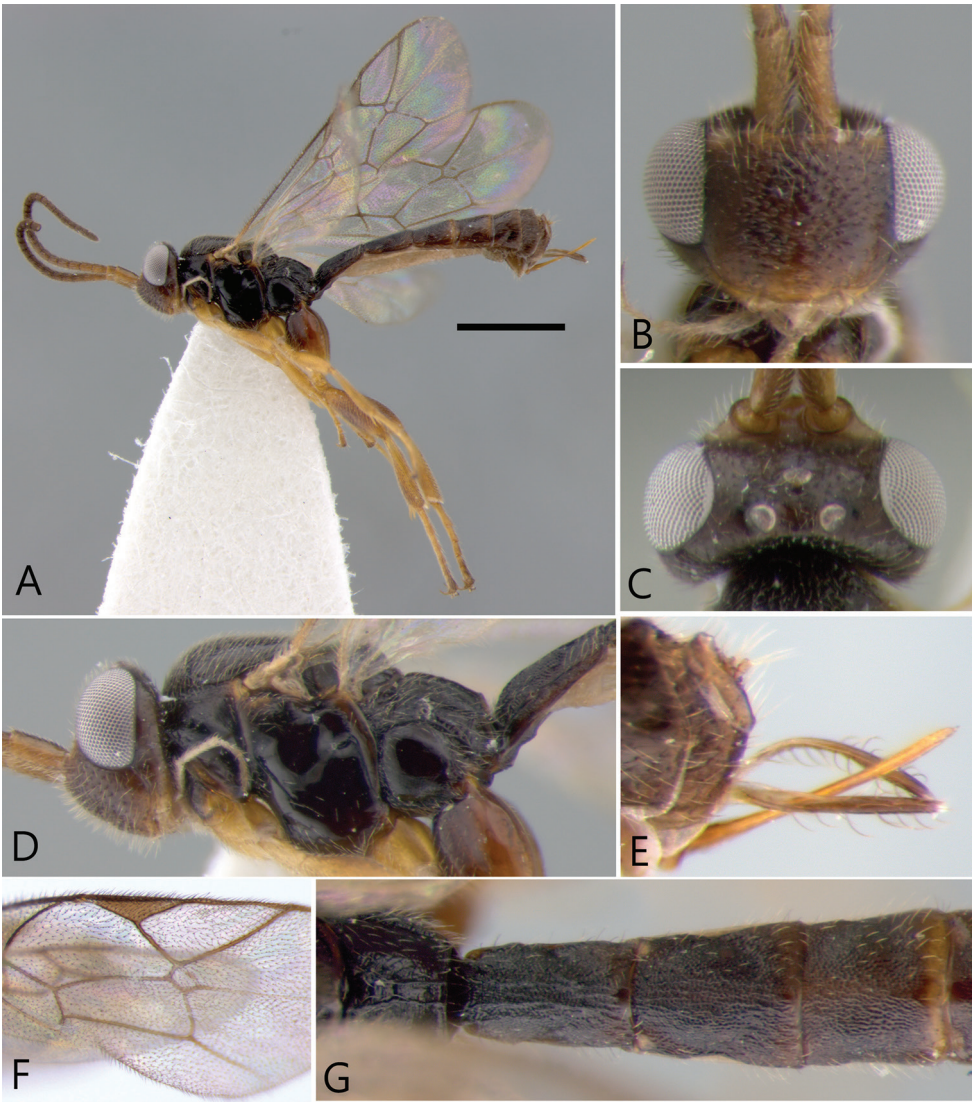

Figure 3. *Orthocentrus caudalis* sp. nov. Holotype. **A** Habitus in lateral view **B** head in frontal view **C** head in dorsal view **D** head and mesosoma in lateral view **E** ovipositor **F** areolet **G** propodeum and first to third tergites in dorsal view.

Mesosoma smooth and polished except postero-ventral corner of pronotum with short striae, mesoscutum with indicated notauli; in profile, scutellum weakly convex, metapleuron somewhat convex; propodeum with coriaceous microsculpture and with complete posterior transverse carina, lateromedian longitudinal carinae indistinct basally, spiracle small.

Legs all slightly flattened, broad; coxae and femora polished, tibiae and tarsi coriaceous-granulate; hind femur 3.1 times as long as high, hind tibia 3.6 times as long as apically wide; tibiae dorsally with spine-like setae; spurs curved apically.

Wings not particularly narrow, fore wing with areolet closed but 3rs-m weak, areolet longer than high, vein 2rs-m shorter than 3rs-m, 2m-cu meeting areolet at apical 0.6, vein Rs nearly straight; nervellus intercepted slightly below middle.

First tergite 2.0 times as long as posteriorly wide, in dorsal view, slightly wider at spiracles; coriaceous, with weak lateromedian longitudinal carinae, with transverse impressions originating at about middle of tergite, sloping posteriorly, not meeting centrally. Second tergite 1.2 times as long as posteriorly wide; coriaceous, with shallow transverse impressions originating at about middle of tergite, sloping anteriorly and posteriorly, not meeting clearly centrally; anterior thyridia small, contrastingly coloured. Third tergite coriaceous; remaining tergites smooth and polished; fourth tergite with coriaceous microsculpture antero-medially. Ovipositor slightly upcurved, thin, as long as hind femur, without dorsal notch; ovipositor sheath narrow, pointed, with setae longer than ovipositor sheath width and curved backwards, sparser basally.

Body setose except eyes, pronotum, mesopleuron, metapleuron; setae on propodeum, anterior tergites and posterior sides of coxae very few.

Blackish brown except mouthparts and malar space pale, antenna dull yellow ventrally, infuscate over entire dorsal side. Clypeus apically and dorsal ridge of upper face between antennae narrowly yellowish, frontal orbits with small yellowish marks close to antennal sockets; sternites creamy, fore and mid legs and hind trochanters and trochantellus yellowish. Hind coxae brown in basal 2/3, hind femur brownish, except for more light basal third. Tergites 3 and 4 with light brown apical margin.

Male. Unknown.

Biology. Hosts unknown.

Etymology. Named from the Latin *cauda* (tail) after the unusually long ovipositor as long as the hind femur.

Comparison. This is a distinctive species on account of the very long, thin, slightly upcurved ovipositor, which is as long as the hind femur (Fig. 3A).

Material examined. ***Holotype:*** female; South Korea, **JN**: Gurye-gun, Gurye-eup, Mt. Jirisan National Park, Nogodan, 35°17'47"N, 127°31'36"E, 20.VI–10.IX.2011, J.W. Lee leg. (DNUE).

Paratype: 1 ♀, China, Jirin-seong, Helong-si, Xicheng-jin, Mingyan-chon, 42°32'48"N, 129°00'38"E, 31.VIII–7.IX.2009, J.W. Lee leg. (ZIN).

Distribution. South Korea (JN), China.

5. *Orthocentrus consobrinus* Humala & Lee, sp. nov.

http://zoobank.org/14312A34-3F11-4F96-8D7F-F2225EEC169E
Fig. 4

Description. Female. Fore wing length 4.0 mm.

Face at level of antennal sockets 1.4 times as wide as high; smooth, polished, slightly punctate; eyes not setose; dorsal ridge of face inbetween antennal sockets with a low median blunt prominence; face profile straight except dorsally very slightly im-

pressed; inner orbits divergent ventrally; edge of clypeus straight, antennal sockets not on a distinct high shelf; subocular sulcus distinct, sharp, slightly bent towards occiput; maxillary palp reaching beyond fore coxa. In dorsal view, head posteriorly moderately concave, temples short but distinct, lateral ocellus separated from eye by its maximum diameter, POL 1.1 times as long as diameter of lateral ocellus; ocellar-ocular grooves present. Minimum distance between antennal sockets about 0.8× diameter of socket; antenna short, with 21 flagellomeres elongate, gradually shortening towards apex of antenna; first flagellomere 1.8 times as long as wide and about half of the scape length; scape slightly convex on inner surface, slightly concave on outer surface.

Mesosoma smooth and polished; mesoscutum anteriorly with distinct notauli; in profile, scutellum weakly convex, metapleuron slightly convex; propodeum with posterior transverse carina complete, strong and raised between lateral longitudinal carinae, lateromedian longitudinal carinae complete, lateral longitudinal carinae distinct, spiracle small.

Legs robust; coxae polished, femora with coriaceous microsculpture, tibiae and tarsi coriaceous-granulate; hind femur 2.7 times as long as high, hind tibia 4.0 times as long as apically wide; tibiae with spine-like setae.

Wings not particularly narrow; fore wing with small narrow areolet, vein Rs straight posteriorly, vein cu-a opposite Rs&M, oblique; nervellus straight, intercepted below.

First tergite slightly widening posteriorly, 1.5 times as long as apically wide; coriaceous, with two indistinct lateromedian longitudinal carinae and indistinct longitudinal striae, with transverse impressions originating at about middle of tergite, sloping posteriorly, not meeting centrally.

Second tergite as long as posteriorly wide; coriaceous and longitudinally striate, anterior corners impressed and transverse groove near posterior margin bending anteriorly near lateral margins, forming a somewhat uplifted area medially; small thyridia rounded. Remainder of metasoma unsculptured, polished; third tergite with coriaceous microsculpture anteriorly. Ovipositor comparatively thin, slightly upcurved, without subapical dorsal notch; ovipositor sheath narrow, with sparse setae.

Body setose except eyes, pronotum, mesopleuron and metapleuron, setae scattered on metasoma and posterior sides of coxae.

Blackish brown; face brown, yellowish along upper margin, inner orbits broadly light yellow from centre of face to level of front ocellus, antenna proximally and ventrally yellowish; malar area yellowish posterior to malar sulcus and up to level of ventral edge of eye; mouthparts, fore and mid coxae, all trochanters and trochantelli yellowish brown, remainder of fore and mid legs orange; hind legs slightly darker, apical margin of second tergite light brown.

Male. Unknown.

Biology. Hosts unknown.

Etymology. Named from the Latin *consobrinus* (relative), after the conspicuous similarity to *O. koreanus*.

Comparison. Compared with the other species that have a lenticular head, flattened and smooth face, short temples, and eyes glabrous, the fore wing areolet is present, unlike

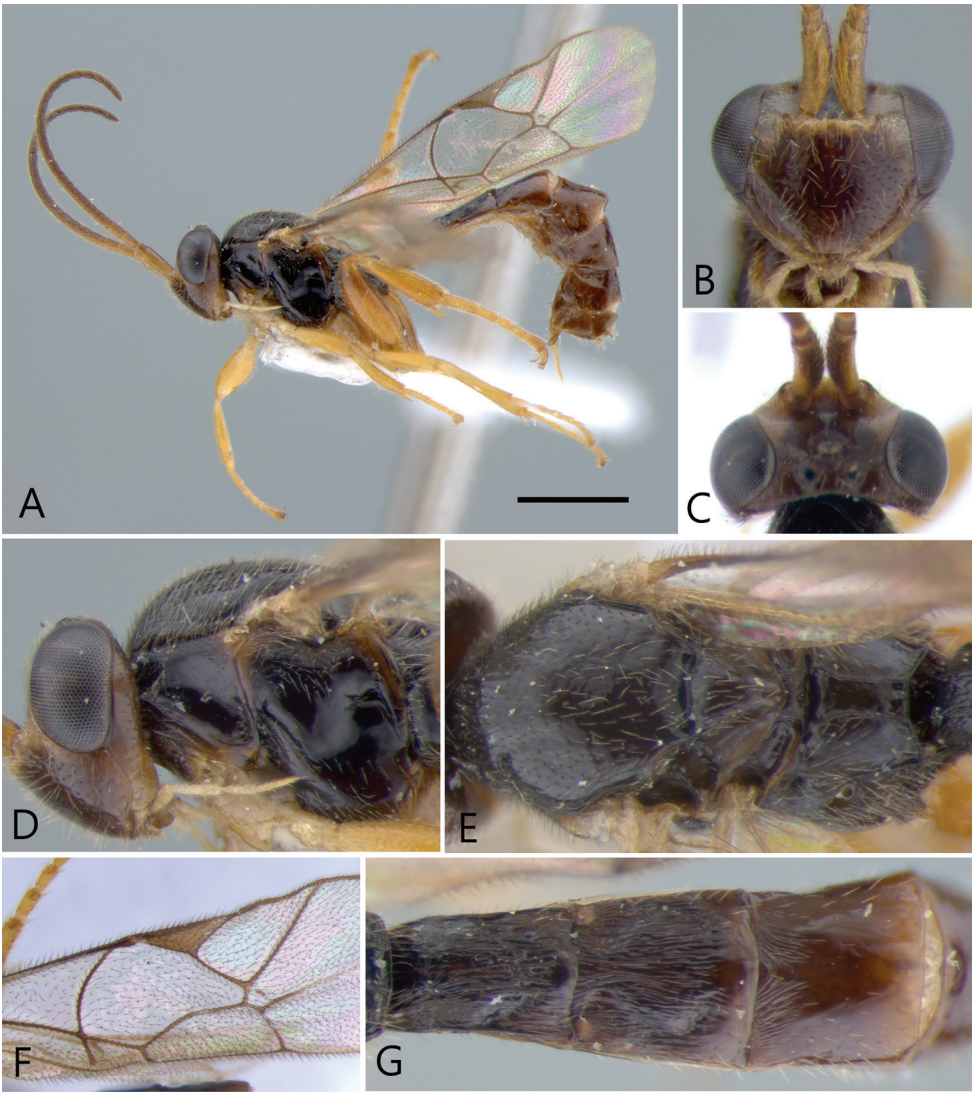

Figure 4. *Orthocentrus consobrinus* sp. nov. Holotype. **A** Habitus in lateral view **B** head in frontal view **C** head in dorsal view **D** head and mesosoma in lateral view **E** mesosoma in dorsal view **F** areolet **G** first to third tergites in dorsal view.

in *O. brachycerus* and *O. leei*. From the allied *O. koreanus* it differs in the brown face, smaller number of antennal flagellomeres and the first tergite 1.5 times as long as apically wide.

Material examined. ***Holotype:*** female; South Korea, **GW,** Mt. Taebaeksan, 14.V–20.VI.1999, D.S. Ku leg. (NIAS).

Paratype: 1♀, Russia, Primorsky Terr., Vladivostok, Sedanka, 100 m, 17.V.2016, S. Belokobylskij leg. (ZIN).

Distribution. South Korea (GW), Russia (Primorsky Terr.).

6. *Orthocentrus flavescens* Humala & Lee, sp. nov.
http://zoobank.org/5182E1AA-288D-46E3-9F0D-356A13F6BB5D
Fig. 5

Description. Female. Fore wing length 3.1 mm.

Face at level of antennal sockets 1.4 times as wide as high; face smooth, polished, sparsely punctate, eyes not setose, dorsal ridge of face in between antennal sockets with a median blunt low prominence; face profile straight except dorsally very slightly impressed, inner orbits slightly divergent ventrally; edge of clypeus straight, antennal sockets not on a distinct high shelf; subocular sulcus well developed, nearly straight; maxillary palp reaching beyond fore coxa. In dorsal view, head posteriorly slightly concave, temples very short, lateral ocellus separated from eye by a distance 1.4 times longer than its maximum diameter, POL 1.6 times as long as diameter of lateral ocellus; ocellar-ocular grooves present. Minimum distance between antennal sockets about 0.4× diameter of socket; antenna with 20 flagellomeres elongate, first flagellomere about 3.0 times as long as wide and about 0.9 times as long as scape; scape slightly convex on inner surface, slightly concave on outer surface.

Mesosoma smooth and polished; mesoscutum anteriorly with distinct notauli; in profile, scutellum particularly high, metapleuron slightly convex; propodeum with posterior transverse carina complete, strong and raised between lateral longitudinal carinae, lateromedian longitudinal carinae complete, lateral longitudinal carinae distinct, spiracle small.

Legs robust; coxae polished, femora with coriaceous microsculpture, tibiae and tarsi coriaceous-granulate; hind femur 2.9 times as long as high, hind tibia 3.5 times as long as apically wide; tibiae with spine-like setae.

Wings not particularly narrow; fore wing without areolet; vein Rs nearly straight, fore wing with vein Rs+2r meeting middle of pterostigma; vein cu-a nearly interstitial (opposite Rs&M); nervellus straight, intercepted below.

First tergite stout, widening posteriorly, 1.2 times as long as posteriorly wide; coriaceous, with two lateromedian longitudinal carinae and longitudinal striae, with transverse impressions originating at about middle of tergite, sloping posteriorly, meeting centrally.

Second tergite 0.8 times as long as posteriorly wide; coriaceous and longitudinally striate, with developed lateromedian longitudinal carinae, anterior corners impressed and transverse groove near posterior margin bending anteriorly near lateral margins, forming a somewhat uplifted striated area medially; small thyridia contrastingly coloured. Third tergite longitudinally striate with transverse impressions originating at about middle of tergite, sloping posteriorly, not meeting centrally. Remainder of metasoma unsculptured, polished. Ovipositor thin, comparatively short, weakly upcurved, without subapical dorsal notch; ovipositor sheath narrow, with sparse setae.

Body setose except eyes, pronotum, mesopleuron and metapleuron, setae scattered on metasoma and posterior sides of coxae.

Yellowish brown; face dusky orange, inner orbits broadly yellow up to occiput; antenna yellowish-brown; malar area yellow posterior to subocular sulcus and up to level of eye middle; mouthparts, legs yellow; propleuron, pronotum, mesopleuron in lower 2/3,

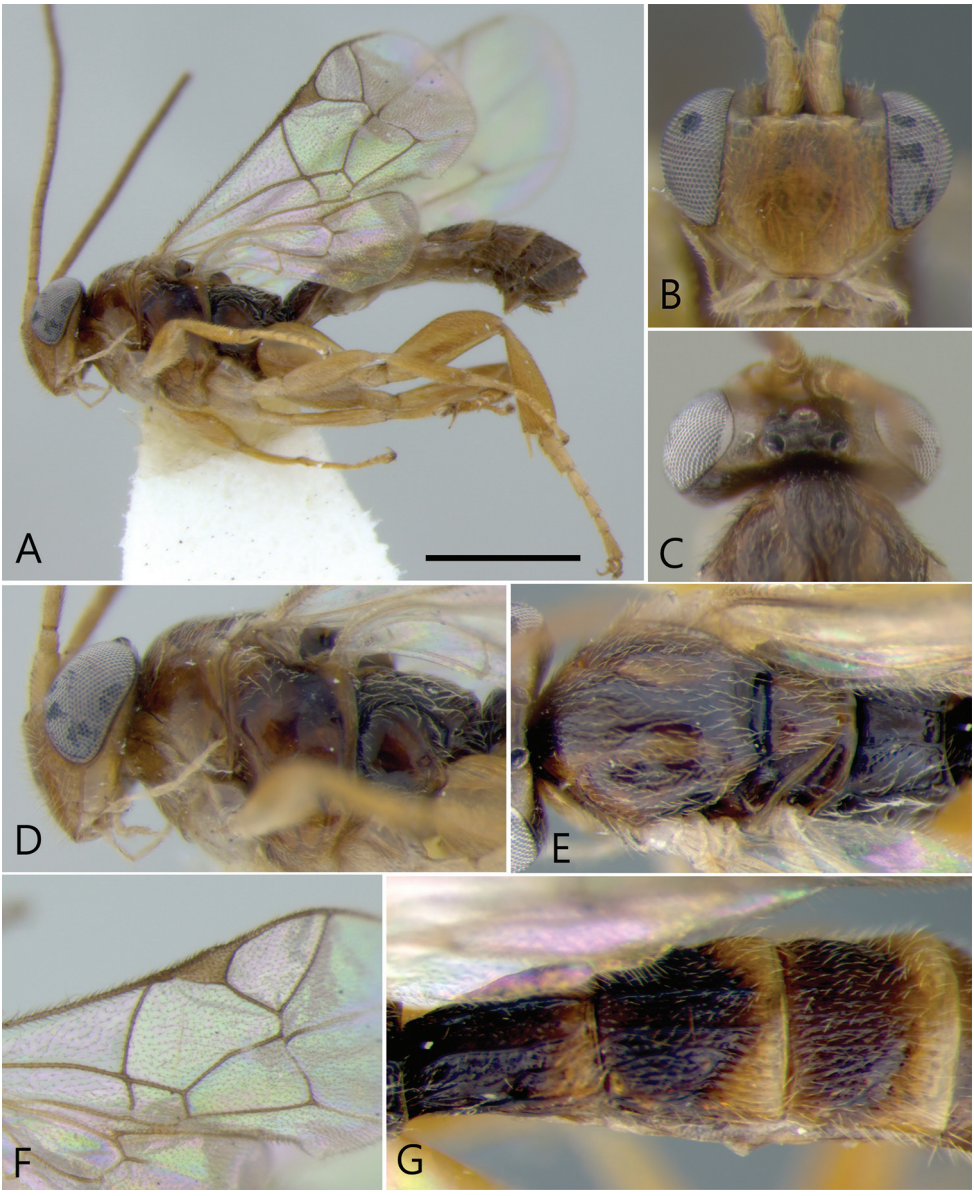

Figure 5. *Orthocentrus flavescens* sp. nov. Holotype. **A** Habitus in lateral view **B** head in frontal view **C** head in dorsal view **D** head and mesosoma in lateral view **E** mesosoma in dorsal view **F** areolet **G** first to third tergites in dorsal view.

mesoscutum anteriorly and longitudinal bars along notauli, scutellum, central part of metapleuron, reddish brown; posterior margins of tergites 1–3 and tergite 4 light-brown.

Male. flagellum with 21 flagellomeres; basic coloration – yellow, frons reddish-yellow. Otherwise as in female.

Biology. Hosts unknown.

Etymology. Named from the Latin *flavesco* (turn yellow) after the yellowish general body colouration.

Comparison. This is a distinctive species on account of the metasomal tergites 2–3 with strong transverse-diagonal furrows separating contrastingly coloured creamy latero-posterior corners. From the closely allied *O. castellanus* it differs in the absence of the fore wing areolet and fewer antennal flagellomeres.

Material examined. ***Holotype:*** female; South Korea, **GW**: Chuncheon-si, Sanong-dong, Gwangwon Provincial Arboretum, 1–14.VIII.2013, I.G. Kim leg. (DNUE).

Paratype: South Korea, **GB**: 1 ♂, Bongjeongsa 10–11.VII.1998, J.W. Lee leg. (DNUE–0135).

Distribution. South Korea (GB, GW).

7. *Orthocentrus fulvipes* Gravenhorst, 1829

Figs 1E, F

Biology. Hosts unknown.

Comments. This is the commonest species of the genus in Korea.

Material examined. South Korea, **GG**: 1♀, Seoul, Cheongyangri-dong, Dongdaemun-gu, MTI, S.N.U. 11–18.VII.2005, W.I. Choi leg., (DNUE–0247); **CB**: 1♀, Eumseong-gun, Eumseong-eup, Mt. Gayeopsan, 36°57'44"N, 127°40'52"E, 24.VII.2013, J.K. Choi leg. (DNUE–0495); 1♂, Boeun-gun, Naesongni-myeon (01), Sinwon-ri, 36°30'41"N, 127°53'26"E, 20.VII.2007, E.J. Hong, Y.R. Jeon & S.K. Lee leg. (DNUE–0275); **CN**: 1♀, Daejeon, Donggu, Daejeon University, MT, 8.X–30XI.2007, J.W. Lee leg. (DNUE–0130); **GB**: 1♀, Gyeongsan-si Dae-dong, Yeungnam University 35°49'N, 128°45'E, 3.VIII.1989, J.W. Lee leg. (DNUE–0115); 2♀, Gyeongsan-si Dae-dong, Yeungnam University 35°58'N, 128°47'E, 20–27.V.2013, J.W. Lee leg. (DNUE–0393,0394); 1♀, Gyeongsan-si Dae-dong, Yeungnam University, 31.VII.1986. S.M. Ryu leg. (DNUE–0139); 1♀, Youngyang-gan, Subi-myeon, Sinwon-ri, 18.V.2001, J.W. Lee leg. (DNUE–0338); 1♂, Gyeongsan-si Dae-dong, Yeungnam University 10.VII.1986. J.W.Lee leg. (DNUE–0138); 3♂, Mungyeong-si Mungyeong-eup Sancho-ri, 14.VIII.1982, J.W. Lee leg. (DNUE–0159,0163,0162); **GG**: Pocheon-si, Soheul-eup, Jikdong-ri, Korean National Arboretum, Gwangneung Forest MTII, 37-45-22 N 127-9-48.9 E, 123 m, 15.vii-2.viii.2013, S.Y. Park, J.O. Lim & J.S. Lim leg. (NIBR); **GW**: 1♀, Chuncheon-si, Sanong-dong, Arboretum, 15–30.V.2013, I.G. Kim leg. (ZIN); 1♀, Chuncheon-si, Sanong-dong, Arboretum, 81 m, 2–15.V.2012, G. Yeong Lee leg. (DNUE–0558); China: 1♀, Jilin-seong, Helong-si, Xicheng-jin, Mingyan-chon, 42°32'48"N, 129°00'38"E, 25–31.VIII.2009, J.W. Lee leg. (DNUE–0227); 1♀, Jirin-seong, Helong-si, Xicheng-jin, Mingyan-chon, 42°32'48"N, 129°00'38"E, 31.VIII–7.IX.2009, J.W. Lee leg. (DNUE–0504); Japan: 1♀,2♂, Hokkaido University, Kita 8, Nishi 5, Kita-ku, Sapporo, Hokkaido, 30.VII–21.VIII.2013, S.H. Oh leg. (DNUE–0056, 0047, 0052).

Distribution. Palaearctic, Oriental; China, Japan; *South Korea (CB, CN, GB, GG, GW).

8. *Orthocentrus hirsutor* Aubert, 1969
Figs 6A, B

Biology. Hosts unknown.

Material examined. 1 ♀ South Korea, **GB**: Yeongju-si, Punggi-eup, Jungyeong (site 104), MT, 22.VI–3.VII.2009, C.J. Kim leg. (DNUE).

Distribution. Palaearctic; *South Korea (GB).

9. *Orthocentrus koreanus* Humala & Lee, sp. nov.
http://zoobank.org/04EAD2D7-DDE8-4B8B-B539-05BC080726D7
Fig. 7

Description. Female. Fore wing length 3.7 mm.

Face at level of antennal sockets as wide as high; face smooth, polished, slightly punctate, frons finely pustulate with hairs, temples with fine matt-like coriaceous sculpture; eyes not setose, face slightly prominent, inner orbits slightly divergent ventrally; dorsal ridge of face in between antennal sockets without a median prominence; profile straight except dorsal third slightly impressed, edge of clypeus straight, antennal sockets on a shelf; subocular sulcus distinct, slightly bent towards occiput; labial palp short; maxillary palp reaching slightly beyond fore coxa. In dorsal view, head posteriorly slightly concave, temples short, lateral ocellus distant from eye by its maximum diameter; POL 1.4 times as long as diameter of lateral ocellus; ocellar-ocular groove somewhat developed. Minimum distance between antennal sockets about 2/3 diameter of socket; antenna with 26–27 elongate flagellomeres (n=18) which gradually shorten apically; basal flagellomere 2.0 times as long as wide and about half of scape length; scape slightly convex on inner surface, slightly concave on outer surface.

Mesosoma smooth and polished; mesoscutum with distinct notauli anteriorly indicated; in profile, scutellum somewhat high, metapleuron slightly convex; propodeum with posterior transverse carina present between lateral longitudinal carinae and pleural carina, area superomedia narrowed posteriorly, spiracle medium-sized.

Legs stout, slightly flattened, rather broad; coxae polished, femora polished-coriaceous, tibiae and tarsi coriaceous-granulate; hind femur 2.9–3.0 times as long as high, hind tibia 3.7 times as long as apically wide; tibiae with spine-like setae.

Wings not particularly narrow; fore wing with vein Rs+2r meeting centre of pterostigma; areolet closed, small, almost petiolate, 2m-cu meeting areolet at apical 0.7, vein Rs bent towards wing apex; vein cu-a inclivous and slightly distad of Rs&M; nervellus intercepted in lower third.

First metasomal tergite elongate, slightly widening apically, 2.1 times as long as posteriorly wide, coriaceous-rugose, with two nearly parallel, complete or posteriorly almost complete lateromedian longitudinal carinae; with deep transverse impressions originating at about middle of tergite, sloping posteriorly, not meeting centrally. Second tergite 1.3 times as long as posteriorly wide, coriaceous-rugose and somewhat

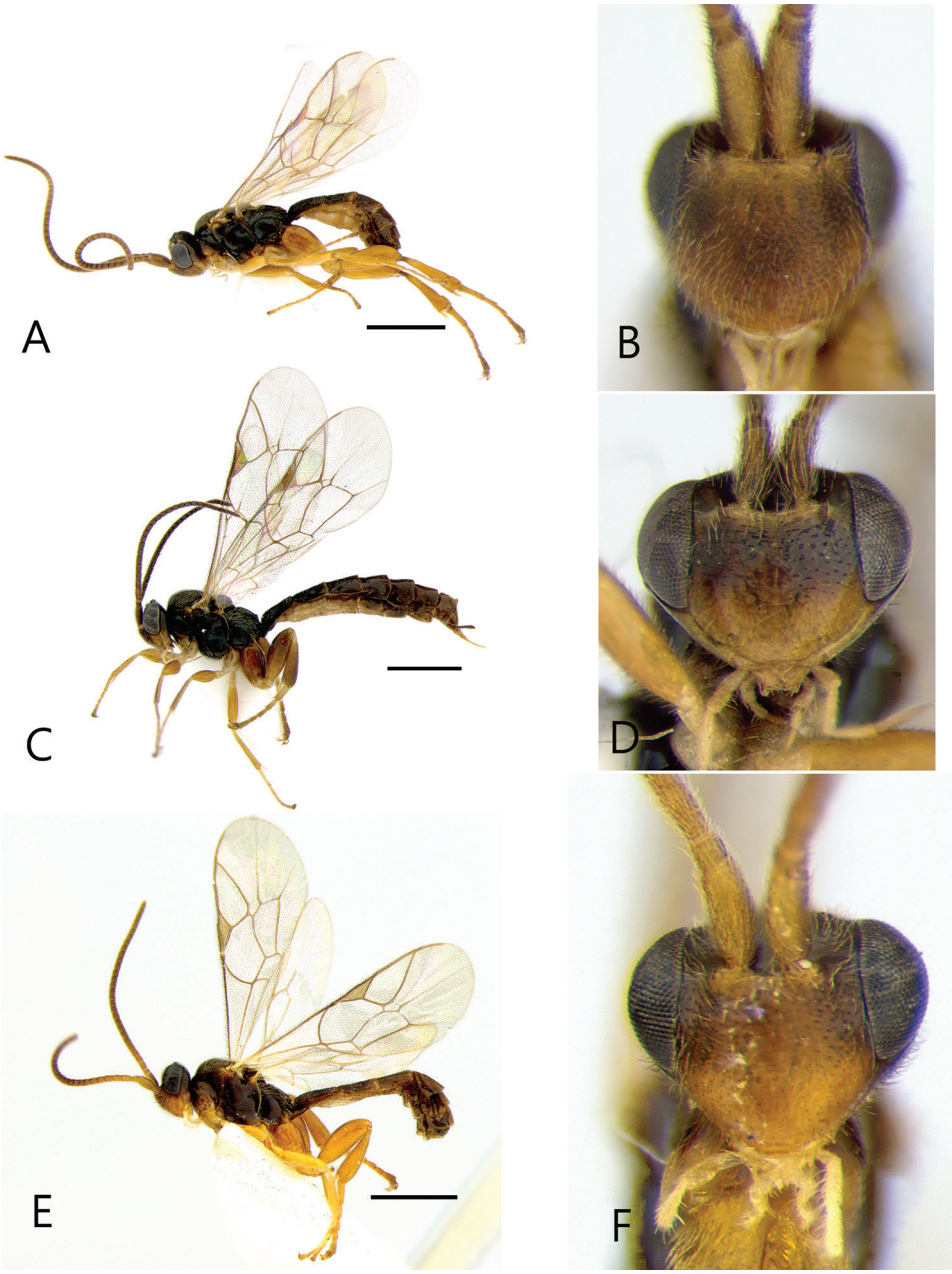

Figure 6. *Orthocentrus* spp. **A** Habitus in lateral view of *O. hirsutor* **B** head in frontal view of *O. hirsutor* **C** habitus in lateral view of *O. marginatus* **D** head in frontal view of *O. marginatus* **E** habitus in lateral view of *O. patulus* **F** head in frontal view of *O. patulus*.

strigose; with the central area convex, bounded by well-defined anterolateral oblique furrows connected with posterior transverse impressions originating at about middle of tergite and meeting centrally; thyridia small, oval, contrastingly coloured. Third ter-

gite slightly coriaceous anteriorly, all remaining tergites smooth and polished. Ovipositor slightly upcurved, thin, without dorsal notch; ovipositor sheath narrow, pointed, with long scarce setae.

Body setose except eyes, propleuron, hind corner of pronotum, mesopleuron and metapleuron; setae very scattered on propodeum, tergites and posterior coxae.

Brown to dark brown except face, frontal orbits, malar space, lower temple, hind corner of pronotum, tegula, wing bases, fore and mid legs, narrow apical bands on tergites 2 and 3; hind trochanter and trochantellus and base of hind tibia yellowish brown, mouthparts and sternites creamy. Sometimes face infuscate laterally. Hind coxa apically yellowish-brown.

Male. Unknown.

Biology. Hosts unknown.

Etymology. Named after the type locality, Korea.

Comparison. Compared with the other species that have a lenticular head, flattened and smooth face, short temples, and eyes glabrous, *O. koreanus* has the fore wing areolet closed and 26–27 antennal flagellomeres, unlike in *O. brachycerus* and *O. leei*. From the allied *O. consobrinus* it differs in the yellowish face, more antennal flagellomeres and the first tergite 2.1 times as long as posteriorly wide.

Material examined. ***Holotype:*** female; South Korea, **GW**: Pyeong-chang-gun Yong-pyeong-myeon Gyebangsan, 28.VI–12.VIII.2012, J.Y. Park leg. (DNUE–0430).

Paratypes: South Korea, **CN**: 1♀, Daejeon, Donggu, Daejeon University, MT, 12.IV–12.V.2007, J.W. Lee leg. (ZIN–0137); **GB:** 1♀, Cheongdo-gun, Unmun-myeon, Mt. Unmun (U2), 35°38'50"N, 128°58'19"E, MT, 30.V–16.VI.2009, C.J. Kim leg. (DNUE); 1♀, Cheongdo-gun, Unmun-myeon, Mt. Unmun 23.V.2008, J.W. Lee leg. (DNUE–0418); 1♀, Mungyeong-si, Gaeun-eup, Wanjang-ri, Mt. Songnisan National Park, Beorimigijae, 36°40'59"N, 127°57'07"E, MT, 17.VII–12.VIII.2013, J.K. Choi leg. (DNUE–0083); 1♀, Chilgok-gun, Dongmyeong-myeon, Hakmyeong-ri, Gansansaseong, 36°02'11.7"N, 128°34'18.17"E, MT, 10.VI–1.VII.2015, J.W. Lee leg. (ZIN); 1♀, **GW**: Donghae-si, Samhwa-dong, Mureung valley, MT, 21–30.V.2005, J.W. Lee leg. (ZIN–0472); 1♀, Donghae-si, Samhwa-dong, Mureung valley, 35°31'N, 126°53'E, MT, 28.VIII–9. IX.2006, K.B. Kim leg. (DNUE); 1♀, Donghae-si, Samhwa-dong, Mureunggyegok, 37°25'45"N, 126°01'17"E, MT, 31.V–5.VI.2005, J.W. Lee leg. (DNUE–0244); 1♀, Wonju-si, Panbu-myeon, Mt. Bangtaesan, MT, 30.VII–28.VIII.2013, J.W. Lee leg. (DNUE–0473); 1♀, Mt. Taebaeksan, MT, 14.V–20.VI.1999, D.S. Ku (NIAS); 5♀, Mt. Taebaeksan, Yuilsa, MT, 20.VI–11.VII.1999, D.S. Ku leg. (NIAS); **JB**: 1♀, Muju-gun, Mupung-myeon, Hyeonnae-ri, San3, Mt. Bakseoksan, 35°59'2.79"N, 127°52'30.74"E, 17.VI–2.VII.2015 J.W. Lee leg. (DNUE); 1♀, Jeongeup-si, Naejang-dong Naejang-san National Park, Geumseongyegok (14 site), MT, 8–14.VI.2008, J.W. Lee leg. (DNUE–0343); **JJ**: 1♀, Jeju-si, Yeon-dong, Halla Arboretum, MT, 1–16.V.2012, S.H. Jeong leg. (DNUE–0039); 1♀, Jeju-si, Jejudaehak-ro, Cheju National University, 33°27'21"N, 126°33'38"E, MT, 19–26.V.2008, J.W. Lee leg. (DNUE–0251).

Distribution. South Korea (CN, GB, GW, JB, JJ).

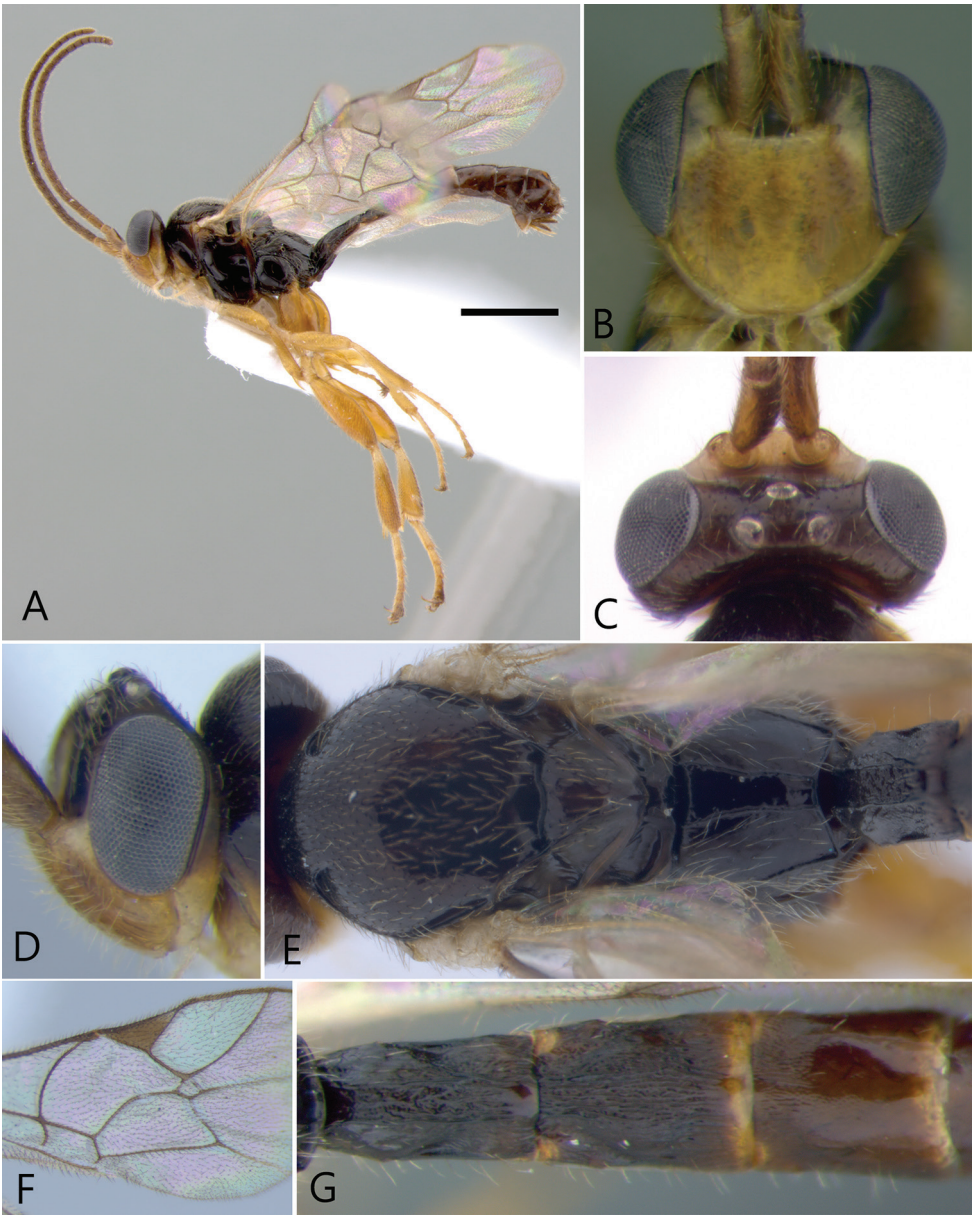

Figure 7. *Orthocentrus koreanus* sp. nov. Holotype. **A** Habitus in lateral view **B** head in frontal view **C** head in dorsal view **D** head in lateral view **E** mesosoma in dorsal view **F** areolet **G** first to third tergites in dorsal view.

10. *Orthocentrus leei* Humala & Choi, sp. nov.
http://zoobank.org/24556892-5675-4781-978D-F79A4D583427
Fig. 8

Description. Female. Fore wing length 2.9 mm.

Face at level of antennal sockets 1.4 times as wide as high; face smooth, polished, slightly punctate, eyes not setose, dorsal ridge of face in between antennal sockets with a median blunt low prominence; face profile straight except dorsally very slightly impressed, inner orbits divergent ventrally; edge of clypeus straight, antennal sockets not on a distinct high shelf; subocular sulcus distinct, gently bent towards occiput; maxillary palp reaching to fore coxa. In dorsal view, head posteriorly concave, temples short but distinct, lateral ocellus separated from eye by its maximum diameter, POL 1.2–1.5 times as long as diameter of lateral ocellus; ocellar-ocular grooves present. Minimum distance between antennal sockets about 0.6× diameter of socket; antenna short, with 18–20 flagellomeres gradually shortening towards apex of antenna; first flagellomere 1.7 times as wide as high and about half of length of scape; scape slightly convex on inner surface, slightly concave on outer surface.

Mesosoma smooth and polished; mesoscutum anteriorly with distinct notauli; in profile, scutellum weakly convex, metapleuron slightly convex; propodeum with posterior transverse carina complete, strong and raised between lateral longitudinal carinae; lateromedian longitudinal carinae complete, lateral longitudinal carinae distinct, spiracle small.

Legs robust; coxae and femora polished, femora partly with coriaceous microsculpture, tibiae and tarsi coriaceous-granulate; hind femur 2.7 times as long as high, hind tibia 3.3 times as long as apically wide; tibiae with spine-like setae.

Wings not particularly narrow; fore wing without areolet; vein Rs nearly straight, fore wing with vein Rs+2r meeting pterostigma at basal 0.45; vein cu-a slightly distad of Rs&M; nervellus intercepted below.

First tergite slightly widening posteriorly, 1.5 times as long as posteriorly wide; coriaceous, with two lateromedian longitudinal carinae and longitudinal striae, with transverse impressions originating at about middle of tergite, sloping posteriorly, not meeting centrally. Second tergite 0.9 times as long as posteriorly wide; coriaceous and longitudinally striate, anterior corners impressed and transverse groove near posterior margin bent anteriorly near lateral margins, forming a somewhat uplifted area medially; thyridia rounded and contrastingly coloured. Third tergite with anterior thyridia and coriaceous microsculpture in anterior half. Remainder of metasoma unsculptured, polished; Ovipositor comparatively thin, slightly upcurved, with shallow subapical notch; sheath narrow, with setae directed backward.

Body setose except eyes, pronotum, mesopleuron and metapleuron, setae scattered on metasoma and posterior sides of coxae.

Blackish brown; face brown, inner orbits with small yellowish marks close to antennal sockets; clypeus and upper face, antenna orange; malar area posterior to malar sulcus yellowish; mouthparts whitish-yellow, fore and mid legs yellow; hind legs dull orange, hind coxa dark brown in basal 3/4, hind femur somewhat infuscate centrally; posterior margin of tergite 2 and tergite 3 anteriorly and posteriorly yellowish-brown; sternites creamy.

Male. Unknown.

Biology. Hosts unknown.

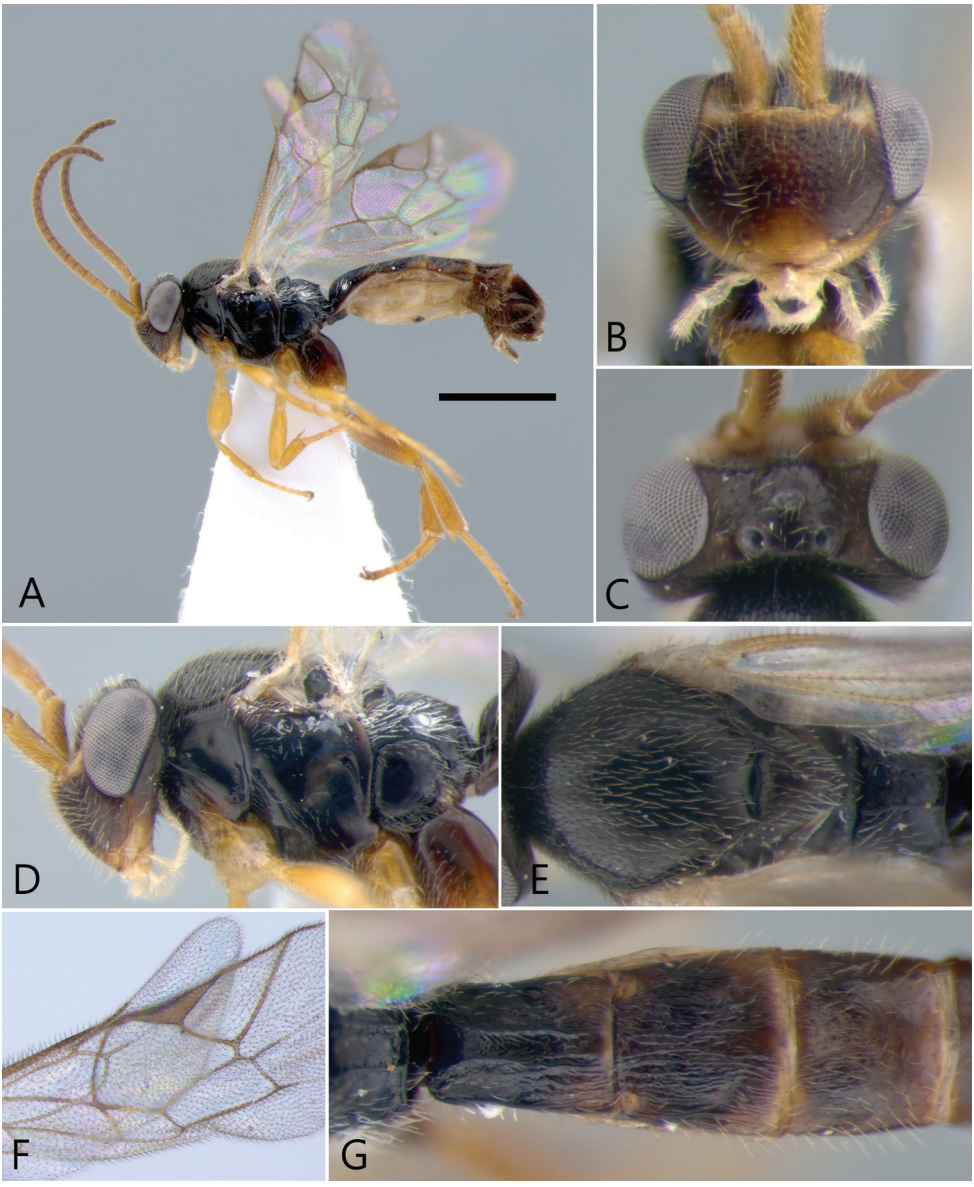

Figure 8. *Orthocentrus leei* sp. nov. Holotype. **A** Habitus in lateral view **B** head in frontal view **C** head in dorsal view **D** head and mesosoma in lateral view **E** mesosoma in dorsal view **F** areolet **G** first to third tergites in dorsal view.

Etymology. This species is named in honor of Professor Jong-Wook Lee, a Korean expert on Ichneumonidae and Head of the Animal Systematic Laboratory of Yeungnam University.

Comparison. Compared with the other species that have a lenticular head, flattened and smooth face, short temples, and eyes glabrous, the fore wing areolet is absent

and the flagellum has fewer than 20 flagellomeres, unlike in *O. koreanus* and *O. consobrinus*. From the allied *O. brachycerus* it differs in the fuscous face and frontal orbits with small yellowish marks, and the POL 1.1 times as long as the diameter of an ocellus.

Material examined. ***Holotype:*** female; South Korea **GG**: Pocheon-si, Soheur-eup, Jikdong-ri, 51–7, Korean National Arboretum, 37°45'1.9"N, 127°08'34.4"E, MT 4, 24.VII–5.VIII.2013, I.G. Kim leg. (DNUE).

Paratype: South Korea, **CB**: 1♀, Geoisan-gun, Chilseong-myeon, Gallon-ri, Gallon valley, 36°43'51.72"N, 127°51'48.89"E, 22.VII–27.X.2011, J.W. Lee leg. (DNUE).

Distribution. South Korea (CB, GG).

11. *Orthocentrus leucostomus* Humala & Lee, sp. nov.

http://zoobank.org/D67B39AA-91FF-4FE3-B067-0BDE87229EBC
Fig. 9

Description. Female. Fore wing length 2.7 mm.

Face at level of antennal sockets as wide as high; head smooth and polished, face granulate, eyes not setose, dorsal ridge of face in between antennal sockets without a median prominence; face profile straight except just before antennal sockets impressed, edge of clypeus straight, antennal sockets on a shelf; malar space with narrow, almost straight subocular sulcus; maxillary palp reaching to beyond fore coxa. In dorsal view, head posteriorly concave, temples short, lateral ocellus distant from eye by a distance 1.1 times longer than its maximum diameter, POL 1.1 times as long as diameter of lateral ocellus, lacking ocellar-ocular grooves. Minimum distance between antennal sockets about 0.4× diameter of socket; antenna comparatively short and thick, with 22 flagellomeres (n = 3) which gradually shorten apically; first flagellomere about 2.0 times as long as wide and about 0.6 times as long as scape; scape nearly parallel-sided.

Mesosoma smooth and polished except postero-ventral corner of pronotum with short striae, mesoscutum with indicated notauli; in profile, scutellum weakly convex, metapleuron convex; propodeum with coriaceous microsculpture and with complete posterior transverse carina, lateromedian longitudinal and lateral longitudinal carinae; spiracle small.

Legs slightly flattened, broad; coxae and femora polished, tibiae and tarsi coriaceous-granulate; hind femur 3.1 times as long as high, hind tibia 3.6 times as long as apically wide; tibiae dorsally with spine-like setae; spurs curved apically.

Wings not particularly narrow, fore wing with narrowly sessile areolet, vein 3rs-m weak, areolet not longer than high, 2rs-m shorter than 3rs-m, 2m-cu meeting areolet at apical 0.6–0.7, nervellus intercepted below middle.

First tergite 1.8 times as long as posteriorly wide, in dorsal view, slightly wider at spiracles; coriaceous, with lateromedian longitudinal carinae, with weak transverse impressions originating at about middle of tergite, sloping posteriorly, not meeting centrally. Second tergite 1.3 times as long as posteriorly wide; coriaceous with dense striae, polished posteriorly, transverse impressions originating at about middle of tergite, sloping anteriorly and posteriorly, not meeting clearly centrally; anterior thyridia

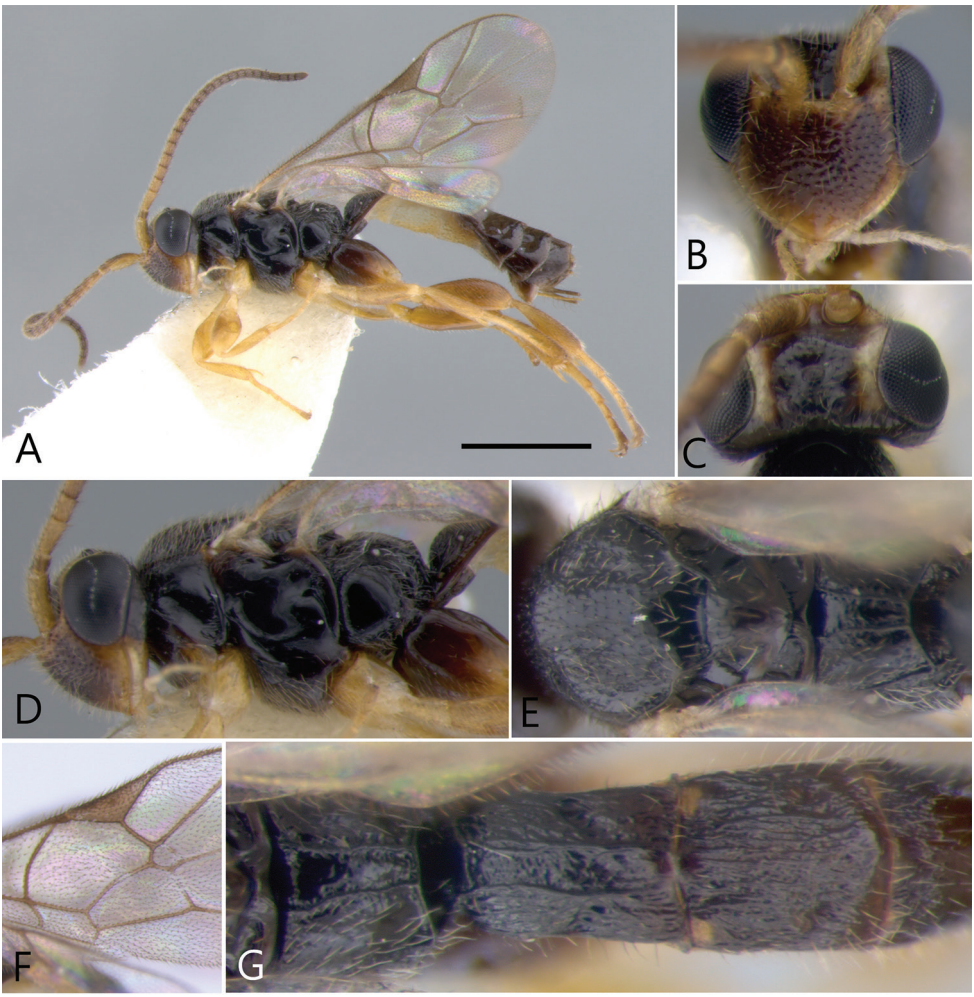

Figure 9. *Orthocentrus leucostomus* sp. nov. Holotype. **A** Habitus in lateral view **B** head in frontal view **C** head in dorsal view **D** head and mesosoma in lateral view **E** mesosoma in dorsal view **F** areolet **G** propodeum and first to second tergites in dorsal view.

rounded, contrastingly coloured. Remaining tergites smooth and polished; third tergite with coriaceous microsculpture antero-medially. Ovipositor straight, thin, comparatively long, without dorsal notch; ovipositor sheath narrow, pointed, with setae longer than sheath width and slightly curved backwards.

Body setose except eyes, pronotum, mesopleuron, metapleuron; setae on propodeum, basal tergites and posterior sides of coxae very few.

Blackish brown except mouthparts and malar space creamy, sternites creamy, fore and mid coxa and all trochanters and trochantelli largely yellow, antenna dull yellow ventrally, infuscate over entire dorsal side. Hind coxae fuscous in basal 2/3, hind femur brownish, except for basal third. Clypeus apically and sometimes dorsal ridge of upper

face between antennae narrowly yellowish, frontal orbits yellow to vertex. One paratype from Cheongdo-gun has a lighter face and hind legs.

Male. Unknown.

Biology. Hosts unknown.

Etymology. Named from the Greek *λευκο* (white) and *στομα* (mouth) after the creamy mouthparts.

Comparison. Compared with the other species that have antennal sockets on a shelf, the face is granulate, the inner orbits yellowish up to the level of the lateral ocelli, antenna comparatively short and thick, with 22 flagellomeres, malar space and mouthparts creamy, notauli well developed.

Material examined. ***Holotype:*** female; South Korea, **GG**: Pocheon-si, Soheur-eup, Jikdong-ri, 51-7, Korean National Arboretum, Saengtae tower, 37°44'56"N, 127°08'54.5"E, 17–30.V.2013, I.G. Kim leg. (DNUE).

Paratypes: South Korea, 1♀, **GB**: Daegu-si, Dong-gu, Palgongsan-ro, 237 gil (site 39), 35°59'19.55"N, 128°42'55.55"E, MT, 12.VI–14.VII.2014, J.W. Lee leg. (DNUE); **GB:** 1♀, Cheongdo-gun, Unmun-myeon, Mt. Unmun 35°38'32"N, 128°57'50"E, 2–16.VIII.2013, J.W. Lee leg. (DNUE).

Distribution. South Korea (GG, GB).

12. *Orthocentrus marginatus* Holmgren, 1858

Figs 6C, D

Biology. Hosts unknown.

Material examined. South Korea, **GB**: 1♀, Gunwi-gun, Bugye-myeon, Dongsan-ri, San 75 Odoam, 10.VII–1.VII.2015, J.W. Lee leg. (NIBR); **GN:** 1♀, Sancheong-gun, Sicheon-myeon, Seseoksanjang, 35°18'N, 127°41'E, 26.VII–12.X.2001, J.W. Lee leg. (DNUE); **GG**: 1♀, Yongin-si Suji-gu Gwanggyosan 6–24.IX.2008, J.O. Lim leg. (DNUE–0131); **GW**: 1♀, Pyeong-chang-gun Yong-pyeong-myeon Gyebangsan 28.VI–12.VIII.2012, J.Y. Park leg. (DNUE–0121); **JB**: 1♀, Muju-gun, Mupung-myeon, Hyeonnae-ri, San 3, Mt. Bakseoksan, 35°59'2.79"N, 127°52'30.74"E, 17.VI–2.VII.2015 J.W. Lee leg. (ZIN).

Distribution. Palaearctic; *South Korea (GB, GN, GG, GW, JB).

13. *Orthocentrus orientalis* Humala & Lee, sp. nov.

http://zoobank.org/2E90BC35-B098-401B-8C14-7A1BD2EF69A7

Fig. 10

Description. Female. Fore wing length 2.4–2.8 mm.

Face at level of antennal sockets 1.1 times as wide as high; face smooth and densely punctate, eyes not setose, dorsal ridge of face in between antennal sockets without a median prominence; face profile straight, slightly impressed dorsally, edge of clypeus

straight, antennal sockets on a shelf; inner orbits subparallel; subocular sulcus distinct, nearly straight; maxillary palp long, reaching beyond to fore coxa. In dorsal view, head posteriorly concave, temples short, lateral ocellus distant from eye by a distance 1.5 times longer than its maximum diameter, POL 1.6 times as long as diameter of lateral ocellus. Minimum distance between antennal sockets about 0.6 × of the socket diameter; antenna with 22–24 flagellomeres (n = 10) which gradually shorten towards apex; first flagellomere 2.3–2.5 times as long as wide and 0.6 times as long as scape; scape nearly parallel-sided.

Mesosoma smooth and polished except pronotum with short striations posteroventrally, propodeum with alutaceous-coriaceous microsculpture; mesoscutum with notauli anteriorly indicated; in profile, scutellum weakly convex, metapleuron slightly convex; propodeum with posterior transverse carina between lateral longitudinal carinae, lateromedian longitudinal carinae complete, lateral longitudinal carinae weak but present posteriorly, spiracle small.

Legs slightly flattened; coxae and femora polished, tibiae and tarsi coriaceous; hind femur 2.8 times as long as high, hind tibia 4.0 times as long as apically wide; tibiae with spine-like setae, spurs of hind tibia distinctly curved apically.

Wings not particularly narrow, fore wing with areolet closed, slightly transverse, narrowly sessile, vein 3rs-m weak; 2m-cu meeting areolet at apical 0.7, vein Rs gently bent towards wing apex; vein cu-a distad of Rs&M; nervellus angled below the middle.

Metasoma slender and considerably compressed from tergite 3 to apex. First tergite elongate, slightly widening posteriorly, 2.1 times as long as posteriorly wide; coriaceous-strigose, lateromedian longitudinal carinae weak and indistinct, with shallow transverse impressions originating at about middle of tergite, sloping posteriorly, not meeting centrally. Second tergite parallel-sided, 1.8 times as long as posteriorly wide; coriaceous and finely strigose, with shallow transverse impressions originating at about middle of tergite, sloping posteriorly, polished apically; small thyridia oval. Third tergite elongate, nearly 2.0 times as long as posteriorly wide, coriaceous medio-basally, polished in posterior half. Remaining tergites unsculptured. Ovipositor thin, slightly upcurved, without dorsal notch, pointed apically; ovipositor sheath narrow, parallel-sided, with dense setae longer than sheath width and curved backwards.

Body largely setose except eyes, pronotum, mesopleuron and metapleuron; setae scattered on anterior tergites and posterior sides of coxae.

Dark brown except face, clypeus, malar space, antennae, hind legs yellowish brown; mouthparts, tegula, propleuron, hind corners of pronotum, fore and mid legs yellowish; metasoma from tergite 4 brown; sternites creamy; sometimes lower inner orbits with blurred reddish-brown marks.

Male. Unknown.

Biology. Hosts unknown.

Etymology. This species is named from the Latin *orientalis* (eastern) after its geographical distribution, as the Korean Peninsula is situated in the Far East.

Comparison. Compared with the other species that have antennae on a shelf, it has a granulate face and no distinct yellow marks along the inner orbits, the first flagellomere

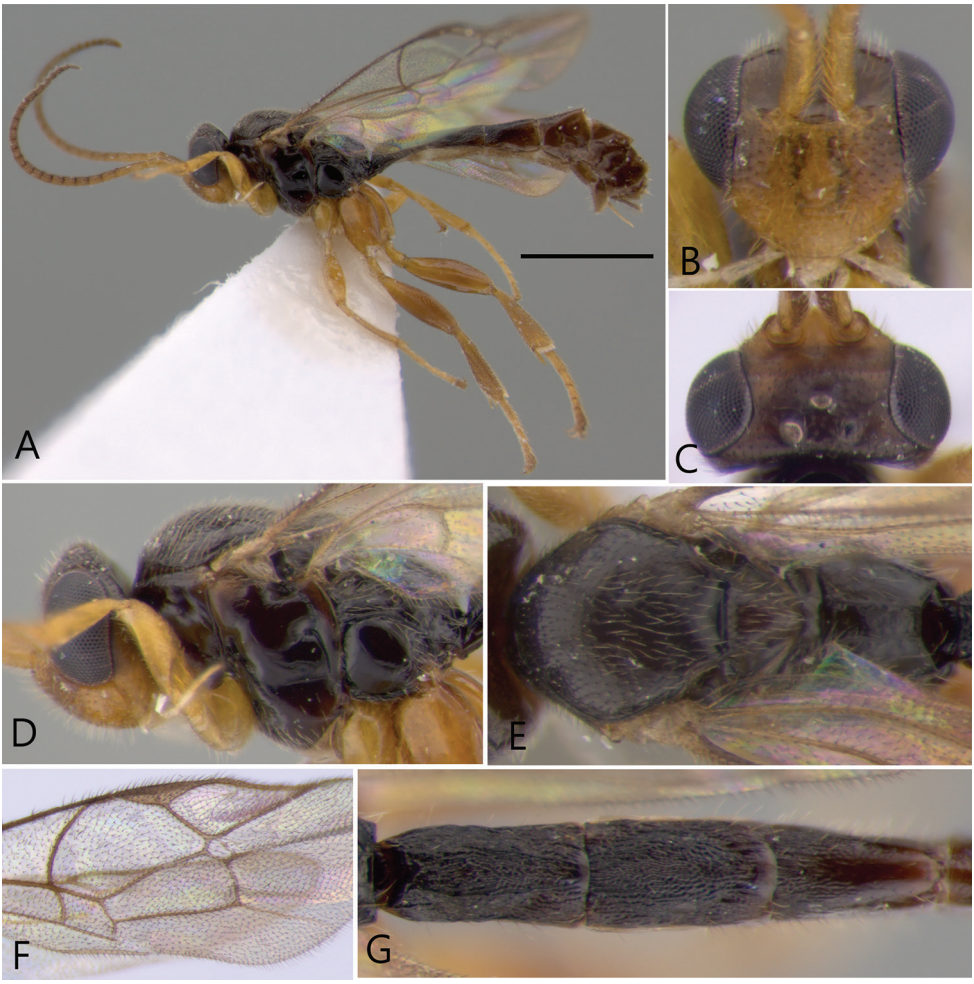

Figure 10. *Orthocentrus orientalis* sp. nov. Holotype. **A** Habitus in lateral view **B** head in frontal view **C** head in dorsal view **D** head and mesosoma in lateral view **E** mesosoma in dorsal view **F** areolet **G** first to third tergites in dorsal view.

2.3–2.5 times as long as wide, the areolet comparatively small, the first tergite 2.1 times as long as posteriorly wide, the second tergite 1.8 times as long as posteriorly wide. Additionally, the subocular sulcus is nearly straight, the POL 1.6 times as long as the diameter of a lateral ocellus, and the fore wing length is 2.4–2.8 mm (unlike in *O. parvus*).

Material examined. ***Holotype:*** female; South Korea **GG**: Mt. Yongmunsan Yeonsu, Yongmun, Yangpyeong, 320 m, MT III, 26.VI–16.VII.2009, J.O. Lim leg. (DNUE–0309).

Paratypes: South Korea, **GB:** 2♀, Mungyeong-si, Gaeun-eup, Wanjang-ri, Mt. Songnisan National Park, Beorimigijae, 36°40'59"N, 127°57'07"E, MT, 17.VII–12.VIII.2013, J.K. Choi leg. (DNUEU–0075, ZIN–0079); **GN**: 1♀, Dapcheon-ri, Ibanseong-myeon, Jinju-si, MT III, 27.VI–4.VII.2005, B.K. Ahn leg. (DNUE–0302); **GG**:

1♀, Mt. Yongmunsan Yeonsu, Yongmun, Yangpyeong, 324 m, MT III, 26.VI–16. VII.2009, J.O. Lim leg. (DNUE–0307); **GW**: 1♀, Chuncheon-si Dong-myeon Jinae-ri, 1–10.VII.2005, S.J. Jang leg., S.N.U. (DNUE–0387); 2♀, Wonju-si, Heungeop-myeon, Yeonse University, MT, 22.VII–11.VIII.2007, J.W. Lee leg. (DNUE–0152, 0035); **JB**: 2♀, Jeongeup-si, Naejang-dong Naejang-san, Geumseongyegok (14 site), MT, 29.VI-6.VII.2008, J.W. Lee leg. (DNUE–0313, 0315); **JN**: 1♀, Kwangju-si, Buk-gu, Geumgok-dong, Mudeungsan Nat. park Wonhyosa, MT, 26.VI–27.VII.2013, J.K. Choi leg. (DNUE–0141);

Distribution. South Korea (GB, GN, GG, GW, JB, JN).

14. *Orthocentrus pacificus* Humala & Lee, sp. nov.

http://zoobank.org/9B35FFE4-6D2E-400A-AB6D-BBFEC3AF82FC
Fig. 11

Description. Female. Body length 2.8–3.0 mm, fore wing length 2.2–2.5 mm.

Face at level of antennal sockets 1.1 times as wide as high; face densely punctate, eyes with short indistinct setae, inner orbits divergent ventrally, vertex somewhat prominent; dorsal ridge of face in between antennal sockets without a median prominence; face profile slightly convex, edge of clypeus convex, antennal sockets on a shelf; subocular sulcus distinct, strongly bent towards occiput; maxillary palp long, reaching beyond to fore coxa. In dorsal view, head posteriorly concave, occipital carina weak, widely interrupted dorsally; temples distinct, lateral ocellus distant from eye by a distance 1.7 times longer than its maximum diameter, POL 1.2 times as long as ocellar diameter of lateral ocellus. Minimum distance between antennal sockets about 0.4× of the diameter of socket; antenna with 24–25 flagellomeres (n=9) which do not gradually shorten towards apex; first flagellomere about 1.1 times as long as wide and about 1/3 of the scape length; scape nearly parallel-sided.

Mesosoma with microsculpture except pronotum with short striations posteroventrally, propodeum with coriaceous microsculpture; mesoscutum with notauli anteriorly indicated; in profile, scutellum weakly convex, metapleuron slightly convex; propodeum with posterior transverse carina and lateral longitudinal carinae complete, lateromedian longitudinal carinae weak, spiracle small.

Legs slightly flattened; coxae and femora polished, tibiae and tarsi coriaceous; hind femur 2.8 times as long as high, hind tibia 3.5 times as long as apically wide; tibiae with spine-like setae.

Wings not particularly narrow, fore wing with areolet closed, clearly transverse, narrowly sessile, 2m-cu meeting areolet at apical 0.7, vein Rs gently bent towards wing apex; vein cu-a distad of Rs&M; nervellus angled below the middle.

First tergite of metasoma elongate, slightly widening posteriorly, 1.6 times as long as posteriorly wide; coriaceous, lateromedian longitudinal carinae weak and indistinct, with shallow transverse impressions originating at about middle of tergite, sloping posteriorly, not meeting centrally. Second tergite nearly parallel-sided, 1.2 times as long

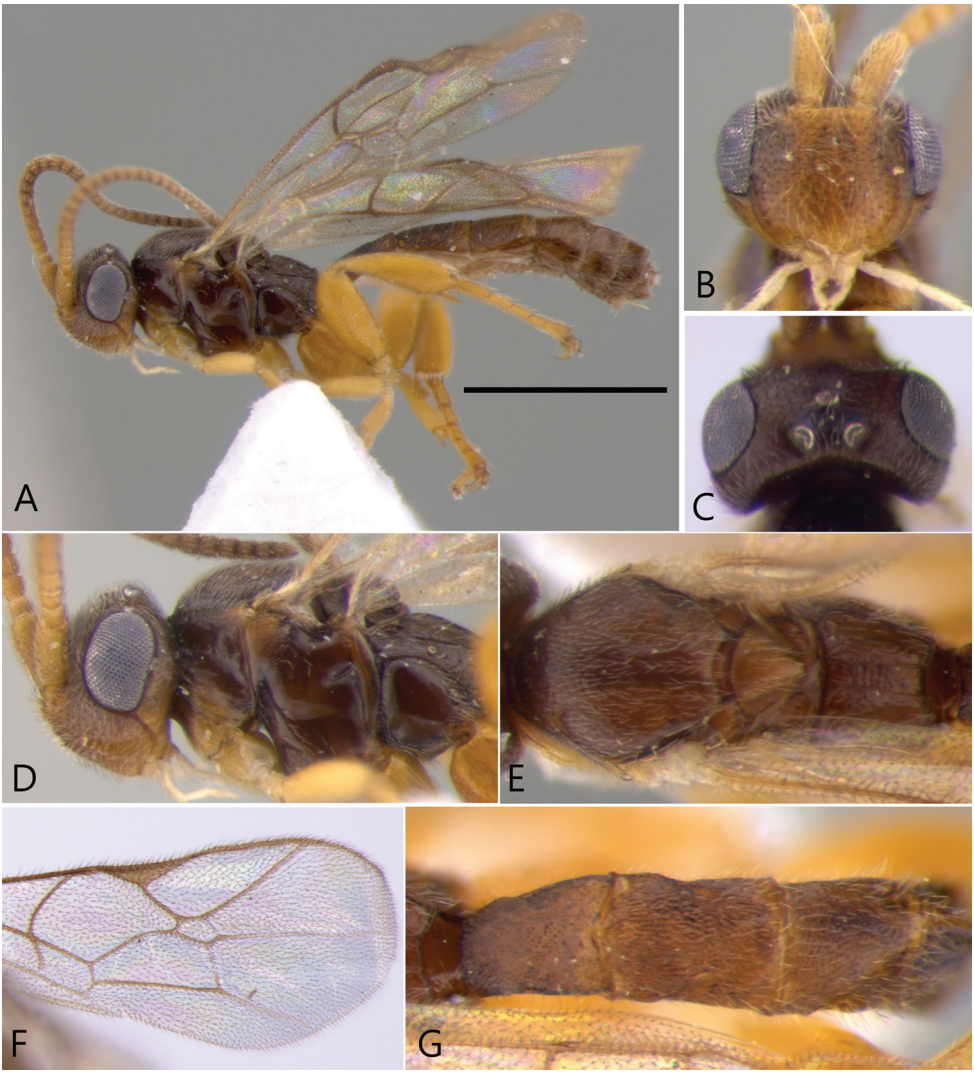

Figure 11. *Orthocentrus pacificus* sp. nov. Holotype. **A** Habitus in lateral view **B** head in frontal view **C** head in dorsal view **D** head and mesosoma in lateral view **E** mesosoma in dorsal view **F** areolet **G** first to third tergites in dorsal view.

as posteriorly wide; coriaceous, with transverse furrows originating at about middle of tergite, sloping posteriorly, meeting centrally; anterior thyridia small, oval, contrastingly coloured; second thyridia vaguely defined, medial, same colour as surrounding cuticle. Third tergite nearly as long as posteriorly wide, coriaceous medio-anteriorly, polished in apical part, with second thyridia round. Remaining tergites unsculptured. Ovipositor not visible; sheaths narrow, with dense setae curved backwards.

Body largely setose except pronotum, mesopleuron and metapleuron; setae scattered on anterior tergites and posterior sides of coxae.

Brown to light-brown except face, clypeus, malar space, lower temple, antenna yellow; mouthparts, tegula, propleuron creamy; all legs yellow; metasoma from tergite 4 light-brown; sternites creamy; sometimes pronotum, propleuron, mesopleuron, scutellum, hind margins of tergites 2–3 orange.

Male. Unknown.

Biology. Hosts unknown.

Etymology. This species name refers to its geographical distribution – relating to the Pacific Ocean and the region where Korea is situated.

Comparison. Similar to *O. fulvipes* Grav. in having an occipital carina, subocular sulcus strongly bent towards the occiput, all legs entirely red, but differs in its smaller size (fore wing 2.2–2.5 mm), the anterior tergites coriaceous without longitudinal striae; the first tergite 1.6 times as long as posteriorly wide, the second tergite 1.2 times as long as posteriorly wide.

Material examined. ***Holotype:*** female; South Korea, **GG:** Namyangju-si, Choanmyeon, Songcho-ri, Mt. Ungilsan, MT (II), Alt. 134 m, 37°34'43.3"N, 127°18'37.5"E, 27.V–10.VI.2009, J.O. Lim leg. (DNUE–0165).

Paratypes: South Korea, **CN:** 1♀, Daejeon-si, Dong-gu, Daejeon University, MT, 8.X–30XI.2007, J.W. Lee leg. (ZIN–0129); 1♀, Daejeon-si, Dong-gu, Daehang-no 62, Daejeon University, MT, 15.VIII–30.IX.2006, J.W. Lee leg. (DNUE–0261); **GB:** 1♀, Gyeongsan-si, Dae-dong, Yeungnam University, MT, 21.IV–19.V.2004, J.W. Lee leg. (DNUE–0126); 1♀, Chilgok-gun, Dongmyeong-myeon, Hakmyeong-ri, San 25, site 23, MT, 36°01'53.45"N, 128°33'46.93"E, 30.VIII–22.IX.2014, J.W. Lee leg. (DNUE); **GN:** 1♀, Hapcheon-gun, Gaya-myeon, Hwangsan-ri, San 124-3, 10.VII–14.VIII.2014, J.W. Lee (DNUE); **GG:** 1♀, Mt. Ungilsan, Songchon, Choan, Namyangiu, 134 m, 37°34'43.3"N, 127°18'37.5"E, MT II, 27.V–10.VI.2009, Jongok Lim leg. (ZIN–0171); 2♀, Anyang-si, Manan-gu, Mt. Gwanaksan, 5–19.VII.2007, J.O. Lim leg. (DNUE–0304, 0305); **GW:** 1♀, Donghae-si, Samhwa-dong, Mureung valley, MT, 1–28.VII.2007, J.W. Lee leg. (DNUE–0298);

Distribution. South Korea (CN, GB, GG, GN).

15. *Orthocentrus parvus* Humala & Lee, sp. nov.

http://zoobank.org/233D2588-17AC-4C8B-A8EB-7CFBE0613CB0
Fig. 12

Description. Fore wing length 1.7 mm.

Face at level of antennal sockets 1.2 times as wide as high; face punctate, eyes not setose, dorsal ridge of face inbetween antennal sockets without a median prominence; face in profile almost evenly round, slightly more so dorsally, edge of clypeus slightly impressed, antennal sockets on a shelf but shelf not particularly high; subocular sulcus distinct, bent towards occiput; maxillary palp reaching to fore coxa. In dorsal view, head posteriorly slightly concave, temples narrow, lateral ocellus separated from eye by a distance 1.2 times longer than its maximum diameter, POL 1.1 times as long as diameter of lateral ocel-

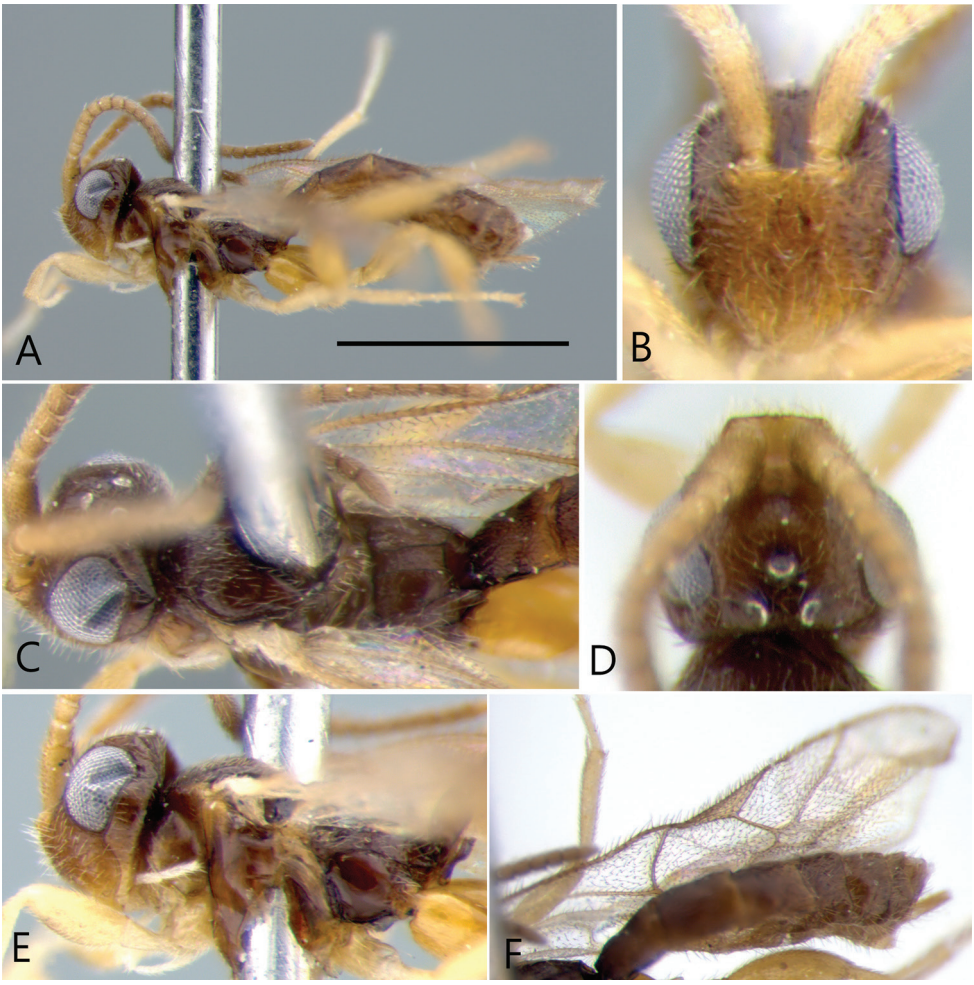

Figure 12. *Orthocentrus parvus* sp. nov. Holotype. **A** Habitus in lateral view **B** head in frontal view **C** head and mesosoma in dorsal view **D** head in dorsal view **E** head and mesosoma in lateral view **F** fore wing.

lus, lacking ocellar-ocular groove. Occipital carina reduced. Minimum distance between antennal sockets slightly more than half diameter of socket; antenna with 23 short flagellomeres which do not gradually shorten towards apex; basal flagellomere subquadrate and about 1/3 of length of scape; scape almost parallel-sided, internal surface slightly convex.

Mesosoma smooth and polished except dorsal propodeum with pustulate microsculpture; mesoscutum with anteriorly indicated notauli; scutellum destroyed by pin, metapleuron slightly convex; propodeum with posterior transverse carina strong, present between lateral longitudinal carinae, lateromedian longitudinal carinae complete, spiracle small.

Legs broad, coxae and femora polished, tibiae and tarsi coriaceous-granulate; hind femur 2.9 times as long as high, hind tibia 4.0 times as long as apically wide; tibiae with spine-like setae.

Wings not particularly narrow; fore wing with areolet closed but 3rs-m weak, areolet nearly as wide as high, 2m-cu meeting areolet at apical 0.7, vein Rs straight; nervellus not intercepted, straight.

First tergite stout, posteriorly slightly widening, 1.4 times as long as posteriorly wide; coriaceous, without lateromedian longitudinal carinae, with transverse impressions originating at about middle of tergite, sloping posteriorly, not meeting centrally. Second tergite 1.2 times as long as posteriorly wide; coriaceous, with faint transverse impressions originating at about middle of tergite, slightly sloping posteriorly, not meeting centrally; thyridia contrastingly coloured. Remaining tergites smooth and polished. Ovipositor straight; ovipositor sheath with dense and long, curved backwards-directed setae.

Body largely setose except pronotum, mesopleuron and metapleuron; setae scattered on propodeum and posterior sides of coxae

Brown except mouthparts, fore and mid coxae, trochanters and trochantelli, creamy to light yellow, sternites creamy, legs, antennae yellow.

Male. Unknown.

Biology. Hosts unknown.

Etymology. Named from the Latin *parvus* (small, inconspicuous) after its small size.

Comparison. Compared with the other species that have antennae on a distinct shelf and face finely punctate, the size is smaller (fore wing 1.7 mm), eyes without short setae, the POL shorter, the temples narrower, occipital carina not developed, unlike in *O. pacificus*. Additionally, compared with other small species, *O. parvus* has narrow temples, the subocular sulcus is bent and the first flagellomere subquadrate (unlike in *O. orientalis*).

Material examined. ***Holotype:*** female; South Korea, **GG**: Mt. Gwanggyo, Sujigu, Yongin-si, 214 m, 37°19'56.8"N, 127°02'37.8"E, 15–25.VII.2008, J.W. Lee leg. (DNUE–0562).

Distribution. South Korea (GG).

16. *Orthocentrus patulus* Holmgren, 1858

Figs 6E, F

Biology. Hosts unknown.

Material examined. South Korea, **CB**: 1♀, Danyang-gun, Danyang-eup, Cheongdong-ri, Chonndong valley, 19–30.IV.2007, J.W. Lee leg. (DNUE– 0038).

Distribution. Palaearctic; *South Korea (CB).

17. *Orthocentrus protervus* Holmgren, 1858

Figs 14A, B

Biology. Parasitoid of *Sciophila hirta* Meigen (Diptera, Mycetophilidae).

Material examined. South Korea, **GG**: 1♀, Pocheon-si, Soheur-eup, Jikdong-ri, 51-7, Korean National Arboretum, Saengtae tower, 37°44'56"N, 127°08'54.5"E, 20–29.VIII.2013, I.G. Kim leg. (DNUE); **GW**: 1♀, Mt. Taebaeksan, Yuilsa, MT, 20.VI–11.VII.1999, D.S. Ku leg. (NIAS).

Distribution. Palaearctic; *South Korea (GG, GW).

18. *Orthocentrus pulchellus* Humala & Lee, sp. nov.

http://zoobank.org/1AF75673-BF1E-450E-9E7E-A5D7602A0318
Fig. 13

Description. Female. Fore wing length 3.1 mm.

Face at level of antennal sockets 1.4 times as wide as high; face smooth, polished, sparsely punctate, eyes not setose, dorsal ridge of face in between antennal sockets with a median blunt low prominence; face profile straight except dorsally very slightly impressed, inner orbits slightly divergent ventrally; edge of clypeus straight, antennal sockets not on a distinct high shelf; subocular sulcus narrow, nearly straight; maxillary palp reaching beyond fore coxa. In dorsal view, head posteriorly concave, temples very short, lateral ocellus separated from eye by a distance of 1.8 times longer than its maximum diameter, POL 1.5 times as long as diameter of lateral ocellus; ocellar-ocular grooves present. Minimum distance between antennal sockets about half of the diameter of socket; antenna moderately long, with 30–31 flagellomeres elongate (n = 4); flagellum considerably thinned apically; first flagellomere about 3.5 times as long as wide and about 0.8 times as long as scape; scape slightly convex on inner surface, slightly concave on outer surface.

Mesosoma smooth and polished; mesoscutum anteriorly with distinct notauli; in profile, scutellum high, metapleuron slightly convex; propodeum with posterior transverse carina complete, strong and raised between lateral longitudinal carinae, lateromedian longitudinal carinae complete, lateral longitudinal carinae distinct, spiracle small.

Legs robust; coxae polished, femora with coriaceous microsculpture, tibiae and tarsi coriaceous-granulate; hind femur 2.9 times as long as high, hind tibia 3.7 times as long as apically wide; tibiae with spine-like setae.

Wings not particularly narrow; fore wing without areolet, vein 2rs-m about 0.6 times as long as portion of 1m-cu between 2rs-m and 2m-cu; pterostigma comparatively wide, vein Rs bent upwards, fore wing with vein Rs+2r meeting apical 0.6 of pterostigma; vein cu-a strongly oblique, distad of Rs&M; nervellus intercepted below.

First tergite 1.8 times as long as posteriorly wide; coriaceous, with two lateromedian longitudinal carinae and longitudinal striae, with transverse impressions originating at about middle of tergite, sloping posteriorly, meeting centrally.

Second tergite 1.6 times as long as posteriorly wide; coriaceous and longitudinally striate, with developed lateromedian longitudinal carinae, anterior corners impressed and transverse groove near posterior margin bending anteriorly near lateral margins, forming a somewhat uplifted area medially; oval thyridia contrastingly coloured.

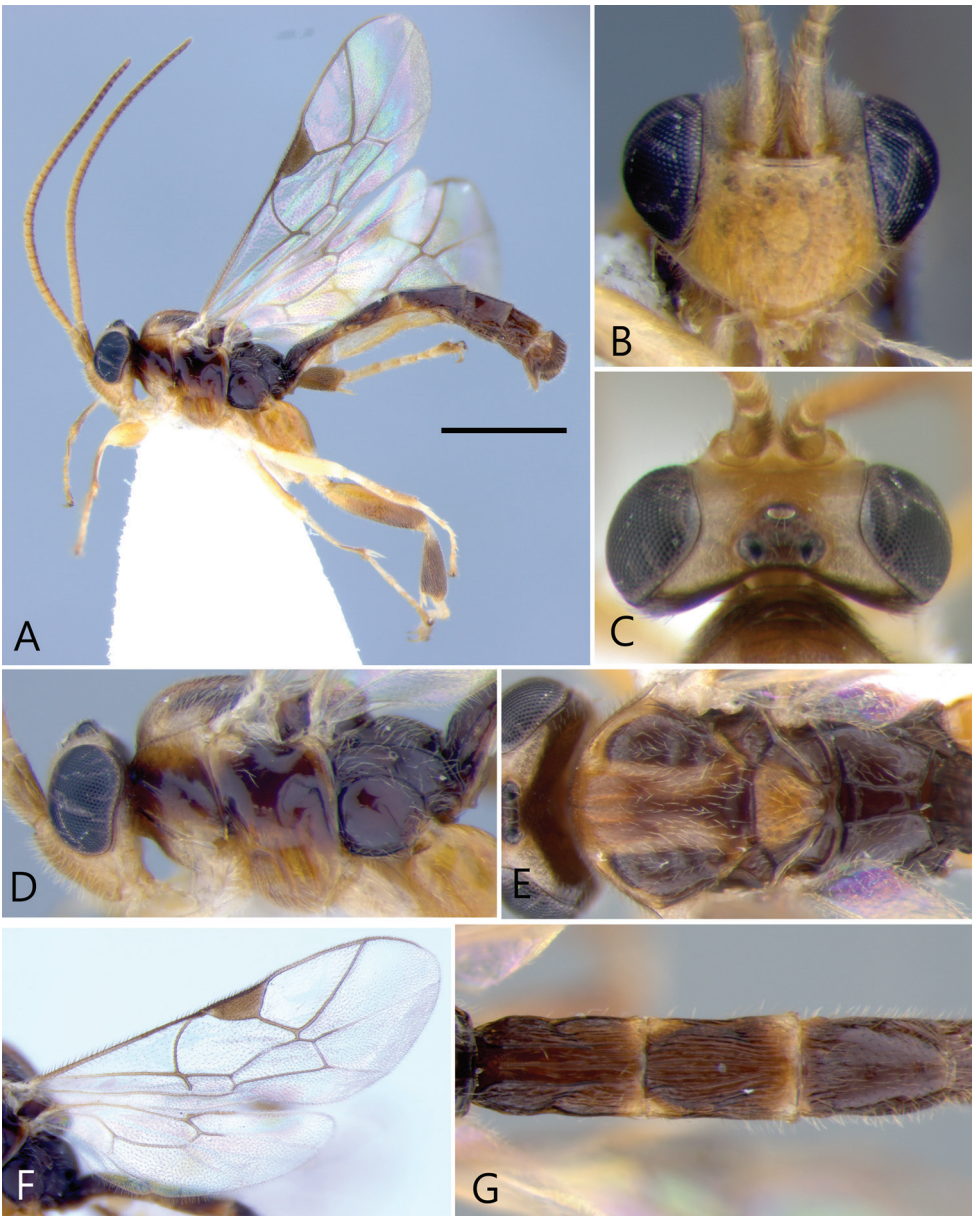

Figure 13. *Orthocentrus pulchellus* sp. nov. Holotype. **A** Habitus in lateral view **B** head in frontal view **C** head in dorsal view **D** head and mesosoma in lateral view **E** mesosoma in dorsal view **F** wings **G** first to third tergites in dorsal view.

Third tergite longitudinally striate anteriorly, remainder of metasoma unsculptured, polished. Ovipositor thin, comparatively short, weakly upcurved, without subapical dorsal notch; sheaths short, concealed by hypopygium.

Body setose except eyes, pronotum, mesopleuron and metapleuron, setae scattered on metasoma and posterior sides of coxae.

Brown; face, frons and vertex yellowish, inner orbits broadly creamy-yellow up to occiput, interocellar area fuscous; antenna yellowish-brown; malar area yellow posterior to subocular sulcus and up to level of half of eye; mouthparts, fore and mid legs, hind coxa, trochanters and tarsi and longitudinal bars along notauli yellow; propleuron, lower and upper pronotum, medial part of mesoscutum anteriorly, scutellum, mesopleuron in lower half, hind coxa and trochanters and tarsi reddish brown; posterior margin of tergite 1and anterior corners and posterior margin of tergite 2 yellowish-brown; sometimes hind femur except basal 0.2 and hind tibia except light basal ring brown.

Male. Unknown.

Biology. Hosts unknown.

Etymology. Named from the Latin *pulchellus* (nice, pretty) after its rich body colouration.

Comparison. This is a distinctive species on account of the entirely yellow face and frons (except for the interocellar area), the absence of the fore wing areolet and the presence of yellow bars along the notauli on the median part of the mesoscutum.

Material examined. ***Holotype:*** female; South Korea, **GB**: Namsa-ri, Hyeongok-myeon, Kyeongju-si, MT II, 15–29.IX.2005, J.T. Mun leg. (DNUE).

Paratypes: South Korea, **CN**: 1♀, Daejeon, Donggu, Daehang-no 65, Daejeon University, MT, 15.VIII–30.IX.2006, J.W. Lee leg. (DNUE–0260); **GG**: 2♀, Seoul, Cheongyangri-dong, Dongdaemun-gu, MT III, S.N.U. 12–20.IX.2005, W.I. Choi leg. (DNUE–0908,0910).

Distribution. South Korea (CN, GB, GG).

19. *Orthocentrus sannio* Holmgren, 1858
Figs 14C, D

Biology. Hosts unknown.

Material examined. South Korea, **GW**: 1♀, Mt. Sundalsan, Yongmok, 28.V.1998 (NIAS); 1♂, Mt. Jirisan National Park, Bamsagol, 23.VII.1989, J.G. Kim leg. (DNUE–0475); **GB**: 1♂, Namsa-ri, Hyeongok-myeon, Kyeongju-si, MT II, 15–29. IX.2005, J.T. Mun leg. (DNUE); 1♂, Yeongcheong-si, Cheongtong-myeon Temp., Eunhaesa, 36°02'11.74"N, 128°34'18.17"E, MT, 21.VII–10.VIII.2015, J.W. Lee leg. (DNUE); **GW**: 2♀, Inje-gun Girin-myeon Jindong-ri Jeombongsan, 37°34'43.2"N, 127°18'40.1"E, 26.VI–28.VII.2012, J.Y. Park leg. (DNUE–0534, 0535).

Distribution. Palaearctic; *South Korea (GB, GW).

20. *Orthocentrus setosus* Humala & Lee, sp. nov.
http://zoobank.org/57490ee5-a30d-4e84-830b-8cf3e52412bd
Fig. 15

Description. Fore wing length 2.0–2.1 mm.

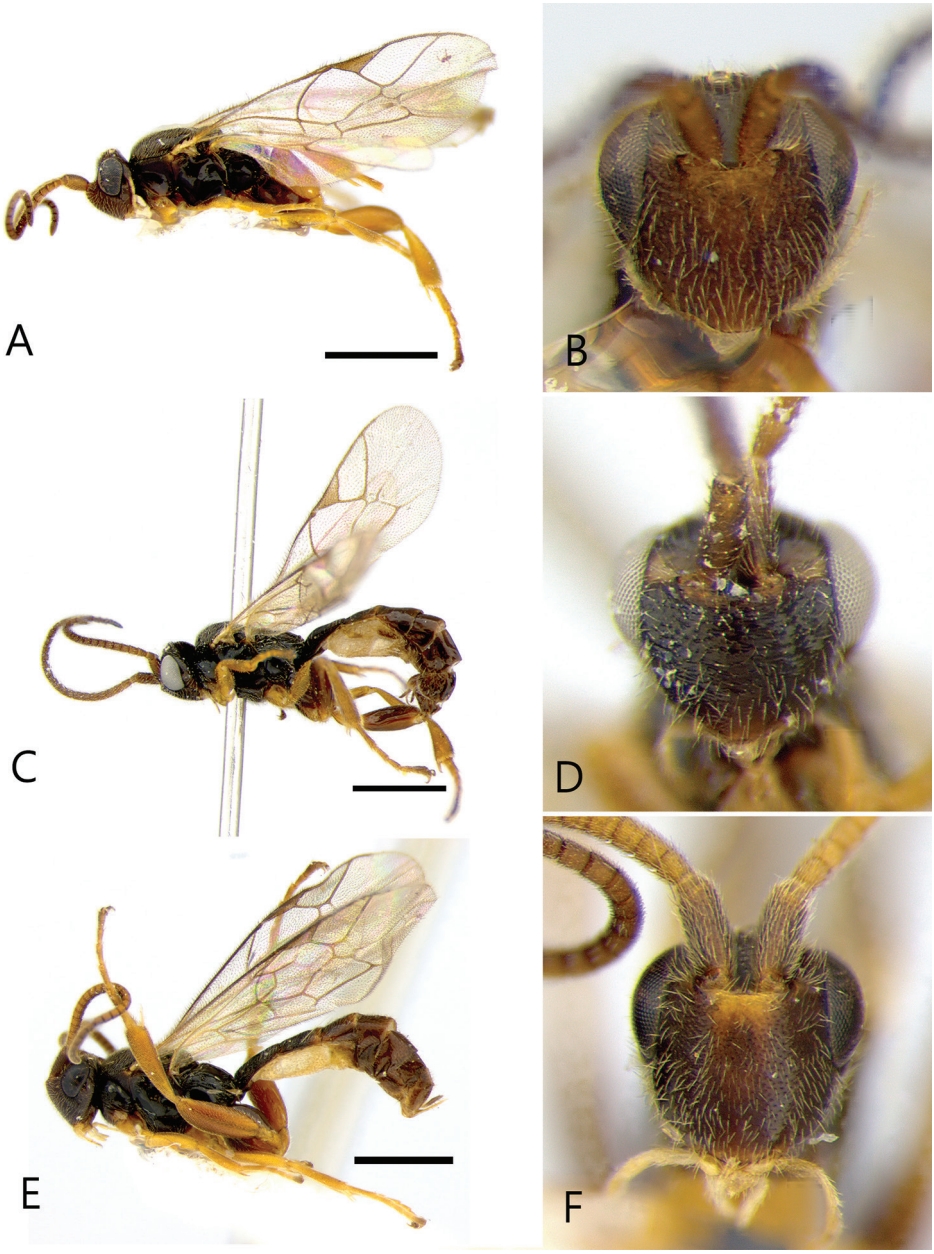

Figure 14. *Orthocentrus* spp. **A** Habitus in lateral view of *O. protervus* **B** head in frontal view of *O. protervus* **C** habitus in lateral view of *O. sannio* **D** head in frontal view of *O. sannio* **E** habitus in lateral view of *O. spurius* **F** head in frontal view of *O. spurius*.

Face at level of antennal sockets 1.2 times as wide as high; face coarsely papillate, eyes densely setose, dorsal ridge of face in between antennal sockets without a median prominence; face in profile almost evenly round, edge of clypeus very slightly im-

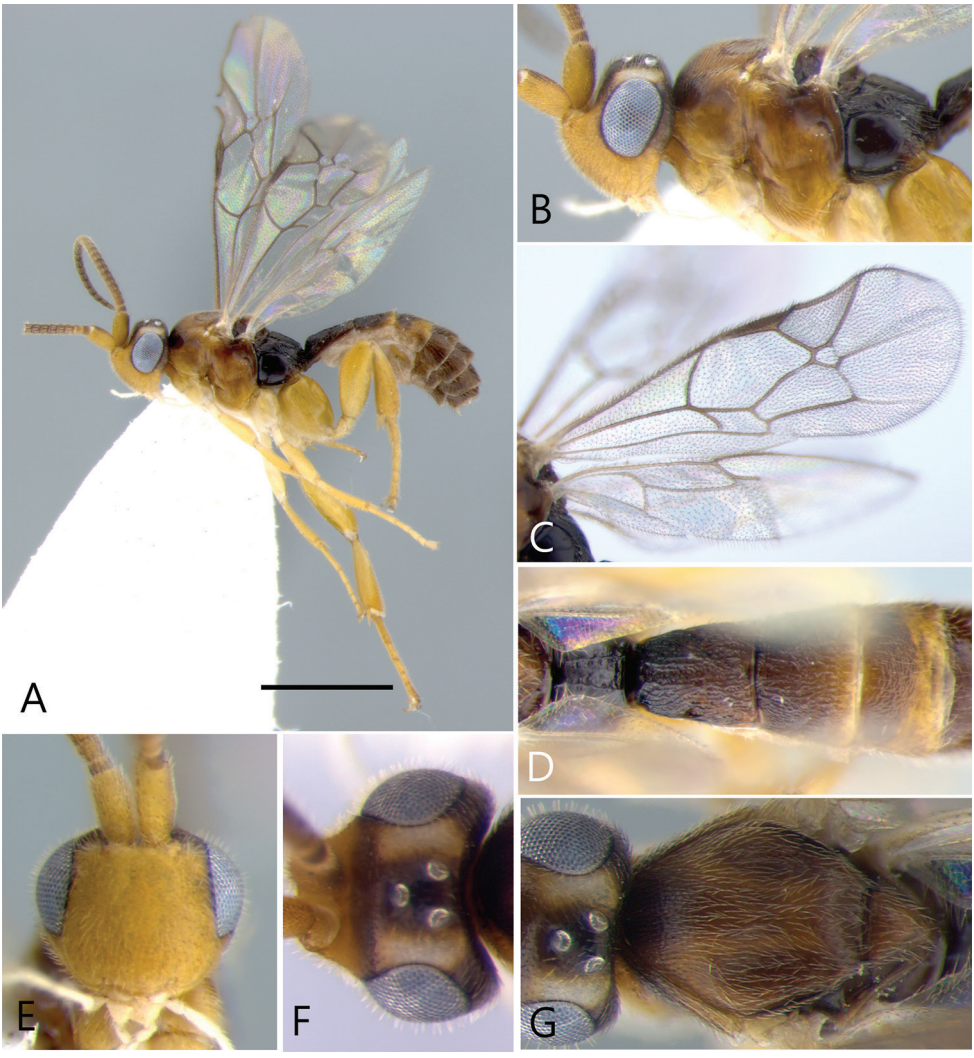

Figure 15. *Orthocentrus setosus* sp. nov. Holotype. **A** Habitus in lateral view **B** head and mesosoma in lateral view **C** wings **D** propodeum and first to third tergites in dorsal view **E** head in frontal view **F** head in dorsal view **G** mesoscutum in dorsal view.

pressed, antennal sockets on a shelf; subocular sulcus weak and shallow, slightly bent towards occiput; maxillary palp reaching to beyond fore coxa. In dorsal view, head posteriorly slightly concave, temples narrow, lateral ocellus separated from eye by a distance of 2 times longer than its maximum diameter, POL 1.1 times as long as diameter of lateral ocellus, lacking ocellar-ocular grooves. Minimum distance between antennal sockets slightly less than half diameter of socket; antenna comparatively short, with 26 short flagellomeres which do not gradually shorten towards apex; first flagellomere 0.8 times as long as wide and about as long as 1/3 of scape; scape almost parallel-sided.

Mesosoma smooth and polished except dorsal propodeum coriaceous with punctures; mesoscutum lacking notauli; in profile, scutellum weakly convex, metapleuron slightly convex; propodeum with posterior transverse carina strong, present between lateral longitudinal carinae, lateromedian longitudinal carinae complete, and lateral longitudinal carinae present as short stubs not reaching spiracles, spiracle small.

Legs broad, hind coxa large; coxae and femora polished, tibiae and tarsi coriaceous-granulate; hind femur 2.6 times as long as high, hind tibia 3.3 times as long as apically wide; tibiae with spine-like setae.

Wings not particularly narrow; fore wing with areolet closed but 3rs-m weak, areolet slightly wider than high, 2m-cu meeting areolet at apical 0.6, vein Rs straight, pterostigma narrow, vein Rs+2r meeting pterostigma at apical 0.6; vein cu-a well distad of Rs&M; nervellus slightly intercepted in lower third, almost straight.

First tergite stout, apically widening, 1.5 times as long as posteriorly wide; coriaceous, without lateromedian longitudinal carinae, with transverse impressions originating at about middle of tergite, sloping posteriorly, not meeting centrally. Second tergite 0.7 times as long as posteriorly wide; coriaceous to rugose, with transverse impressions originating at about middle of tergite, slightly sloping posteriorly, meeting centrally; small transverse thyridia contrastingly coloured. Third tergite coriaceous with transverse furrow, posteriorly polished; remaining tergites smooth and polished. Ovipositor short, straight, without dorsal notch; ovipositor sheath invisible.

Body largely setose except pronotum, mesopleuron and metapleuron; setae scattered on propodeum and posterior sides of coxae.

Brown, except mouthparts, orbital marks between eyes and ocelli, fore and mid coxae, trochanters and trochantelli, creamy to light yellow, sternites creamy to brownish creamy, face, clypeus, malar space, scape, propleuron, pronotum, anterior part and lateral patches on mesoscutum, scutellum, mesopleuron, legs, posterior margins of second and third tergites yellow to dull orange.

Male. Unknown.

Biology. Hosts unknown.

Etymology. Named from the Latin *setosus* (setose) after the largely setose body, including eyes.

Comparison. Compared with the other species that have densely setose eyes, the antennae are comparatively short, with 26 flagellomeres, unlike in *O. hirsutor* and *O. trichophthalmus.* From the allied *O. trichoptilus* it differs in the yellowish face, mesoscutum, propleuron and mesopleuron, the creamy vertex marks and the subocular sulcus hardly visible.

Material examined. ***Holotype:*** female; South Korea, **JB**: Muju-gun, Mupung-myeon, Hyeonnae-ri, San 3, Mt. Bakseoksan, 35°59'2.79"N, 127°52'30.74"E, 5–18. VIII.2015, J.W. Lee leg. (DNUE).

Paratype: South Korea, **GB**: 1♀, Gyeongsan-si Dae-dong, Yeungnam University, 4–23.IX.2008, J.W. Lee leg. (DNUE– 0140).

Distribution. South Korea (GB, JB).

21. *Orthocentrus spurius* Gravenhorst, 1829
Figs 14E, F

= *protuberans* Holmgren 1858

Biology. Hosts unknown.

Material examined. South Korea, **GW:** 1♀, Mt. Taebaeksan, MT, 14.V–20.VI.1999, D.S. Ku leg. (NIAS).

Distribution. Holarctic; *South Korea (GW).

22. *Orthocentrus stigmaticus* Holmgren, 1858 (stat. rev.)
Figs 19A, B

Biology. Hosts unknown.

Material examined. South Korea, **CN**: 1♀, Daejeon, Donggu, Daejeon University, MT, 12.IV–12.V.2007, J.W. Lee leg. (DNUE–0117); 1♂, Seosan-si Haemi-myeon Hanseo University, MT, 4–29.VI.2006, J.W. Lee leg. (DNUE–0369); 1♀, Buyeo-gun Gyuam-myeon Sumok-ri. 35°15'N, 126°50'E, MT, 13.VII–16.VIII.2005, J.W. Lee leg. (DNUE–0265); 1♂, Buyeo-gun Gyuam-myeon Sumokri, MT, 16–2.VI.2005, J.W. Lee leg. (DNUE–0263); **GB**: 1♀, Namsa-ri, Hyeongok-myeon, Kyeongju-si, MT II, 11–18.VIII.2005, J.T. Mun leg. (DNUE–0308); 1♂, Gyeongsan-si, Dae-dong, Yeungnam University, 18.V.1989, J.K. Kim leg. (DNUE–0457); 1♂, Gyeongsan-si Daehak-ro280 Yeungnam University, 35°49'30"N, 128°45'39"E, 13.VI.2013, J.W. Lee leg., (DNUE–0437); 1♀, Mungyeong-si, Mungyeong-eup, Sangcho-ri, Mungyeongsaejae, 10.VI.1992 (DNUE); 1♂, Namsa-ri, Hyeongok-myeon, Kyeongju-si, MT II, 15–29.IX.2005, J.T. Mun leg. (DNUE); 1♀, Namsa-ri, Hyeongok-myeon, Kyeongju-si, MT I, 18–25.VIII.2005, J.T. Mun leg. (NIBR–0276); **GG**: 1♀, Mt. Yongmunsan Yeonsu, Yongmun, Yangpyeong, 324 m, MT III, 26.VI–16.VII.2009, J.O. Lim leg. (DNUE–0301); **GG:** 1♂, [Arb.] Kwanga, Manan-gu, Anyang-si, 37°2'21.6"N, 126°56'56.8"E, 133 m, MT III. 26.VII–8.VIII.2008, S.N.U. Jongok Lim leg. (DNUE–0235); 1♂, Pocheon-si, Soheur-eup, Jikdong-ri, 51–7, Korean National Arboretum, Saengtae tower, 37°45'9.1"N, 127°09'4.7"E, 28.VI–24.VII.2013, I.G. Kim leg. (DNUE); **GN**: 1♂, Dapcheon-ri Ibanseong-myeon Jinju-si, MT III, 27.VI–4.VII.2005 S.N.U. B.K. Ahn leg. (DNUE–0300); **GW:** 1♀, Donghae-si, Samhwa-dong, Mureung valley, 8–16.X.2005, J.W. Lee leg. (DNUE–0555); 1♂, Chuncheon-si Dong-myeon Jinae-ri, 1–8.VIII.2005, S.J. Jang leg., S.N.U. (DNUE–0123); 1♀3♂, Chuncheon-si, Sanong-dong, Gwangwon Provincial Arboretum, 30.VIII–17.IX.2013, I.G. Kim leg. (DNUE); 1♀, same data as for preceding, 30.IV–15.V.2013, I.G. Kim leg. (DNUE); 1♂, Taebaek-si, Hyeol-dong, Yuilsa, 37°06'41.79"N, 128°55'26.46"E, 30.VI.1991, J.W. Lee leg. (DNUE); 1♀, Hongcheon-gun, Bukbang-myeon, Gwangwon Prov., Environment Research Park, 37°45'15.6"N, 127°51'1.7"E, 3–15.X.2013, S.J. Jang leg.

(DNUE); **JB:** 1♀, Wanju-gun, Dongsang-myeon, Daea-ri, San 1, Daea Arboretum, 35°58'24.24"N, 127°18'13.53"E, 1–15.IX.2013, J.M. Park leg. (DNUE); 2♀, same data as for preceding, 16–31.VII.2013 (DNUE); 1♀, Muju-gun, Mupung-myeon, Hyeonnae-ri, San, Mt. Bakseoksan, MT, 37°59'2.79"N, 127°52'30.74"E, 5–16. VI.2015, J.W. Lee leg. (DNUE).

Distribution. Palaearctic; *South Korea (CN, GB, GG, GN, GW, JB).

Remarks. The name *O. stigmaticus* is removed from synonymy with *O. winnertzii* and its status of valid species is resurrected, as both these species occur in the same areas and have distinct morphological differences, what do not meet the criteria for the subspecies definition.

23. *Orthocentrus tenuiventris* Humala & Lee, sp. nov.

http://zoobank.org/B8524C51-FB9F-47EC-8143-2293E5F5688D
Fig. 16

Description. Female. Fore wing length 3.0–3.5 mm.

Face at level of antennal sockets 1.1 times as wide as high; face smooth and densely punctate, eyes not setose, dorsal ridge of face in between antennal sockets without a median prominence; face profile straight, slightly impressed dorsally, edge of clypeus straight, antennal sockets on a shelf; subocular sulcus distinct, bent towards occiput; maxillary palp long, reaching beyond to fore coxa. In dorsal view, head posteriorly slightly concave, temples distinct, lateral ocellus distant from eye by its maximum diameter, POL as long as diameter of lateral ocellus. Minimum distance between antennal sockets about 0.6× of the diameter of socket; antenna with 31–36 flagellomeres (n=10) which gradually shortening towards apex; first flagellomere 2.3–2.5 times as long as wide and about 1/2 of the scape length; scape nearly parallel-sided.

Mesosoma smooth and polished except pronotum with short striations posteroventrally, propodeum coriaceous with punctures; mesoscutum with distinct notauli; in profile, scutellum somewhat high, metapleuron not convex; propodeum without posterior transverse carina between lateral longitudinal carinae, lateromedian longitudinal carinae weak but complete, lateral longitudinal carinae weak, present posteriorly, spiracle small.

Legs slightly flattened; coxae and femora polished, tibiae and tarsi coriaceous; hind femur 3.4 times as long as high, hind tibia 3.8 times as long as apically wide; tibiae with spine-like setae, spurs of hind tibia distinctly curved apically.

Wings somewhat narrow, cells thus comparatively long and narrow; fore wing with areolet closed, large, conspicuously transverse, 2m-cu meeting areolet at apical 0.7, vein Rs gently bent towards wing apex; vein cu-a clearly distad of Rs&M; nervellus angled in the middle.

First tergite elongate, slightly widening posteriorly, 2.5–3.1 times as long as posteriorly wide; coriaceous-strigose, with weak lateromedian longitudinal carinae, with shallow transverse impressions originating at about middle of tergite, sloping poste-

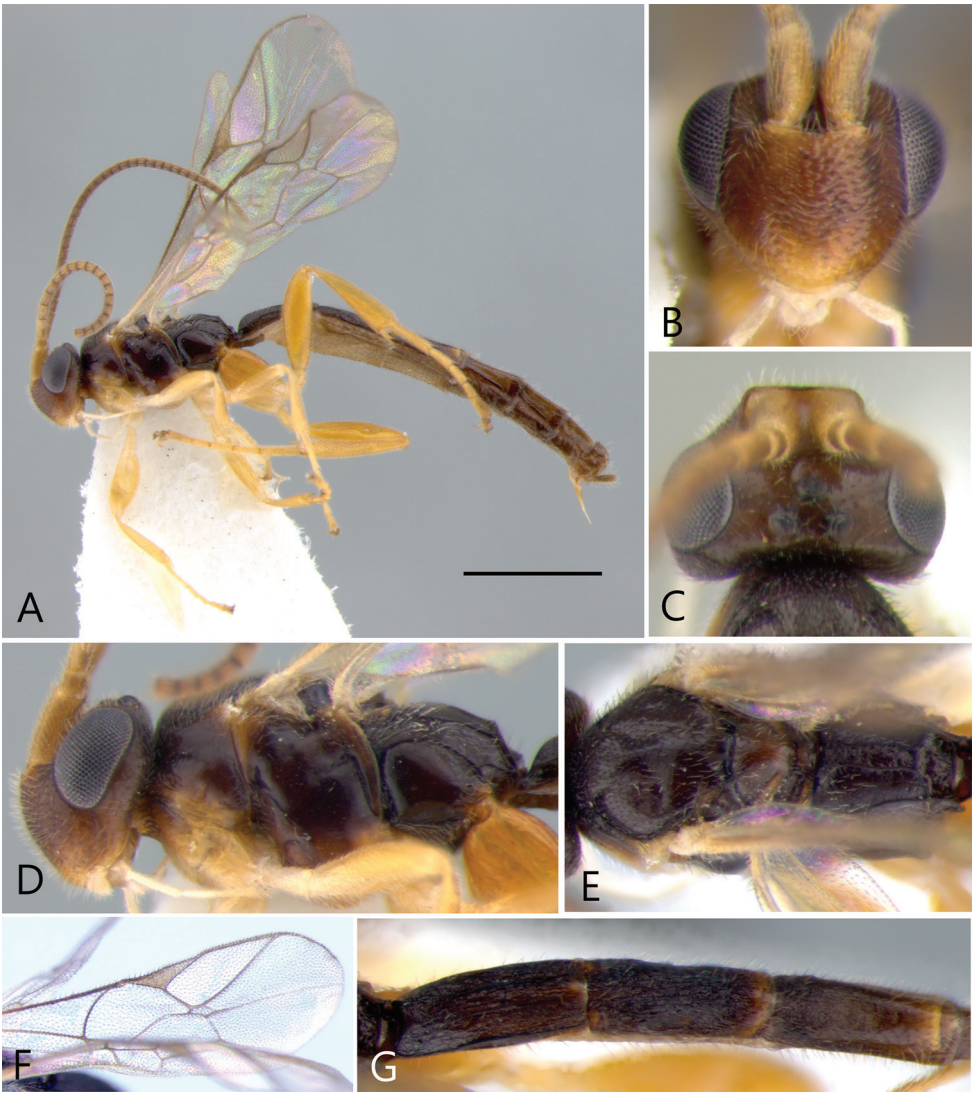

Figure 16. *Orthocentrus tenuiventris* sp. nov. Holotype. **A** Habitus in lateral view **B** head in frontal view **C** head in dorsal view **D** head and mesosoma in lateral view **E** mesosoma in dorsal view **F** fore wing **G** first to third tergites in dorsal view.

riorly, not meeting centrally. Second tergite parallel-sided, 2.0–2.9 times as long as posteriorly wide; coriaceous, longitudinally striate, with shallow transverse impressions originating at about middle of tergite, sloping posteriorly, polished apically; small thyridia oval. Third tergite elongate, 2.0–2.9 times as long as posteriorly wide, coriaceous, longitudinally striate, polished posteriorly. Remaining tergites unsculptured. Ovipositor thick basally, strongly narrowed and pointed apically, straight, without notch; ovipositor sheath parallel-sided, with dense setae longer than sheath width and strongly curved, backwards pointing.

Body largely setose except eyes, pronotum, mesopleuron and metapleuron; setae conspicuous on tergites and sternites from metasomal segment 3, and very scattered on anterior tergites and posterior sides of coxae.

Dark brown except propleuron, hind corners of pronotum, lower mesopleuron yellowish; antenna, legs, clypeus dull yellow; mouthparts, tegula, and sternites creamy.

Male. Similar to female but laterally paler, creamy white, and antenna pale yellow, creamy white basally; antenna with 29 flagellomeres (n = 2). Otherwise as in female.

Biology. Hosts unknown.

Etymology. Named from the Latin *tenuis* (thin, slender) and *venter* (abdomen) after its long and narrow metasoma.

Comparison. This is a distinctive species on account of the unusually long and slender metasoma (Fig. 16A), the anterior tergites of which are strongly elongate and longitudinally striate (Fig. 16G); the wings are narrow, antenna with 31–36 flagellomeres, basal flagellomere 2.3–2.5 times as long as wide.

Material examined. ***Holotype:*** female; South Korea, **JN**: Gwangyang-si, Okryong-myeon, Chusan-ri, Mt. Baekun, MT (DNUE).

Paratypes: South Korea, **GB**: 1♀, Mungyeong-si Mungyeong-eup Sangcho-ri 288–1 Mungyeongsaejae 10.VI.1992 (DNUE–0248); 1♀, Uljin-gun, Mt. Baekamsan, 20.VI–12.VII.1999, D.S. Ku leg. (NIAS); **GG**: 2♀, Annyang-si, Manan-gu, Gwanaksan, 37°25'06"N, 126°50'56"E, 26.VI–4.VII.2007, J.W. Lim leg. (DNUE–0233,0234); 3♀, Gapyeong-si, Cheongpyeong-myeon Soseong-ri, Mt. Homyeong, 37°43'15"N, 127°29'18.9"E, 11–25.VII.2009, J.O. Lim leg. (DNUE–0906, ZIN–0904,0905); 1♀, Pocheon-si, Soheul-eup, Jikdong-ri, 51-7, Korean National Arboretum, 37°45'9.1"N, 127°08'34.4"E, MT 4, 14–28.VI.2013, I.G. Kim leg. (ZIN); **GW:** 1♀, Donghae-si, Samhwa-dong, Mureung valley, MT, 16–28.VI.2005, J.W. Lee leg. (ZIN–0118); 2♂, Mt. Taebaeksan, Yuilsa, MT, 20.VI–11.VII.1999, D.S. Ku leg. (NIAS); **JB**: 1♀, Jeongeup-si, Samgan-dong, Dapgok-ri, MT, 18.VI.2006, J.W. Lee leg. (DNUE–0401).

Distribution. South Korea (GB, GG, GW, JB, JN).

24. *Orthocentrus trichophthalmus* Humala & Lee, sp. nov.

http://zoobank.org/F1AAAEC7-5A3D-4677-80BE-E7501A058598
Fig. 17

Description. Female. Fore wing length 3.8 mm.

Face at level of antennal sockets 0.9 times as wide as high; face fairly sparsely punctate, shining, eyes setose, dorsal ridge of face in between antennal sockets without a median prominence; face profile gently curved, edge of clypeus somewhat impressed, margin straight, antennal sockets not on a distinct high shelf; subocular sulcus gently curved; maxillary palp long, reaching back to fore coxae. In dorsal view, head posteriorly moderately concave, temples distinct, lateral ocellus distant from eye by its maximum diameter, POL 1.1 times as long as diameter of lateral ocellus, ocellar-ocular grooves

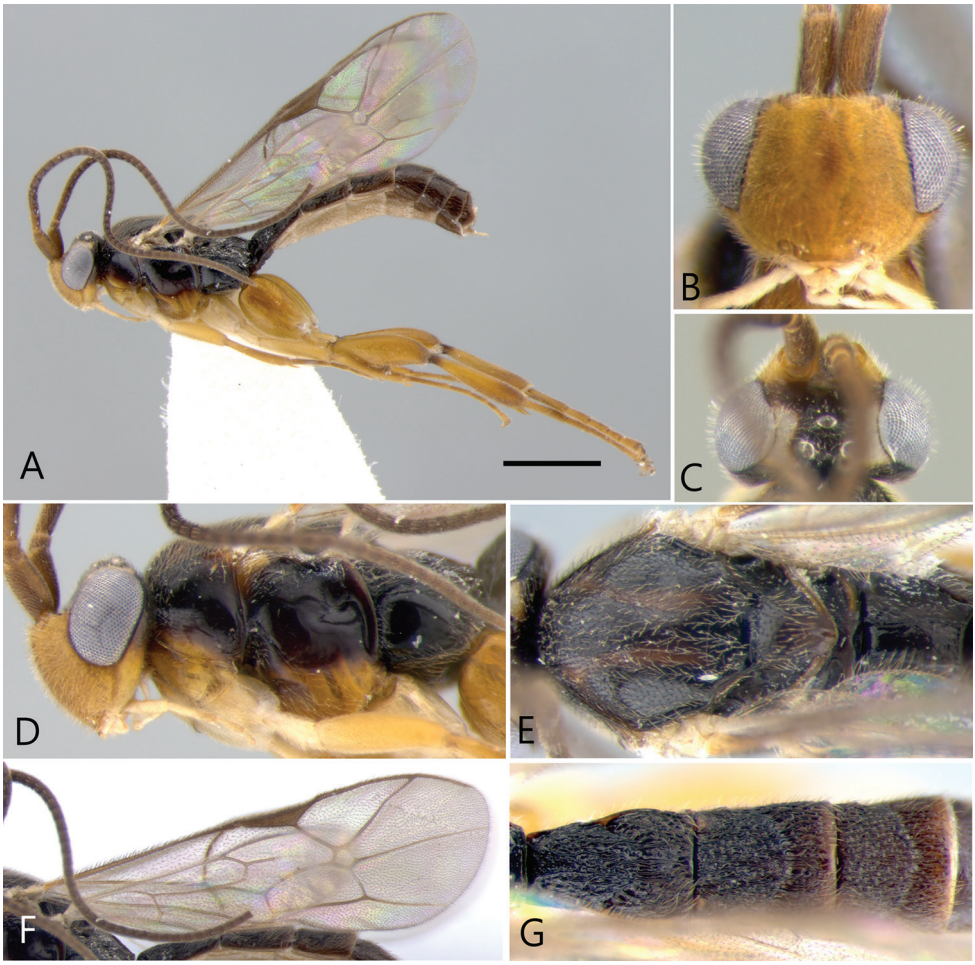

Figure 17. *Orthocentrus trichophthalmus* sp. nov. Holotype. **A** Habitus in lateral view **B** head in frontal view **C** head in dorsal view **D** head and mesosoma in lateral view **E** mesosoma in dorsal view **F** fore wing **G** first to third tergites in dorsal view.

absent. Minimum distance between antennal sockets about 0.4× diameter of socket; antenna long, slender, with 45 flagellomeres which gradually shorten towards apex of antenna; first flagellomere 2.1 times as long as wide and 0.6 times as scape length; scape slightly curved, in frontal view a little concave on lateral surface, convex on inner surface.

Mesosoma smooth, polished, impunctate except mesoscutum with shallow punctures, some faint coriaceous/rugose microsculpture on propodeum; mesoscutum lacking notauli; in profile, scutellum weakly convex, metapleuron slightly convex; propodeum with posterior transverse carina strong and raised, lateromedian longitudinal carinae complete, spiracle not particularly large.

Legs stout, hind leg massive; hind femur 3.1 times as long as maximum depth, hind tibia 4.1 times as long as apical width; tibiae lacking spine-like setae.

Wings not particularly narrow; fore wing with narrowly sessile areolet, slightly shorter than high, pterostigma narrow, vein Rs+2r meeting pterostigma at apical third; vein Rs nearly straight; nervellus intercepted below, angulate.

First tergite somewhat elongate and apically slightly widening, 1.6 times as long as posteriorly wide; heavily rugose without lateromedian longitudinal carinae, with transverse impressions originating at about middle of tergite, sloping posteriorly, and meeting centrally by transverse furrow. Second tergite 1.2 times as long as posteriorly wide; heavily rugose, with transverse impressions originating at about middle of tergite, sloping posteriorly, meeting centrally, delimiting vaguely defined rhombic area centrally; thyridia present. Third tergite with rugose/strigose sculpture, sculpture towards posterior edge smoother, with transverse impressions originating at about middle of tergite, sloping anteriorly, meeting centrally. Posterior tergites slightly coriaceous. Ovipositor thin, straight, without dorsal notch; ovipositor sheaths short, concealed by large hypopygium.

Setae over whole body except pronotum, mesopleuron, metapleuron, scattered on propodeum and dorsal sides of coxae.

Blackish-brown; flagellomeres brown, dull orange basally; face clypeus and malar space dull yellow/pale orange, frons fuscous, vertex with creamy orbital marks between eyes and ocelli, small pale area behind subocular sulcus; indistinct reddish-brown patches at anterolateral margins and whole course of notauli (if they were impressed), scutellum brown; propleuron, ventrally on pronotum and lower third of mesopleuron pale orange; legs basically dull yellow/orange, narrow basal band on hind tibia dark brown, fore and mid coxa, all trochanters and trochantelli pale. Tergites dark brown, second and third tergites narrowly dull orange apically. Sternites creamy with yellow more sclerotized patches.

Male. Unknown.

Biology. Hosts unknown.

Etymology. Named from the Greek *τρίχα* (hair) and *οφθαλμός* (eye) after the densely setose eyes.

Comparison. Compared with the other species that have densely setose eyes, it is much larger, the mesoscutum with reddish bars along notauli, antennae comparatively long, with 45 flagellomeres, unlike in *O. trichoptilus*, *O. hirsutor* and *O. setosus*.

Material examined. ***Holotype:*** female; South Korea, **GW**: Wonju-si, Heungeop-myeon, Maeji-ri 234, Yonseidae, MT, 31.VII–5.IX.2014, H.Y. Han leg. (DNUE).

Distribution. South Korea (GW).

25. *Orthocentrus trichoptilus* Humala & Lee, sp. nov.

http://zoobank.org/CD88033B-260C-4849-AE85-F11B59BCB724
Fig. 18

Description. Female. Fore wing length 2.6 mm.

Face at level of antennal sockets 1.1 times as wide as high; face matt, finely and densely pustulate, frons finely pustulate with hairs, temples with fine matt-like coriaceous sculpture; eyes setose; dorsal ridge of face in between antennal sockets without a median

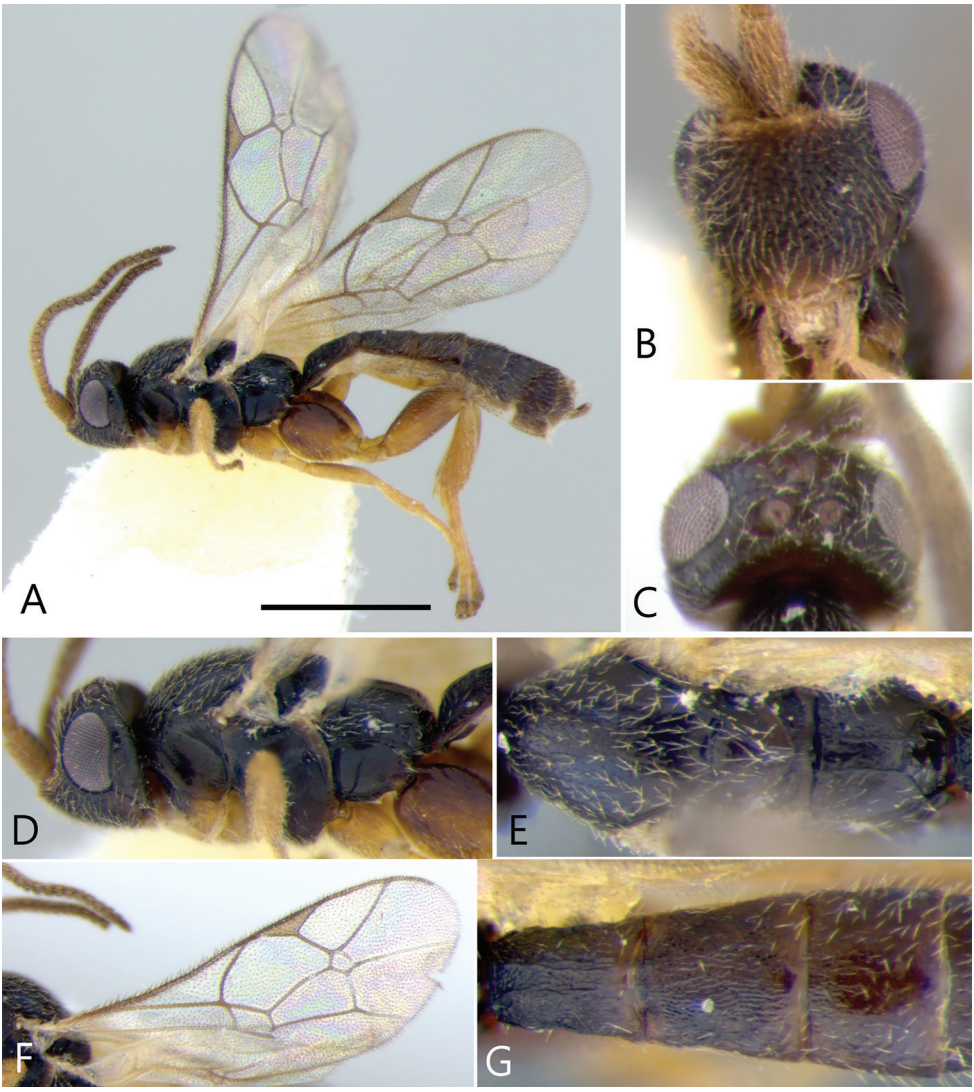

Figure 18. *Orthocentrus trichoptilus* sp. nov. Holotype. **A** Habitus in lateral view **B** head in frontal view **C** head in dorsal view **D** head and mesosoma in lateral view **E** mesosoma in dorsal view **F** fore wing **G** first to third tergites in dorsal view.

prominence; face in profile almost straight, slightly impressed dorsally, edge of clypeus straight, antennal sockets on a high shelf; subocular sulcus distinct, sharp, bent towards occiput; maxillary palp reaching to about epicnemial carina. Head in dorsal view posteriorly deeply concave, temples distinct, lateral ocellus separated from eye by a distance 2 times 1.3 times longer than its maximum diameter, POL 0.9 times as long as diameter of lateral ocellus, ocellar-ocular grooves lacking. Minimum distance between antennal sockets very narrow, sockets almost touching each other; antenna short, moniliform,

with 24 transverse flagellomeres, apical flagellomeres subquadrate, first flagellomere 0.8 times as long as wide and about 1/3 of the scape length, scape nearly parallel-sided.

Mesosoma smooth and polished except mesoscutum and scutellum regularly punctate, dorsal propodeum with coriaceous microsculpture; mesoscutum lacking notauli; in profile, scutellum weakly convex, metapleuron slightly convex; propodeum with posterior transverse carina present between lateral longitudinal carinae, lateromedian longitudinal carinae complete, diverging anteriorly; spiracle small.

Legs broad, coxae polished, femora polished-coriaceous, tibiae and tarsi coriaceous-granulate; hind femur 2.5 times as long as high, hind tibia 3.8 times as long as apical width, with spine-like setae.

Wings not particularly narrow; fore wing with areolet closed, areolet comparatively large, about as high as wide, 2m-cu meeting areolet at apical 0.7, vein Rs straight; nervellus not intercepted, gently curved.

First tergite elongate, posteriorly widening, 1.6 times as long as posteriorly wide; coriaceous-rugose, without developed lateromedian longitudinal carinae. Second tergite 0.7 times as long as posteriorly wide; coriaceous-rugose, posteriorly polished, with shallow transverse impressions originating at about middle of tergite, sloping posteriorly and meeting centrally; anterior thyridia oval-rectangular. Remaining tergites smooth and polished, third tergite with shallow punctures, without thyridia; third tergite sometimes anteriorly narrowly coriaceous-strigose. Ovipositor straight, without notch; ovipositor sheaths slightly widened apically with sparse backward-pointing setae.

Body largely setose except pronotum, mesopleuron and metapleuron; setae few and scattered on propodeum and posterior sides of coxae.

Dark brown except mouthparts, upper margin of face and small marks between inner orbits and antennal sockets, fore and mid legs, tegula, light yellow; sternites creamy, propleuron ventrally, legs largely except dorsal half of hind coxa and hind femur dorsally yellow; division of dark and pale colours blurred.

Male. Unknown.

Biology. Hosts unknown.

Etymology. Named from the Greek *τρίχα* (hair) and *οπτικθσ* (optics, eye) after the relatively dense setae on the surface of the eyes.

Comparison. Compared with the other species that have densely setose eyes, the face, mesoscutum, propleuron and mesopleuron are fuscous, the subocular sulcus distinct, the antennae comparatively short with 24 flagellomeres, unlike in *O. trichophthalmus*, *O. hirsutor* and *O. setosus*.

Material examined. ***Holotype:*** female; South Korea; **JB**: Muju-gun, Mupung-myeon, Hyeonnae-ri San 3, Mt. Bakseoksan, MT, 17.VI–2.VII.2015, J.W. Lee leg. (DNUE).

Distribution. South Korea (JB).

26. *Orthocentrus winnertzii* Förster, 1850

Figs 19C, D

Biology. Parasitoid of *Sciophila rufa* Meigen (Diptera, Mycetophilidae).

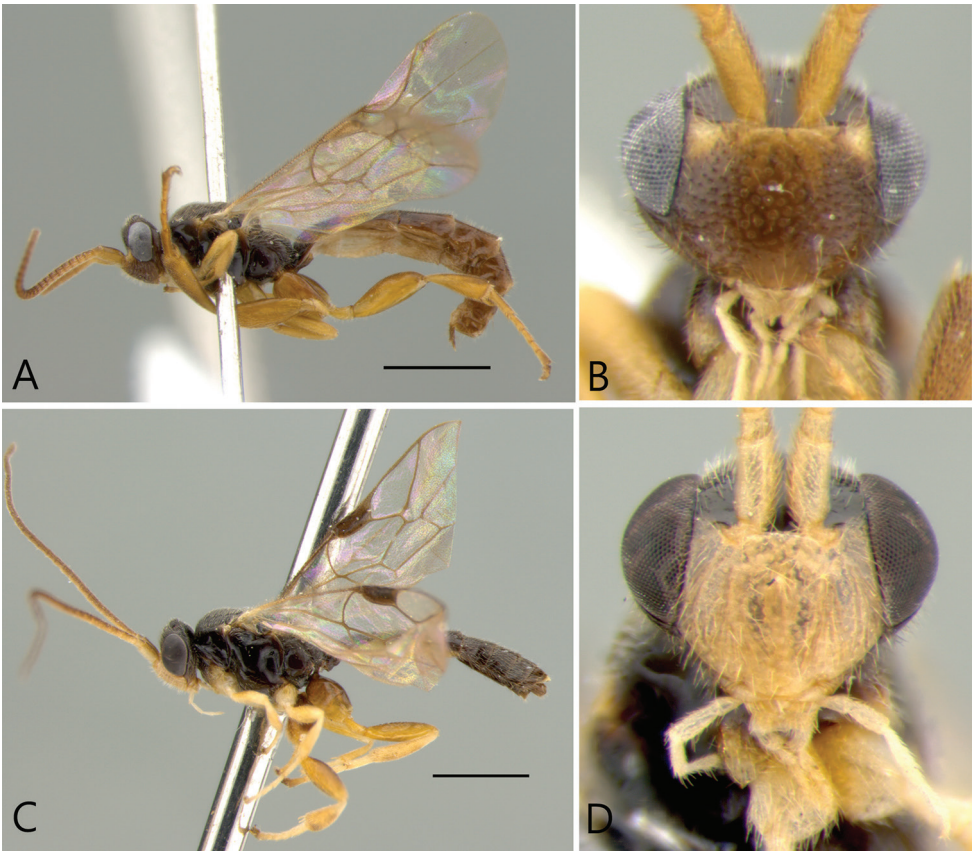

Figure 19. *Orthocentrus* spp. **A** Habitus in lateral view of *O. stigmaticus* **B** head in frontal view of *O. stigmaticus* **C** habitus in lateral view of male of *O. winnertzii* **D** head in frontal view of male of *O. winnertzii*.

Material examined. South Korea, **GB:** 1♂, Gyeongsan-si, Yeungnam University, 19.IV.1989, J.G. Kim leg. (DNUE–0478); **GW**: 1♀, Wonju-si, Panbu-myeon, Mt. Baegunsan, MT, 5.IX–16.X.2013, H.Y. Han leg. (DNUE); 1♂, Taebaek-si, Hyeol-dong, Yilsa, 37°0'41.79"N, 128°55'26.46"E, 30.VI.1991, J.W. Lee leg. (DNUE); Japan: 1♀, Hokkaido University, Kita 8, Nishi 5, Kita-ku, Sapporo, Hokkaido, 30.VII–21.VIII.2013, S.H. Oh leg. (DNUE–0050).

Distribution. Holarctic; *South Korea (GB, GW), *Japan.

Discussion

Altogether 25 species of *Orthocentrus* are found to occur in South Korea, previously none of these had been reported from this country, and neither had the genus *Orthocentrus*. Among them, 15 species are new to science and 10 are known species of Palaearctic or Holarctic distribution. After this work, the Korean fauna of *Orthocentrus* can be considered the best studied in the East Palaearctic. Unfortunately not all the

available males were associated with specific females, and probably the use of molecular methods could help to solve this problem in a future study.

All of the scarce reliable observations of *Orthocentrus* hosts are restricted to the genera *Sciophila* Meigen and *Neoempheria* Osten Sacken (Diptera, Mycetophilidae): *O. asper* was reared from *Sciophila lutea* Macquart (Šedivý and Ševčik 2003), *O. protervus* from *Sciophila hirta* Mg. (Roman 1923), *O. stigmaticus* from *Sciophila rufa* Mg. (Kolarov 1986), and unidentified *Orthocentrus* species from *Neoempheria carinata* Sueyoshi (Mukai and Kitajima 2019). No biological information concerning *Orthocentrus* hosts is available from South Korea.

Veijalainen et al. (2014), after studying *Orthocentrus* in the Neotropics, concluded that the genus is not monophyletic and perhaps should be divided. They proposed five species-groups, and some of them (e.g. *O. maculae* and *O. shieldsi* species-groups), could be found also in the Palaearctic fauna. We agree with their opinion in general; however, to address the possible split of *Orthocentrus*, a more comprehensive analysis is needed, ideally including specimens from all regions of the world. For the moment, this division could not be applied to the Palaearctic species of the genus, as many distinctive characters overlap and consequently the species-group definitions do not fit well to many species from our study.

Orthocentrinae still remains an incompletely investigated group if compared with other ichneumonid subfamilies and requires much more taxonomic attention; however, the efforts of several researchers resulted in some progress in this field during the last few decades. Despite this the number of unknown Orthocentrinae species remains very high, especially in the tropical regions.

Acknowledgments

We are deeply grateful to the reviewers and the subject editor Gavin Broad for reviewing this manuscript and constructive criticism that improved this paper. Also, our thanks to Dr Hae-Chul Park (NIAS curator) for providing material for this study. This work was carried out under state order to the Karelian Research Centre of the Russian Academy of Sciences (Forest Research Institute) and supported by a grant from the National Institute of Biological Resources (NIBR), funded by the Ministry of Environment (MOE) of the Republic of Korea (NIBR201801201 and NIBR201902205).

References

Aubert JF (1978) Révision préliminaire des Ichneumonides Orthocentrinae européennes (I) (Hymenoptera, Ichneumonidae). Eos 52: 7–28.

Eady RD (1968) Some illustrations of microsculpture in the Hymenoptera. Proceedings of the Royal Entomological Society of London (A) 43: 66–72. https://doi.org/10.1111/j.1365-3032.1968.tb01029.x

Gauld ID (1991) The Ichneumonidae of Costa Rica 1. Memoirs of the American Entomological Institute 47: 1–539.

Gravenhorst JLC (1829) Ichneumonologia Europaea. Pars III. Vratislaviae, 1097 pp. https://doi.org/10.5962/bhl.title.65750

Humala AE (2007) Subfamily Orthocentrinae. In: Lelej AS (Ed.) Opredelitel' nasekomykh Dal'nego Vostoka Rossii [Keys to the Insects of the Russian Far East], Dal'nauka, Vladivostok, Vol. 4, 680–718. [In Russian]

Humala AE (2019) Mexican species of the genus *Orthocentrus* (Hymenoptera, Ichneumonidae: Orthocentrinae). Zootaxa. 4709 (1): 1–83, https://doi.org/10.11646/zootaxa.4709.1.1

Humala AE, Choi JK, Lee JW (2016) A review of the genera *Gnathochorisis* Förster and *Symplecis* Förster of South Korea with notes on Korean orthocentrines (Hymenoptera: Ichneumonidae: Orthocentrinae). ZooKeys 562: 85–104. https://doi.org/10.3897/zookeys.562.7303

Humala AE, Choi JK, Lee JW (2018) A review of the genus *Eusterinx* Förster (Hymenoptera, Ichneumonidae, Orthocentrinae) from South Korea with descriptions of five new species. Entomological Science 21: 97–111. https://doi.org/10.1111/ens.12287

Kasparyan DR, Khalaim AI, Tereshkin AM, Humala AE, Proschalykin MYu (2012) 47. Ichneumonidae. In: Lelej AS (Ed.) Annotated Catalogue of the insects of Russian Far East. Hymenoptera, Dal'nauka, Vladivostok, Vol. 1, 210–299. [In Russian]

Kolarov J (1986) A revision of the Orthocentrinae of Bulgaria (Hymenoptera, Ichneumonidae). Annales Historico-Naturales Musei Nationalis Hungarice 78: 255–264.

Mukai H, Kitajima H (2019) Parasitoid wasps regulate population growth of fungus gnats *Neoempheria* Osten Sacken (Diptera: Mycetophilidae) in shiitake mushroom cultivation. Biological Control 134: 15–22. https://doi.org/10.1016/j.biocontrol.2019.03.016

Roman A (1923) Ichneumonids reared from Diptera Nematocera. Entomologist's Monthly Magazine 59: 71–76.

Šedivý J, Ševčik J (2003) Ichneumonid (Hymenoptera: Ichneumonidae) parasitoids of fungus gnats (Diptera: Mycetophilidae): rearing records from the Czech Republic. Studia Dipterologica 10: 153–158.

Townes HK (1971) The genera of Ichneumonidae, part 4. Memoirs of the American Entomological Institute 17: 1–372.

Veijalainen A, Broad GR, Sääksjärvi IE (2014) Twenty seven new species of *Orthocentrus* (Hymenoptera: Ichneumonidae; Orthocentrinae) with a key to the Neotropical species of the genus. Zootaxa 3768(3): 201–252. https://doi.org/10.11646/zootaxa.3768.3.1

Watanabe K (2016) Discovery of the Genus *Neurateles* Ratzeburg, 1848 (Hymenoptera, Ichneumonidae, Orthocentrinae), from the Eastern Palearctic Region, with Description of a New Species from Japan. Bulletin of the Kanagawa Prefectural Museum (Natural Science) 45: 81–84.

Watanabe K (2018) Discovery of the Genus *Terminator* Humala, 2007 (Hymenoptera: Ichneumonidae: Orthocentrinae) from Japan. Japanese Journal of Systematic Entomology 24(2): 254–256.

Watanabe K (2019a) New Distribution Records of the Subgenus *Fugatrix* Rossem, 1987 of the Genus *Plectiscidea* Viereck, 1914 (Hymenoptera: Ichneumonidae: Orthocentrinae) from Japan. Japanese Journal of Systematic Entomology 25(1): 49–52.

Watanabe K (2019b) Review of the Genera *Aniseres* Förster, 1871 and *Catastenus* Förster, 1868 (Hymenoptera: Ichneumonidae: Orthocentrinae) from Japan. Japanese Journal of Systematic Entomology 25(1): 81–85.

Yu DSK, Achterberg van C, Horstmann K (2016) Taxapad 2016, Ichneumonoidea 2015. Database on flash-drive. Nepean, Ontario, Canada.

JHR 75: 67–85 (2020)
doi: 10.3897/jhr.75.47880
http://jhr.pensoft.net

RESEARCH ARTICLE

JOURNAL OF Hymenoptera RESEARCH
A peer-reviewed open-access journal
The International Society of Hymenopterists

Larval morphology and life history of *Eutrichosoma mirabile* Ashmead and description of a new species of *Eutrichosoma* (Hymenoptera, Chalcidoidea)

Austin J. Baker[1], John M. Heraty[1]

1 *Department of Entomology, University of California, Riverside, CA 92521, USA*

Corresponding author: Austin J. Baker (abake005@ucr.edu)

Academic editor: Petr Jansta | Received 1 November 2019 | Accepted 6 January 2020 | Published 27 February 2020

http://zoobank.org/2D542983-8FC8-4616-834F-47625EDBB5F0

Citation: Baker AJ, Heraty JM (2020) Larval morphology and life history of *Eutrichosoma mirabile* Ashmead and description of a new species of *Eutrichosoma* (Hymenoptera, Chalcidoidea). Journal of Hymenoptera Research 75: 67–85. https://doi.org/10.3897/jhr.75.47880

Abstract

The larval morphology and life history of the weevil parasitoid *Eutrichosoma mirabile* Ashmead (Hymenoptera, Chalcidoidea, Pteromalidae) are described, and the phylogenetic placement of the subfamily Eutrichosomatinae within Chalcidoidea is determined using larval morphological characters. A description of *Eutrichosoma burksi* **sp. nov.** and key to the species of *Eutrichosoma* are provided.

Keywords

Eutrichosomatinae, larval morphology, planidia, Planidial Larva Clade, weevil parasitoid

Introduction

Eutrichosoma is a widespread, but infrequently collected, genus of weevil parasitoids in the subfamily Eutrichosomatinae (Hymenoptera, Chalcidoidea, Pteromalidae). Three species are known: *Eutrichosoma mirabile* Ashmead found throughout North America and Brazil, *E. flabellatum* Bouček from Brazil, and *E. burksi* sp. nov. from California, USA. The natural history is only known for *E. mirabile*, which parasitizes seed-feeding weevil larvae in the genera *Auleutes* and *Smicronyx* (Curculionidae) found on *Parthenium* and *Helianthus* (Asteraceae) (Crawford 1908; Bouček 1974; Charlet and Seiler 1994). *Auleutes* (Ceutorhynchinae) is typically associated with plants in the family Onagraceae and *Smicronyx* (Curculioninae) is typically associated with plants in the

families Asteraceae and Convolvulaceae, however, the plant hosts for the weevils and the weevil hosts for the wasps are likely broader than what is currently known.

Eutrichosomatinae includes two other monotypic genera: *Peckianus laevis* Provancher, a parasitoid of *Apion* (Brentidae) (Bouček and Heydon 1997), ranging from Canada to Brazil; and *Collessina pachyneura* Bouček from Australia, whose natural history is unknown. The taxonomic placement of this group was originally in Cleonyminae (Cleonymidae) by Ashmead (1899), who later placed it within Tanaostigmini (Encyrtidae) when he first provided the species name *Eutrichosoma mirabile* without a description (Ashmead 1904). It was first published as its own family, Eutrichosomatidae, by Peck (1951) and then reclassified as the subfamily Eutrichosomatinae within Pteromalidae by Bouček (1974). The digitate labral morphology of adult *E. mirabile* was regarded as similar to that of Eucharitidae and Perilampidae but independently derived (Darling 1988); however, the phylogenetic placement of this group based on a combination of morphological and molecular data suggests that Eutrichosomatinae belong within the Perilampidae+Eucharitidae clade (Heraty et al. 2013), which we here term the 'Planidial Larva Clade' (PLC) for their highly derived first-instar larvae.

Planidia, which means "diminutive wanderers," are hypermetamorphic, active first-instar larvae (Clausen 1940a). The eggs are often laid away from the host, which requires the planidia to be adapted for free-living, being more mobile and more sclerotized than typical parasitoid larvae and showing host-seeking behavior. Planidia undergo metamorphosis between the first and second instar, with the latter typically resembling sessile, non-planidial larvae that, within Hymenoptera, are termed hymenopteriform (Clausen 1940a; Pinto 2009). Within the PLC, planidia first attach externally to the host larva and begin further development through later instars on the host pupa (Clausen 1940b; Darling and Miller 1991; Darling 1992; Darling 1999). Until the host pupates, the planidia need to be mobile and able to find/recognize their hosts so that they can detach and reattach when their hosts molt. There are several groups of Diptera that have planidial first-instar larvae (Acroceridae, Nemestrinidae, Bombyliidae, Tachinidae, Asilidae) as well as Hymenoptera (Eucharitidae, Perilampidae, *Euceros* in Ichneumonidae), with multiple origins of planidial larvae present in both orders. We predict a single origin for planidial larvae in Chalcidoidea, and thus, if part of the PLC, the first-instar larvae of *Eutrichosoma mirabile* should have planidial morphology or otherwise some transitional form. We were able to collect and study the larvae of *E. mirabile* in Arizona to better understand their life history, and we provide support for the phylogenetic placement within the PLC based on larval morphology. In the process of examining museum material, we discovered a distinctive new species from California.

Materials and methods

Eutrichosoma mirabile was collected at a field site close to Portal, Arizona, along Foothills Rd (31.952N, 109.139W) in August 2016, 2018, and September 2018.

Adult *Eutrichosoma mirabile* were swept off of whitethorn acacia (*Vachellia constricta* (Benth.) Seigler & Ebinger; Fabaceae). Seedpods of whitethorn acacia were collected and individually dissected in lab. Larvae of hosts and parasitoids were collected into 95% ethanol. Voucher specimens were assigned individual plasticized barcodes and deposited in the Entomology Research Museum at the University of California Riverside (**UCRC**). For slide mounting, larvae were cleared with 10% KOH, and then slide mounted in Hoyer's medium; after drying, slides were sealed with clear nail polish. Some larval specimens were retained in 95% ethanol. For scanning electron microscopy (SEM), larvae were dried using hexamethyldisilazane (Heraty and Hawks 1998), mounted on double sided sellotape, and sputter coated with palladium. SEM images were taken at the University of California Riverside using a Tescan Mira3 GMU. Stacked digital images were taken using a Leica Imaging System with a Z16 APO A microscope.

Morphological terms

Terms used for adult morphology follow Heraty et al. (2018). Terms used for larval morphology follow Heraty and Darling (1984), Darling and Miller (1991), and Darling (1992).

Molecular sequencing

Specimens were extracted using the DNeasy blood and tissue kit manufactured by Qiagen (Valencia, CA, USA) with 1 µL RNAse A added after incubation. Two gene regions were sequenced. The ribosomal gene 28S D2 used the following primers and thermocycler protocol: D2F (CGG GTT GCT TGA GAG TGC AGC) and D2Ra (CTC CTT GGT CCG TGT TTC); initial denaturization: 94 °C 3 min; (denaturization: 94 °C 1 min; annealing: 55 °C 1 min; extension: 72 °C 1 min) ×34; final extension: 75 °C 7 min. The mitochondrial gene COI-barcoding (COI-BC) used the following primers and thermocycler protocol: LCO1490 (GGT CAA CAA ATC ATA AAG ATA TTG G) and HCO2198 (TAA ACT TCA GGG TGA CCA AAA AAT CA); initial denaturization: 93 °C 3 min; (denaturization: 93 °C 15 sec; annealing: 46 °C 45 sec; extension: 68 °C 45 sec) ×34; final extension: 68 °C 7 min. PCR products were purified with DNA Clean & Concentrator™ -5 kits by Zymo Research (Irvine, CA, USA). PCR product concentrations were measured using Nanodrop 2000c (Thermo Scientific™). Each gene was PCR amplified individually and Sanger sequenced using both primers. Samples for Sanger sequencing were sent to Retrogen Inc. (San Diego, CA, USA) for sequencing on an Applied Biosystems 3730xl DNA Analyzer. Chromatograms were inspected for base calling errors and edited in Mesquite v.3.31 (Maddison and Maddison 2017b) using Chromaseq v.1.2 (Maddison and Maddison 2017a).

Molecular identification

We attempted to identify (or verify) specimens of parasitoid and host by comparing sequences with the online databases NCBI BLAST (Johnson et al. 2008) and BOLD (Ratnasingham and Hebert 2007) (Suppl. material 1: Tables S1, S2).

Morphological phylogenetics

We tested the placement of Eutrichosomatinae within the PLC by first using the planidial morphology data matrix developed by Heraty and Darling (1984) and later modified by Darling (1992). Within the PLC, the subfamilies of Perilampidae are paraphyletic in recent molecular studies (Munro et al. 2011; Heraty et al. 2013), and we treat Chrysolampinae, Perilampinae, and Philomidinae as separate terminal taxa and equivalent to Eucharitidae. We refined these previous character sets to include only informative and unambiguous characters at the family or subfamily level. Parsimony analyses were performed in PAUP* v4.0a (Swofford 2002) with default settings. We provide a detailed list of the characters, including character states, polarity inferences, and modifications from earlier studies (Heraty and Darling 1984; Darling 1992), with justifications for inclusion or exclusion of those characters.

Character 1. *Egg shape*: 0 = ovoid; 1 = stalked. Stalked eggs were regarded by Heraty and Darling (1984) as a synapomorphy for Eucharitidae, however at least three genera within Eucharitidae (*Indosema*, *Orasemorpha*, and *Timioderus*) lack egg stalks (Heraty 1994), and Chrysolampinae (Darling and Miller 1991), Philomidinae (Heraty et al. 2019), and Eutrichosomatinae all have egg stalks. The polarity cannot be inferred because the presence of egg stalks seems to be widespread throughout Chalcidoidea (e.g. *Aphelinus*, *Leucospis*, *Tetrastichus*, *Torymus*, and many more (Parker 1924)). We excluded this character from the analysis.

Character 2. *Egg sculpture*: 0 = smooth; 1 = ridged. Smooth eggs were inferred to be plesiomorphic by Heraty and Darling (1984), with ridged eggs only appearing in Perilampinae. This character is an autapomorphy for Perilampinae, thus excluded.

Character 3. *Sclerotization of terga* (=*tergites*): 0 = absent; 1 = present. Heraty and Darling (1984) treated this character as a combination of sclerotization and distinctiveness of terga, which was present in all of our ingroup taxa. Darling (1992) made this into two distinct characters: character 3 was sclerotization and character 3' was the shape of the terga (0 = completely encircling body; 1 = incomplete ventrad). All ingroup taxa were coded as sclerotized, and all ingroup taxa except Chrysolampinae and Eutrichosomatinae were coded as incomplete ventrad. The interpretation that Chrysolampinae and Eutrichosomatinae are more sclerotized than outgroup taxa with the terga completely encircling the body seems to be questionable, so we did not include the sclerotization character (3) but only used the shape character (3'), which is treated here as character 20.

Character 4. *Setal pattern of tergum III* (*TIII*): 0 = ventral setae absent; 1 = present. Heraty and Darling (1984) treated this character as a loss of the ventral setae in

Chrysolampinae and Oraseminae (Eucharitidae). The ventral pair of setae are difficult to define by position and are more accurately coded as the third pair of setae on TIII that are located ventrolaterally. Having the seta located on the ventrolateral margin is an autapomorphy of Eucharitidae, although it is not found in all taxa (Heraty and Barber 1990). However, these ventrolateral setae do appear to be present in both Chrysolampinae (Darling and Miller 1991) and Eutrichosomatinae, rendering this character uninformative for this analysis, thus it was excluded.

Character 5. *Distribution of dorsal setae*: 0 = absent; 1 = setae present on TI–III, V, VII, IX, XI; 2 = setae present on TI–III, V, VII, IX; 3 = setae present on TI–III, V. Heraty and Darling (1984) and Darling (1992) treated the absence of setae as the plesiomorphic condition, which is not easily justified given the widespread presence of setae in chalcidoid first-instar larvae (e.g. *Leucospis*, *Torymus*, *Eupelmus*, *Eurytoma* (Parker 1924)). For this analysis, the only informative dorsal seta is on TX. We excluded character 5, but added the presence of a seta on TX as character 21.

Character 6. *Dorsal fusion of terga I and II* (*TI and TII*): 0 = absent; 1 = present. Heraty and Darling (1984) treated this as a synapomorphy of Eucharitidae, however Oraseminae lack this fusion, and *Monacon* and *Krombeinius* (Perilampinae) have the terga fused (Darling 1995; Darling and Roberts 1999). This character is uninformative for this analysis and therefore excluded.

Character 7. *Ventral spines*: 0 = absent; 1 = present. Heraty and Darling (1984) noted that ventral spines are present in many ectoparasitic chalcidoid larvae. Spines of any kind are absent in Eucharitidae, and because Perilampidae are polymorphic, they interpreted the absence of spines as a synapomorphy of these two families. Darling (1992) combined character 7 (spines) with character 8 (tubercles) using the states: 0 = absent; 1 = tubercles present; 2 = spicules (spines) present. This is problematic because multiple terms have been applied to these spines (e.g. the ventral spines in *Chrysolampus* have been referred to as tubercles, pustules, and spicules without any clear distinction (Darling and Miller 1991)). Additionally, Chrysolampinae and Philomidinae were coded as having spicules (but not tubercles), and Perilampinae are coded as having tubercles (but not spicules) despite contradicting descriptions (cf. Darling and Miller 1991). We treat spines as a separate character from tubercles. Spines, represented as hook-like structures on the ventral region of the body segments and located between the tergal margins (cf. figs 17, 34, 37 in Heraty and Darling 1984), are a feature found only in some Perilampinae. They are uninformative for this analysis and excluded.

Character 8. *Lateral tubercles*: 0 = absent; 1 = present. Eutrichosomatinae have a series of tubercles across the ventral region of body segments II–XII (Fig. 1B, D, F; *tbs*). Heraty and Darling (1984) treated this as an autapomorphy of Chrysolampinae based on the description by Askew (1980). This character was further explored and illustrated on two species of *Chrysolampus* by Darling and Miller (1991), occurring on body segments II–XII. A similar patch of tubercles was found on the ventral region of body segment I in Philomidinae (Darling 1992). We excluded this character because of the difficulty assessing the homology of the various types of ventral and lateral protuberances.

Character 9. *Spiracles*: 0 = spiracles on TII, IV, V, VI; 1 = spiracles on TII; 2 = absent. Heraty and Darling (1984) noted that the plesiomorphic condition in Chalcidoidea is having pairs of spiracles on TII, IV, V, and VI, which is the state found in Eutrichosomatinae and several outgroup taxa (Parker 1924). Perilampinae and Philomidinae have lost all spiracles except on TII, and Eucharitidae and Chrysolampinae lack spiracles entirely.

Character 10. *Tergopleural line*: 0 = absent; 1 = present. This longitudinal line of thin, unpigmented cuticle going through the lateral sides of TII–IX is found in most Eucharitidae. It is absent in most Oraseminae, although present in *Orasemorpha* (Heraty 2000). In Eucharitinae, it is absent only in *Pseudochalcura* (Heraty and Barber 1990). It is present in Gollumiellinae, which is sister to Oraseminae + Eucharitinae (Heraty 2004), hence it is interpreted as a synapomorphy of Eucharitidae. It is uninformative for this analysis and was excluded.

Character 11. *Caudal cerci*: 0 = present as undifferentiated setae; 1 = absent; 2 = present as differentiated (longer and/or stouter) setae. These structures are defined as setae arising on the dorsum of TXII (Heraty and Darling 1984), which are larger than the setae on other body segments and often prolonged as stout spines or long hairs. If this character is treated as a synapomorphy of Eucharitidae and Perilampidae, the definition is not adequate because several groups have short setae (e.g. *Gollumiella longipetiolata* Hedqvist (Heraty 2004), *Hydrorhoa stevensoni* (Risbec) (Heraty 2002), *Australosema valgius* (Walker) and *Orasemorpha didentata* (Girault) (Heraty 2000)) and some have other setae on the body as long as the setae on TXII (e.g. *Perilampus chrysopae* Crawford (Clancy 1946), *Steffanolampus salicetum* (Steffan) (Darling 1999)). Eutrichosomatinae and Philomidinae both have short socketed setae on TXII and TXIII that are located more laterally (Eutrichosomatinae; Fig. 1H) or ventrally (Philomidinae). These setae appear to be homologous with cerci but without the enlargement and proposed specialized locomotion functions associated with Perilampinae and Eucharitidae (e.g. providing support to hold the body in an upright posture); therefore, we created another character state (state 0) for these taxa. Only Chrysolampinae has entirely lost setae on TXII. The position of the cerci on Eucharitidae appears to be between TXII and TXIII, which is a synapomorphy for the family but uninformative for this analysis.

Character 12. *Caudal pad*: 0 = absent; 1 = present. The last segment (TXIII) is membranous and expanded in Eucharitidae and Perilampinae to adhere to surfaces (Heraty and Darling 1984). However, the morphology does not appear to be different from other taxa in the PLC. We also think that polarity (absent ancestrally) cannot be assumed for this character because multiple other chalcidoid taxa have differentiated posterior segments with "suckers" or other ornamentations (e.g. *Leucospis* (Parker 1924)). This was excluded from the analysis.

Character 13. *Antenna*: 0 = present; 1 = reduced; 2 = absent. The short, conical, papilliform antenna (state 0) is considered plesiomorphic (Heraty and Darling 1984). These are present in Eutrichosomatinae and Chrysolampinae and are widespread across Chalcidoidea (e.g. *Leucospis*, *Torymus*, *Eupelmus*, *Eurytoma*, and more (Parker 1924)). Philomidinae have low, broad swellings that may indicate reduced antennae (Darling 1992).

Character 14. *Cranial setae*: 0 = present; 1 = absent. It is noted by Darling (1992) that the distinction and homology between cranial setae and cranial spines is not clear, which resulted in a combination of characters 14 and 15 with the states: 0 = 3–4 pairs; 1 = reduced number. Philomidinae was the only taxon coded as having complete cranial setae, however, all Perilampinae have 3 pairs of setae on the cranium. Because of the difficulty assessing polarity and homology for this character, it has been excluded.

Character 15. *Cranial spines*: 0 = present; 1 = absent. Some species of *Perilampus* have stout, recurved spines (Heraty and Darling 1984), which may be derived setae. This character is uninformative and excluded from this analysis.

Character 16. *Prelabium*: 0 = membranous; 1 = with sclerotized marginal rim. The prelabium is a depressed area with a sclerotized marginal rim and labial palpi on the margins (Heraty and Darling 1984). Presence of the labial sclerite was considered a synapomorphy for Eucharitidae and Perilampidae and is most easily identified when the palpi appear within or on the marginal rim. In Philomidinae, the labial palpi are not associated with a sclerite, which is thought to be the plesiomorphic condition (Darling 1992). This structure is extremely minute and difficult to score for most slide-mounted larvae. It is excluded from this analysis because the structure could not be verified in many of the taxa, although it is clearly present in *Eutrichosoma* (Fig. 1B, D, E, G; *prl*).

Character 17. *Postlabium*: 0 = non-eversible; 1 = enlarged and eversible. In Eucharitidae and Perilampinae, the postlabium is an eversible membranous sac surrounding the prelabium (Heraty and Darling 1984). This may be the same in Philomidinae (Darling 1992). Observations of specimens with everted postlabia are the only accurate way to code this character, and we could not observe this in Eutrichosomatinae, therefore it was excluded.

Character 18. *Labial plates*: 0 = absent; 1 = present. These are two sclerites found posterior to the prelabium in Eucharitidae (absent in Oraseminae). This character is uninformative for this analysis and excluded.

Character 19. *Pleurostomal setae*: 0 = present; 1 = spine-like; 2 = fused spines. These are setae lateral to the mouth, and they are present in most chalcidoid taxa (Heraty and Darling 1984). These setae do not appear to be modified in Eutrichosomatinae, Chrysolampinae, Philomidinae, or most Perilampinae, despite being previously coded as spine-like (Darling 1992). In Eucharitidae this has been coded as fused spines, but what was observed was not a socketed seta but instead a pointed projection of the cranial cuticle. This character was excluded from the analysis.

Character 20. *Shape of terga*: 0 = completely encircling body; 1 = incomplete ventrad. This is character 3' from Darling (1992). Terga encircling the body is seen in all other known chalcidoid first-instar larvae (Parker 1924) and is considered plesiomorphic for the PLC. Philomidinae, Perilampinae, and Eucharitidae all have incomplete terga. One exception is in the genus *Monacon* (Perilampinae), where the posterior terga (VII–XI) are ventrally fused, while the anterior terga are not (Darling and Roberts 1999). This could be treated as a third character state for a polymorphic coding of Perilampinae, but it would not have an impact on the relationships in this analysis.

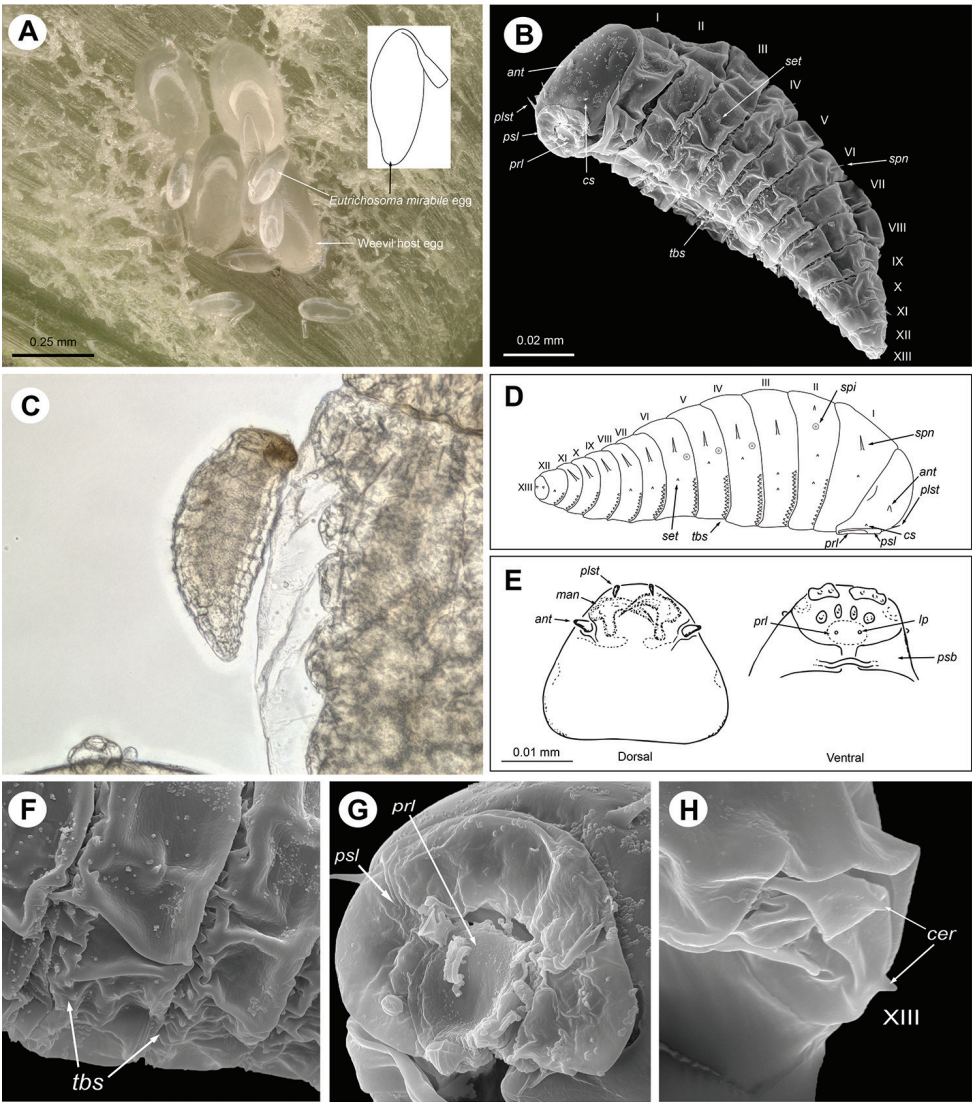

Figure 1. *Eutrichosoma mirabile* immature stages. **A** Eggs of *Eutrichosoma mirabile* (small, stalked) laid on top of the eggs of their weevil host (large, unstalked) within a seed pod of *Vachellia constricta*; inset: *Eutrichosoma mirabile* egg **B** SEM ventrolateral habitus image of a planidium of *Eutrichosoma mirabile* **C** planidium attached to host weevil larva **D** setal map of a *Eutrichosoma mirabile* planidium, modified from an illustration by Darling & Miller (1991) **E** head capsule of planidium, dorsal and ventral views **F** planidium TIII–IV, ventral tubercles **G** head, anterolateral view, showing the labial structure **H** TXIII with cerci, dorsolateral view. Abbreviations: *ant* = antenna, *cer* = cerci, *cs* = cranial spine, *lp* = labial palp, *man* = mandible, *plst* = pleurostomal seta, *prl* = prelabium, *psb* = pleurostomal bridge, *psl* = postlabium, *set* = seta, *spi* = spiracle, *spn* = spine, *tbs* = tubercles, I–XIII = terga numbered from anterior to posterior.

Character 21 (new). *Seta on tergum X:* 0 = present; 1 = absent. Setae present on all terga is treated here as the plesiomorphic state for the PLC based on the presence in many other chalcidoid taxa. Most taxa in the PLC have lost setae on TX, with the exception of Eutrichosomatinae, which maintains the ground plan configuration. We chose to focus on TX because the presence of setae on other terga are either present in all taxa (TI–III, V), only lost in Eucharitidae (TVII, IX), or require interpretation of the dorsal/lateral/ventral homology of the multiple setae present (TIV, VI, VIII).

Character 22 (new). *Seta on tergum XI*: 0 = present; 1 = absent. Loss of setae on TXI is a synapomorphy of Eucharitidae and Perilampinae.

Character 23 (new). *Behavior*: 0 = not ectoparasitic koinobiont; 1 = ectoparasitic koinobiont. All members of the PLC are ectoparasitic koinobionts. There are several examples of planidia residing internally (e.g. *Perilampus* spp.) or transdermally (e.g. *Orasema* spp.) within a host, but they always emerge to an external position to continue development through later instars; therefore, we do not consider these taxa endoparasitic sensu Heraty and Murray (2013). No other chalcidoids (where behavior is known) are ectoparasitic koinobionts because of the unique challenge of reattaching to the host after each molt, which requires increased mobility and host-recognition.

Results

Morphological phylogenetics of planidia

Our dataset was reduced to seven characters (9, 11, 13, 20–23) for the parsimony analysis. We chose to discuss all of the characters previously used because they can be valuable for future phylogenetic analyses at different levels (e.g. the genera of Eucharitidae). The major limitation for this analysis was finding informative characters with minimal ambiguity in the interpretation of their homology, which can be difficult for groups with simple morphology and large evolutionary gaps between sampled taxa. The most parsimonious tree was 11 steps and included only one homoplastic character (Fig. 2). We recovered the same topology as Heraty and Darling (1984) and Darling (1992) with the addition of Eutrichosomatinae, which was placed as the most plesiomorphic member of the PLC.

Eutrichosoma adult generic diagnosis

The inclusion of the new species of *Eutrichosoma* has modified the generic diagnosis (Bouček 1974). Margin of clypeus without incision; advanced occipital ridge directly posterior to the ocelli present or absent; the anterior transverse carina on the pronotal collar present or absent; mesoscutal midlobe completely separating the axillae medially, posteriorly reaching the mesoscutellum; fore wing without marginal fringe; postmarginal vein on the fore wing present, rudimentary (difficult to distinguish), or

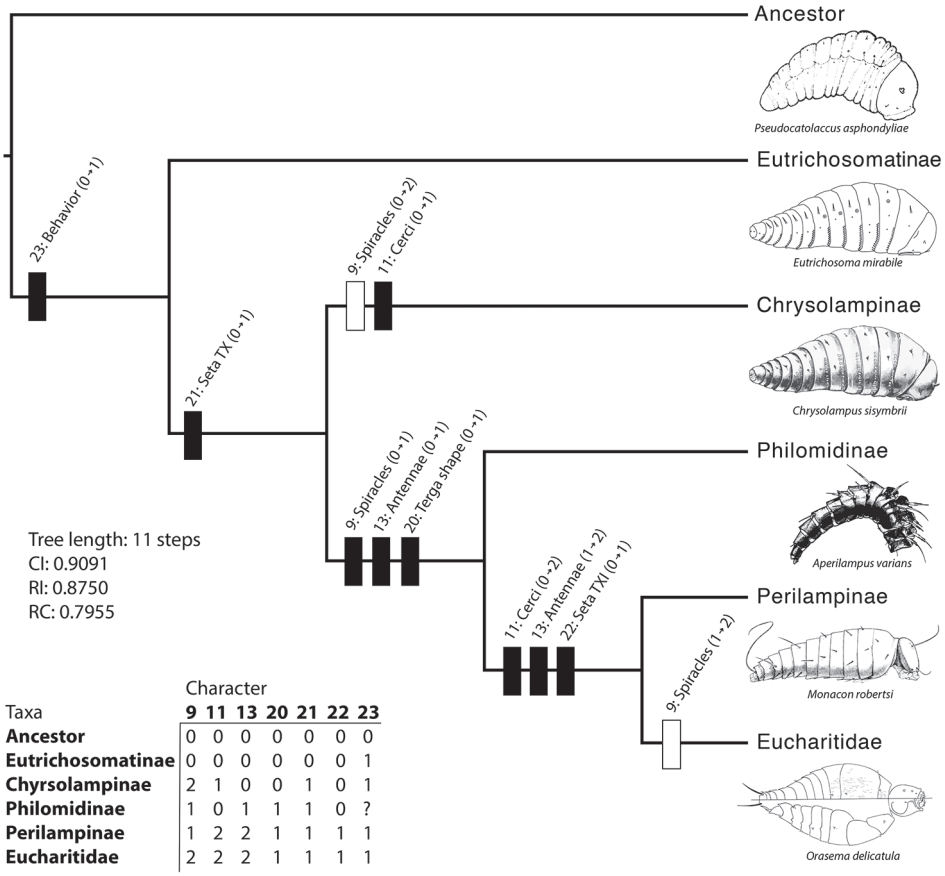

Taxa	Character 9	11	13	20	21	22	23
Ancestor	0	0	0	0	0	0	0
Eutrichosomatinae	0	0	0	0	0	0	1
Chyrsolampinae	2	1	0	0	1	0	1
Philomidinae	1	0	1	1	1	0	?
Perilampinae	1	2	2	1	1	1	1
Eucharitidae	2	2	2	1	1	1	1

Figure 2. Most parsimonious tree from larval morphology, PAUP* analysis. Character state changes on branches are indicated by black bars (synapomorphies) and white bars (homoplasies). Character state matrix and tree statistics included. *Pseudocatolaccus asphondyliae* is shown as an example of a generic hymenopteriform larva with morphology that fits a hypothetical ancestor to the PLC. Illustrations of *Pseudocatolaccus asphondyliae* modified from Parker (1924); *Chrysolampus sisymbrii* modified from Darling and Miller (1991); *Aperilampus varians* modified from Darling (1992); *Moncacon robertsi* modified from Darling and Roberts (1999); *Orasema delicatula* modified from Burks et al. (2015).

absent. It differs from *Peckianus* by the iridescent blue or green coloration of the body, posterior end of the mesoscutal midlobe broadly separating the axillae (by 0.18–0.23× the length of the mesoscutal midlobe; 0.08–0.09× in *Peckianus*), marginal vein on fore wing short (0.1–0.13× the length of the fore wing; 0.2–0.21× in *Peckianus*). It differs from *Collessina* by having a moderately setose body (setae sometimes spatulate), head and mesosoma more coarsely reticulate, antenna with two anelli, scape not reaching median ocellus, notauli and scutoscutellar sulcus distinct, marginal vein on fore wing with a continuous width (not increasing distally).

Key to the species of *Eutrichosoma*

1 Body covered with distinctly wide, spatulate setae; stigmal vein angulate medially..... ***Eutrichosoma mirabile*** **Ashmead**

– Body covered with thin, simple setae; stigmal vein nearly straight, without obvious angle..... **2**

2 Occipital carina present; mesoscutellar disc finely granulate; male antenna flabellate (females unknown); body length 2.9–3.1 mm..... ..... ***Eutrichosoma flabellatum*** **Bouček**

– Occipital carina absent; mesoscutellar disc transversely imbricate; female antenna simple (males unknown); body length 1.9 mm... ***Eutrichosoma burksi*** **sp. nov.**

Eutrichosoma mirabile **Ashmead**
Fig. 1A–H

Eutrichosoma mirabile Ashmead 1904: 375. Lectotype designated by Gahan and Peck (1946: 315): USA: Montana: Helena (female). Deposited in USNM.
Eutrichosoma albipes Crawford 1908: 158–159. Synonymy by Bouček, 1975. Holotype: USA: Texas: Dallas (female). Deposited in USNM.
E. mirabile; Bouček 1975: 132–133. Redescription and identification key.

Biology and life history. Eggs and first-instar larvae were found inside the early (green) seedpods of *Vachellia constricta* and associated with the presence of weevil eggs and larvae (Curculionidae). *Eutrichosoma mirabile* eggs are laid among the host eggs inside the seedpods between the ovule and the inner wall of the pod. Hatching of the parasitoid seems to coincide with or precede hatching of the host because parasitoid eggs were never observed without host eggs. The majority of planidia found were parasitizing first- or second-instar weevils (~85%). Typically, only one planidium was found per host, positioned anterodorsally on the body just behind the head attached by the mandibles; always on the external surface and never penetrating the cuticle. The remaining unattached planidia were observed crawling around near clusters of host eggs. Eggs and planidia were the only life stages of the wasps observed in the seedpods. While there may be several eggs and early instars of weevil (up to ~10) per ovule within a seedpod, by the time the weevils are in their fourth instar, there is only one individual per ovule remaining. Considering the wasps are ectoparasitic koinobionts, they are likely detaching then reattaching and repositioning themselves on their hosts between host molts or transferring between individual host larvae. Given the similarities between *E. mirabile* and chrysolampines (discussed below), it is assumed that the *E. mirabile* planidia remain attached externally to the weevil when it leaves the seedpod to pupate in the soil, where the parasitoid likely finishes development. We were not able to keep the weevil larvae alive outside of the pods to allow the parasitoid to develop further. Parasitism rates shown in Suppl. material 1: Table S3.

Egg (Fig. 1A). Egg body length approximately 0.2 mm, maximum width approximately 0.07 mm; ovoid; caudal stalk about half as long as the body of the egg. Eggs separate, not forming tight clusters.

Planidium (Fig. 1B–H). Length approximately 0.13 mm, maximum width approximately 0.05 mm; fusiform in shape. Body and cranium white, darkened around mouth (Fig. 1C). Cranium with one pair of short, papilliform antennae (*ant*), one pair of longer, thinner pleurostomal setae (*plst*), and one pair of minute, lateral cranial spines (*cs*); postlabium (*psl*) large, flat, circular, and surrounding prelabium (*prl*); labial palp (*lp*) present; pleurostomal bridge (*psb*) present and connected by thin integument (Fig. 1E). Thirteen body segments beyond head; terga lightly sclerotized and ring-like, encircling the body; band of 1–2 irregular rows of tubercles (*tbs*) on anteroventral side of terga II–XII; prominent dorsolateral spines (*spn*) on terga I and III–XI; setae (*set*) present on terga I–VIII and XII, with three pairs on tergum II and two pairs on tergum III; short cerci present on XIII (*cer*); spiracles on terga II, IV–VI (*spi*) (Fig. 1B, D, F–G).

Determining if a first-instar larva is a type I planidium (i.e. undergoes hypermetamorphosis sensu Pinto (2009)) requires examination of subsequent instars, which we did not find for *Eutrichosoma*. However, the mobility of the larvae observed in the seedpods and inferred from their koinobiont ectoparasitc behavior suggests that *Eutrichosoma* behavior is congruent with other PLC larvae, even if their morphology is not as derived as Eucharitidae, Perilampinae, or Philomidinae, which are all more heavily sclerotized and generally lack ventral fusion of the terga. Larvae of Eutrichosomatinae and Chrysolampinae appear to be somewhat intermediate between typically hymenopteriform first instars of other chalcidoid taxa and the highly derived planidial larvae in the PLC.

Material examined. USA: Arizona: Cochise Co.: Canadian Lane, Portal, 1426m, 31°55'1"N, 109°07'37"W, 28.viii.2016, A. Baker & S. Heacox, **AB16.024** [2 larvae slide mounted, UCRCENT00513221–2]; 4.viii.2018, A. Baker, S. Heacox, L. Kresslein, **AB18.007** [larvae in alcohol, UCRCENT00513223] **deposition UCRC**.

Eutrichosoma burksi sp. nov.

http://zoobank.org/A3F880D1-467D-4201-A113-E39BE80A644F
Fig. 3A–F

Diagnosis. Recognized from other *Eutrichosoma* by the following combination of characters: body with metallic green coloration; stigma enlarged, stigmal vein short and not elbowed; setae relatively thin and sparse; transversely imbricate sculpture on mesosoma dorsally; lacking vertexal carina.

Female. Length 1.9 mm.

Color. Head, mesosoma, scape, pedicel, and coxae dark green; anellus and flagellum brown; mandible reddish brown; maxilla and labium brown. Femora and tibiae dark brown with green reflections medially, pale at tips. Fore wing hyaline, venation pale brown. Gaster dark brown with green iridescence.

Head (Fig. 3B). Head in frontal view subcircular; head width:height 1.24; face reticulate; scrobal depression shallow, laterally rounded; eyes with minute setae; malar

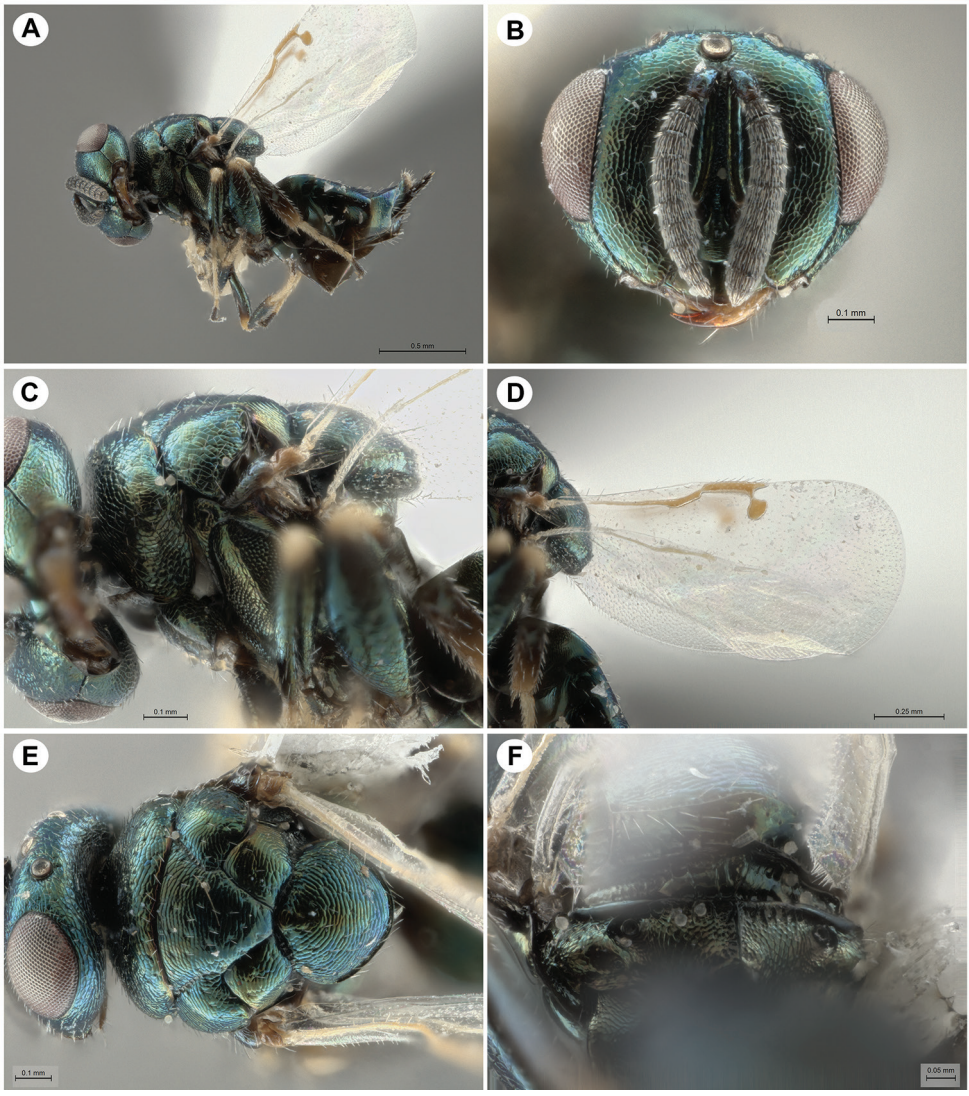

Figure 3. *Eutrichosoma burksi* sp. nov. holotype, adult female. **A** Lateral habitus **B** anterior head **C** lateral mesosoma **D** lateral wing **E** dorsal mesosoma **F** posterior propodeum.

sulcus present; clypeus smooth with rounded margin; epistomal sulcus distinct and sharply defined; anterior tentorial pit shallow; anteclypeus distinct, broadly rounded; palpal formula 4:3; mandibular formula not observed; occiput strigate, emarginate in dorsal view, dorsal margin evenly rounded; temples present, rounded. Antennal scape not reaching median ocellus; pedicel elongate, more than 1.5× as long as broad; antenna with 12 flagellomeres, including small terminal button (F12) at end of clava (clava 4-segmented); flagellum length:head height 0.81; anellus disc-shaped; second flagellomere (F2) 0.78× as long as broad, 0.75× as long as F3; following flagellomeres subequal in length, gradually broader; clava subconical.

Mesosoma (Fig. 3C–F). Mesosoma length:height 1.28; mesoscutal midlobe, lateral lobe, axilla, and mesoscutellum transversely imbricate to coriacious, sparsely setose (Fig. 3E); notauli deeply impressed along entire length; axilla dorsally rounded, on roughly same plane as mesoscutellar disc; scutoscutellar sulcus broad, irregularly foveate, fused with transscutal articulation medially; propodeal disc broadly rounded, reticulate, with median carina (Fig. 3F); callus bulbous, projecting posteriorly beyond the lateral margins of the propodeum, reticulate, with several long hairs; mesepisternum reticulate; upper mesepimeron smooth; lower mesepimeron reticulate; transepimeral sulcus distinct; propleuron nearly flat, transversely imbricate. Hind femur 3.39× as long as broad, with long stout setae; hind tibia with long stout setae. Fore wing 2.13× as long as broad, basal cell and speculum bare, costal cell sparsely setose, wing disc moderately setose; marginal fringe absent; submarginal vein with nine long setae dorsally; marginal vein with eight long setae along the margin; parastigmal vein slightly thicker than submarginal, constricted at connection with marginal vein; stigmal vein straight, narrow, short; stigma large, slightly angled; uncus absent; postmarginal vein short but obvious; hind wing costal cell with a broad bare area medially.

Metasoma. Gaster appears sessile, petiole short and indistinct; first gastral tergum longer than subsequent terga; sparsely setose dorsally, with more setae laterally. Ovipositor sheaths protruding a short distance past the last gastral tergum.

Male. Unknown.

Biology. Unknown

Material examined. ***Holotype*****: USA: California:** San Bernardino Co.: Kelso Dunes Rd, 775m, 34°53'23"N, 115°43'05"W, 19.v.2001, D. Yanega [1 ♀, UCRCENT00221857], **deposition UCRC**.

Etymology. Named in honor of Roger A. Burks, whose expertise led to the recognition of this specimen as a new species.

Discussion

The larval morphology and life history of *Eutrichosoma mirabile* is quite similar to species of *Chrysolampus* (Chrysolampinae). Both taxa lay their eggs in seedpods infested with seed-feeding weevil larvae (Darling and Miller 1991). The larvae of these wasps are strikingly similar, with the position of the spines and setae being the most obvious means to differentiate the two. These observations along with the digitate labral morphology for adults (Darling 1988) and the molecular phylogenetic support from both traditional Sanger sequencing datasets (Heraty et al. 2013) and next-generation sequencing datasets (Heraty et al. unpublished; Rasplus et al. unpublished), make placement of Eutrichosomatinae in the PLC highly supported. The position of this subfamily within the PLC, however, is far less certain. While the planidia of *E. mirabile* may morphologically appear plesiomorphic to the rest of the PLC (Darling 1988), it is not consistently placed as sister to the remaining PLC with molecular data (Heraty et al. unpublished). Our analysis of a limited number of morphological characters of the

first-instar larvae supports the sister-group relationship between Eutrichosomatinae and the remaining PLC, but interpretations of larval character homologies at the family level are very difficult to make.

Pinto (2009) defines planidium as a legless type I hypermetamorphic first-instar larva; type I is characterized by the larva having to locate its own food source, survive for considerable time without desiccating or feeding, and being active, slender, and well-sclerotized. This definition accurately describes the larvae of Eucharitidae, Perilampinae, and Philomidinae, but it cannot be unambiguously applied to Chrysolampinae or Eutrichosomatinae. Females of these two taxa oviposit into seedpods, their larvae are not directly exposed to an external environment, and heavy sclerotization of the body segments is less necessary. As well, the enclosed environment does not necessitate the need for the various ornamentation of setal modifications of the other taxa that may be associated with extreme mobility. Highly mobile ectoparasitic first-instar larvae are known in other Chalcidoidea, but these are usually idiobionts where eggs are laid onto and develop on a single developmental stage of the host, with the larvae searching for an appropriate place to initiate feeding (i.e. *Spalangia* (Richardson 1913; Clausen 1940a)) or even using the first instar to cruise the host and kill competing sibling larvae before initiating feeding (i.e. *Leucospis* (Graenicher 1906; Clausen 1940a)). *Eutrichosoma mirabile* and *Chrysolampus* are unique in Chalcidoidea in that they are both ectoparasitic koinobionts, with the first instars not only highly mobile but able to pass through different life stages of the host, in this case from the host first instar to pupa. This combination is rare in Hymenoptera, being found in some Ichneumonidae, Braconidae, and Dryinidae (Gauld and Bolton 1988; Gauld and Hansen 1995; Quicke 1997). Some Eulophidae have been designated ectoparasitic koinobionts: *Eulophus larvarum* (L) (Shaw 1981) and *Euplectrus* sp. (Neser 1973); however, these taxa are fundamentally different than all of the other ectoparasitic koinobionts because they develop on a single instar of their host caterpillar, which will continue to feed for a time but does not continue developing and renders the parasitoids' status as koinobionts ambiguous. The first-instar larvae of Chrysolampinae and Eutrichosomatinae appear to represent the transition between idiobiont hymenopteriform larvae (limited mobility, weakly sclerotized) and koinobiont planidia (highly mobile, heavily sclerotized). We feel that the application of a combination of behavioral characters (koinobiont, ectoparasitoid, with eggs not directly placed on the host) allows inclusion of these transitional forms into what we term planidial larvae.

While the 28S-D2 gene region confirmed the identity of the parasitoid, which had an exact match between larva and adult (Suppl. material 1: Table S1), the identification of the larval host weevils remains a mystery. There were no exact matches between the sequenced larval weevils and any adult weevils that we collected from the acacia. Furthermore, the BLAST and BOLD results for the host larva were inconclusive past the family level (Curculionidae) for both gene regions, with the top hits being distant matches to multiple subfamilies, including Curculioninae, Ceutorhynchinae, and Tychiinae (Suppl. material 1: Table S2).

Acknowledgements

We would like to thank Roger Burks for his help recognizing the new species and verifying morphological terminology, Doug Yanega for collecting the specimen, and Scott Heacox and Luke Kresslein for assistance collecting and examining acacia seed pods. Support was provided by an NSF-DEB 1555808 award and UCR Hatch project funds to JMH and a UC van den Bosch fellowship and UC Lauren and Mildred Anderson Immature Insects Award to AJB. The authors have declared that no competing interests exist.

References

Ashmead WH (1899) On the genera of the Cleonymidae. Proceedings of the Entomological Society of Washington 4: 200–206.

Ashmead WH (1904) Classification of the chalcid flies or the superfamily Chalcidoidea, with descriptions of new species in the Carnegie Museum, collected in South America by Herbert H. Smith. Memoirs of the Carnegie Museum 1: 225–533.

Askew RR (1980) The biology and larval morphology of *Chrysolampus thenae* (Walker) (Hym., Pteromalidae). Entomologist's Monthly Magazine 115: 155–159.

Bouček Z (1974) The pteromalid subfamily Eutrichosomatinae (Hymenoptera: Chalcidoidea). Journal of Entomology 43: 129–138.

Bouček Z, Heydon SL (1997) Pteromalidae. In: Gibson, GAP, Huber, JT , Woolley, JB (Eds) Annotated keys to the genera of Nearctic Chalcidoidea (Hymenoptera). Monograph Publishing Program, Canada, 541–692.

Charlet LD, Seiler GJ (1994) Sunflower seed weevils (Coleoptera: Curculionidae) and their parasitoids from native sunflowers (*Helianthus*) in the Northern Great Plains. Annals of the Entomological Society of America 87: 831–835. https://doi.org/10.1093/aesa/87.6.831

Clancy DW (1946) The insect parasites of the Chrysopidae (Neuroptera). University of California Press, Berkeley and Los Angeles, 403–496.

Clausen CP (1940a) Entomophagous Insects. McGraw-Hill Book Company, Inc., New York and London.

Clausen CP (1940b) The immature stages of the Eucharidae. Proceedings of the Entomological Society of Washington 42: 161–170.

Crawford JC (1908) Some new Chalcidoidea. Proceedings of the Entomological Society of Washington 9: 157–160.

Darling DC (1988) Comparative morphology of the labrum in Hymenoptera: The digitate labrum of Perilampidae and Eucharitidae (Chalcidoidea). Canadian Journal of Zoology 66: 2811–2835. https://doi.org/10.1139/z88-409

Darling DC (1992) The life history and larval morphology of *Aperilampus* (Hymenoptera: Chalcidoidea: Philomidinae), with a discussion of the phylogenetic affinities of the Philomidinae. Systematic Entomology 17: 331–339. https://doi.org/10.1111/j.1365-3113.1992.tb00554.x

Darling DC (1995) New species of *Krombeinius* (Hymenoptera: Chalcidoidea: Perilampidae) from Indonesia, and the first description of first-instar larva for the genus. Zoologische Mededelingen (Leiden) 69: 209–229.

Darling DC (1999) Life history and immature stages of *Steffanolampus salicetum* (Hymenoptera: Chalcidoidea: Perilampidae). Proceedings of the Entomological Society of Ontario 130: 3–14.

Darling DC, Miller TD (1991) Life history and larval morphology of *Chrysolampus* (Hymenoptera: Chalcidoidea: Chrysolampinae) in western North America. Canadian Journal of Zoology 69: 2168–2177. https://doi.org/10.1139/z91-303

Darling DC, Roberts H (1999) Life history and larval morphology of *Monacon* (Hymenoptera: Perilampidae), parasitoids of ambrosia beetles (Coleoptera: Platypodidae). Canadian Journal of Zoology 77: 1768–1782. https://doi.org/10.1139/z99-155

Gahan AB, Peck O (1946) Notes on some Ashmeadian genotypes in the hymenopterous superfamily Chalcidoidea. Journal of the Washington Academy of Sciences 36.

Gauld ID, Bolton B (1988) The Hymenoptera. Oxford University Press, New York.

Gauld ID, Hansen P (1995) Carnivory in the larval Hymenoptera. In: Hansen, P, Gauld ID (Eds) The Hymenoptera of Costa Rica. Oxford University Press, Oxford, 893.

Graenicher S (1906) On the habits and life-history of *Leucospis affinis* (Say). A parasite of bees. Bulletin of Wisconsin Natural History Society 4: 153–160.

Heraty JM (1994) Classification and evolution of the Oraseminae in the Old World, including revisions of two closely related genera of Eucharitinae (Hymenoptera: Eucharitidae). Life Sciences Contributions 157: 1–174. https://doi.org/10.5962/bhl.title.53489

Heraty JM (2000) Phylogenetic relationships of Oraseminae (Hymenoptera: Eucharitidae). Annals of the Entomological Society of America 93: 374–390. https://doi.org/10.1603/0013-8746(2000)093[0374:PROOHE]2.0.CO;2

Heraty JM (2002) A revision of the genera of Eucharitidae (Hymenoptera: Chalcidoidea) of the world. Memoirs of the American Entomological Institute 68: 1–359.

Heraty JM (2004) Three new species of Gollumiella Hedqvist (Hymenoptera: Eucharitidae). Zootaxa 497: 1–10. https://doi.org/10.11646/zootaxa497.1.1

Heraty JM, Barber KN (1990) Biology of *Obeza floridana* (Ashmead) and *Pseudochalcura gibbosa* (Provancher) (Hymenoptera: Eucharitidae). Proceedings of the Entomological Society of Washington 92: 248–258.

Heraty JM, Burks RA, Cruaud A, Gibson GAP, Liljeblad J, Munro J, Rasplus JY, Delvare G, Jansta P, Gumovsky A, Huber J, Woolley JB, Krogmann L, Heydon S, Polaszek A, Schmidt S, Darling DC, Gates MW, Mottern J, Murray E, Dal Molin A, Triapitsyn S, Baur H, Pinto JD, van Noort S, George J, Yoder M (2013) A phylogenetic analysis of the megadiverse Chalcidoidea (Hymenoptera). Cladistics 29: 466–542. https://doi.org/10.1111/cla.12006

Heraty JM, Burks RA, Mbanyana N, Van Noort S (2018) Morphology and life history of an ant parasitoid, *Psilocharis afra* (Hymenoptera: Eucharitidae). Zootaxa 4482. https://doi.org/10.11646/zootaxa.4482.3.3

Heraty JM, Darling DC (1984) Comparative morphology of the planidial larvae of Eucharitidae and Perilampidae (Hymenoptera: Chalcidoidea). Systematic Entomology 9: 309–328. https://doi.org/10.1111/j.1365-3113.1984.tb00056.x

Heraty JM, Derafshan HA, Moghaddam MG (2019) Review of the Philomidinae Ruschka (Hymenoptera: Chalcidoidea: Perilampidae), with description of three new species. Arthropod Systematics and Phylogeny 77: 39–56.

Heraty JM, Hawks D (1998) Hexamethyldisilazane – A chemical alternative for drying insects. Entomological News 109: 369–374.

Heraty JM, Murray E (2013) The life history of *Pseudometagea schwarzii*, with a discussion of the evolution of endoparasitism and koinobiosis in Eucharitidae and Perilampidae (Chalcidoidea). Journal of Hymenoptera Research 35: 1–15. https://doi.org/10.3897/jhr.35.6025

Johnson M, Zaretskaya I, Raytselis Y, Merezhuk Y, McGinnis S, Madden TL (2008) NCBI BLAST: a better web interface. Nucleic Acids Research 36: W5–9. https://doi.org/10.1093/nar/gkn201

Maddison DR, Maddison WP (2017a) Chromaseq: a Mesquite package for analyzing sequence chromatograms. Version 1.3. http://mesquiteproject.org/packages/chromaseq

Maddison WP, Maddison DR (2017b) Mesquite: a modular system for evolutionary analysis. Version 3.31. http://mesquiteproject.org

Munro JB, Heraty JM, Burks RA, Hawks D, Mottern J, Cruaud A, Rasplus JY, Jansta P (2011) A molecular phylogeny of the Chalcidoidea (Hymenoptera). PLoS ONE 6: e27023. https://doi.org/10.1371/journal.pone.0027023

Neser S (1973) Biology and behaviour of *Euplectrus* species near *Laphygmae* Ferrière (Hymenoptera: Eulophidae). Entomology Memoir, Department of Agriculture Techincal Services, Republic of South Africa, No. 32: 1–31.

Parker HL (1924) Recherches sur les formes post-embryonnaires des chalcidiens. Annales de la Societe Entomologique de France 93: 264–379.

Peck O (1951) Superfamily Chalcidoidea. In: Muesebeck, CFW, Krombein, KV, Townes HK (Eds) Hymenoptera of America north of Mexico – Synoptic catalog. Agriculture Monographs U.S. Department of Agriculture, Washington D.C., 410–594.

Pinto JD (2009) Hypermetamorphosis. In: Resh VH, Carde RT (Eds) Encyclopedia of Insects. Academic Press, 484–486. https://doi.org/10.1016/B978-0-12-374144-8.00137-5

Quicke DLJ (1997) Parasitic Wasps. Chapman & Hall, London.

Ratnasingham S, Hebert PDN (2007) BOLD: The barcode of life data system (www.barcodinglife.org). Molecular Ecology Notes.

Richardson CH (1913) Studies on the habits and development of a hymenopterous parasite, *Spalangia muscidarum* Richardson. Journal of Morphology 24: 513–557. https://doi.org/10.1002/jmor.1050240404

Shaw MR (1981) Delayed inhibition of host development by the nonparalyzing venoms of parasitic wasps. Journal of Invertebrate Pathology 37: 215–221. https://doi.org/10.1016/0022-2011(81)90078-1

Swofford DL (2002) PAUP* v.4.0: phylogenetic analysis using parsimony (* and other methods). Sinauer, Sunderland, Massachusetts, USA.

Supplementary material 1

Tables S1–S3

Authors: Austin J. Baker, John M. Heraty

Data type: molecular data

Explanation note: **Table S1.** Parasitoid larva. Top hits from NCBI BLAST and BOLD online databases for two gene sequences (28S-D2 rDNA and COI-BC mtDNA) obtained from the parasitoid first-instar larva and confirming the identity as *Eutrichosoma mirabile*. **Table S2.** Host larva. Top hits from NCBI BLAST and BOLD online databases for two gene sequences (28S-D2 rDNA and COI-BC mtDNA) obtained from the host larva and confirming the identity as Curculionidae but leaving the subfamily, genus, and species unconfirmed. **Table S3.** Parasitism rates. Summary data from two collecting trips to southeastern Arizona (August 2016 and 2018) showing the rates of parasitism for the host and parasitoid, eggs and larvae on whitethorn acacia (*Vachellia constricta*).

Link: https://doi.org/10.3897/jhr.75.47880.suppl1

JHR 75: 87–95 (2020)
doi: 10.3897/jhr.75.47507
http://jhr.pensoft.net

SHORT COMMUNICATION

JOURNAL OF Hymenoptera RESEARCH
A peer-reviewed open-access journal
The International Society of Hymenopterists

One-year-old flower strips already support a quarter of a city's bee species

Michaela M. Hofmann[1], Susanne S. Renner[1]

1 *Systematic Botany and Mycology, Department of Biology, University of Munich (LMU), Menzinger Straße 67, Munich 80638, Germany*

Corresponding author: Susanne S. Renner (renner@lmu.de)

Academic editor: Jack Neff | Received 22 October 2019 | Accepted 15 December 2019 | Published 27 February 2020

http://zoobank.org/C3F78D31-0DC8-4897-B12D-AFD3F3CDB914

Citation: Hofmann MM, Renner SS (2020) One-year-old flower strips already support a quarter of a city's bee species. Journal of Hymenoptera Research 75: 87–95. https://doi.org/10.3897/jhr.75.47507

Abstract

To combat the loss of flower-rich meadows, many cities are supporting greening measures, including the creation of flower strips. To assess the effectiveness of these measures in supporting flower-visiting insects, their faunas need to be compared to the background fauna at various distances from the flower strips. To meet this goal, we quantified the bee faunas of nine 1000 m^2-large and newly established flower strips in the city of Munich, all planted with a regional seed mix, and compared them to the fauna recorded between 1997 and 2017 within 500, 1000, and 1500 m from the respective strip. The 68 species recorded during the flower strips' first season represent 21% of the 324 species recorded for Munich since 1795 and 29% of the 232 species recorded between 1997 and 2017. Non-threatened species are statistically over-represented in the strips, but pollen generalists are not. These findings illustrate the conservation value of urban flower strips for common species that apparently quickly discover this food source. To our knowledge, this is the first quantitative assessment of the speed and distance over which urban flower strips attract wild bees.

Keywords

Urban ecosystem, attraction effect, flower strips, wild bees

Introduction

Insects that rely on a mix of floral resources for their survival, such as bees and many butterflies and flies, are rapidly decreasing in diversity and abundance (Mandery et al. 2003, Potts et al. 2010, Westrich et al. 2011). One reason for this is the loss of flower-rich meadows, which are becoming increasingly rare. In Germany, for example, meadows covered 5.3 Million hectares (Mio. ha) in 1991, but only 4.7 Mio. ha in 2019 (Statistisches Bundesamt, accessed May 2019). To address the loss of flower-rich areas, the European Union is supporting 'greening' measures, which include the creation of flower strips (European Commission 2011). Flower strips are man-made patches of flowering plants that provide foraging resources for flower-visiting insects, especially bees, butterflies, and flies. Monitoring and experiments have shown that such strips enhance the local plant and insect diversity in agricultural landscapes (e.g. Scheper et al. 2015, Jönsson et al. 2015, Buhk et al. 2018, Dicks et al. 2017 review 80 studies of flower strips).

Despite the work demonstrating the diversity-enhancing effects of flower strips near crops, it is unclear what proportion of bee diversity these usually small, young, and artificial plantings may be 'capturing' and how strongly their faunas may be biased towards common insect species. From first principles, the success of flower strips in maintaining populations of solitary bees will depend on their floristic composition, distance from suitable nesting sites, and distance from other habitats that maintain stable populations. To study the attractiveness of flower strips in an urban landscape, we took advantage of nine 1000 m²-large flower strips newly established in Munich, all with autochthonous seed mixtures selected by the Bavarian bird protection society (Landesbund für Vogelschutz, acronym LBV) and Munich's Department of Horticulture (Gartenbaureferat München). We identified and counted the bees visiting flowers on each strip and then related these numbers to the total diversity of Munich's bee fauna and to the diversity at different distances from the strips. Our expectation was that newly planted flowers strips would attract a small subset of mostly generalist, non-threatened species and that oligolectic species (species using pollen from a taxonomically restricted set of plants) would be underrepresented compared to the city's overall species pool.

Material and methods

Study sites and plant species inventories

In April 2017, the Regional Society for the Protection of Birds (LBV) and the Department of Horticulture of the city of Munich created eight 1000 m²-large flower strips; besides these eight strips, we included another 1000 m²-strip established by the same group in 2015 (Fig. 1). All strips, which initially were covered by lawn or roadside greenery, were ploughed by machine and then sown with regional seeds from the seed

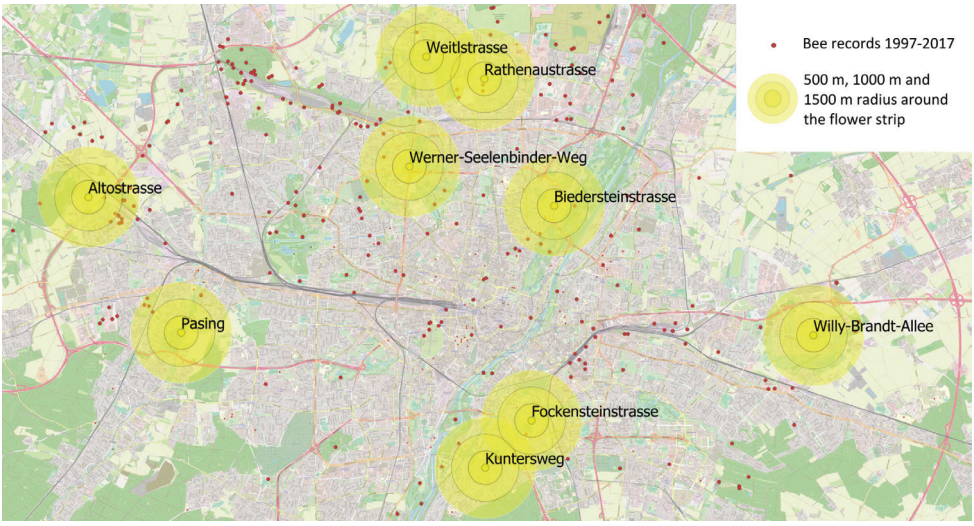

Figure 1. The nine flower strips monitored for this study (modified from https://www.openstreetmap.org, using QGIS 3.8.2 (QGIS Development Team 2019) and Munich's bee records (sightings and/or specimens) between 1997 and 2017.

supplier Kirmer (http://www.krimmer-naturnahes-gruen.de), adapted either for nutrient-rich or nutrient-poor sites, and the LBV also provided man-made nesting sites for cavity-breeding bees at the sites. They therefore all started from bare soil. Flowering plants present after the initial sowing were identified in randomly placed plots of one square-meter per strip at the strips Fockensteinstraße (established in 2015), Willy-Brandt-Allee and Rathenaustraße (nutrient-poor sites established in 2017), and Pasing Stadtpark, and Werner-Seelenbinder-Weg (nutrient-rich sites established in 2017). Plant species found on each strip are listed in Suppl. material 1, Table S1, along with information on herbarium voucher specimens deposited in the Munich herbarium (Botanische Staatssammlung, international acronym M).

Bee species inventories

From March to August in 2017 and 2018, each flower strip was visited four to five times. Visits were made between 10 a.m. and 4 p.m. on sunny, warm days with little or no wind. Where possible, bee species were identified directly in the field and were documented via macro-photography in a standardized setup: for close-up pictures, the bees were caught with an insect net and cooled down for 10 minutes in an Eppendorf screw-capped plastic vial stored on ice in a cooled box. When they fell into rigor of cold, they were transferred onto scale paper (using a small box lined with millimetre paper on its bottom) and photographed from all sides (SLR camera: Pentax K-x; Lens: Sigma DG 17-70 mm, 1:2.8, macro). Within one to two minutes, bees warmed up again and were released at the location where they had been caught. For

species that are difficult to identify by morphology alone, such as species of *Sphecodes*, *Lasioglossum* or *Halictus*, voucher specimens, preferably males (for re-identification by genitalia preparations), were collected and identified morphologically and via DNA barcoding (methods and primers as described in Hofmann et al. 2018). The voucher specimens are deposited in the Zoologische Staatssammlung Munich (ZSM). Photo vouchers are accessible at the Diversity Workbench server (DWB; https://diversityworkbench.net/Portal/Diversity_Workbench), and DNA barcodes at NCBI GenBank (https://www.ncbi.nlm.nih.gov/genbank). Suppl. material 2, Table S2 in the Online Supporting Material shows all GenBank and DWB accession numbers. Additionally, Suppl. material 2, Table S2 shows each species' Red List status based on Westrich et al. (2011) as well as foraging and nesting preferences based on Scheuchl and Willner (2016).

To investigate the catchment area of each flower strip, we analysed 7589 records with Gauß-Krüger coordinates made between 1997 and 2017 of single bees or populations and documented either by specimens stored at the Zoological Collections in Munich and/or by taxonomic assessments in Munich's red lists. We focused on the area within a radius of 500, 1000, and 1500 m from each strip using QGIS 3.8.2 (QGIS Development Team 2019). For species that were recorded on a flower strip, but not within the 1500 m radius from the strip, we measured the distance from the strip to the nearest sighting of the respective species (Suppl. material 3, Table S3). For Fockensteinstraße and Willy-Brandt-Allee, we increased the radius to 1600 m, as there were too few records within the 1500 m radius, while a 1600 m radius yielded comparable numbers of records to those of the other sites.

Results

Oligolecty and Red List status of the species on the flower strips compared to the total Munich species pool

On the nine 1000 m²-large flower strips, we found 83 species of flowering plants, 35 of them coming from the regional seed mix *(Materials and Methods*) and 17 self-sown at Fockensteinstraße (Fig. 2), 27 from the seed mix and 28 self-sown at Rathenaustraße and Willy-Brandt-Allee, and all 23 from the seed mix at Pasinger Stadtpark and Werner-Seelenbinder-Weg (see Suppl. material 1, Table S1 for species lists for each site). The flowers of these plants were visited by honey bees and 68 species of wild bees, that is 21% of the 324 species recorded for Munich since 1795 and 29% of the 232 re-observed or newly observed species over the last twenty years (1997–2017).

Of the 68 species, 62 (91%) have the Red List category 'not threatened,' three (4%) are listed on the pre-warning-list, and three are 'threatened' (Suppl. material 2, Table S2). The respective percentages for the 324-species-pool are 54% (n = 174) not threatened, 11% (n = 35) on the pre-warning list, and 27% (n = 89) threatened. Twenty-two

Figure 2. The flower strip at Fockensteinstraße as an example of the urban context of the flower strips studied here.

of the 324 species are not Red-listed due to a lack of data, and three are considered locally extinct. There are thus significantly more non-threatened species on the flower strips than in Munich overall (chi-square test with 2 df, $\chi^2 = 26.4$, $P = 1.8 \times 10^{-6}$). Of the 232-species-pool recorded for 1997–2017, 156 (67%) species are non-threatened, 29 (13%) on the pre-warning list, 38 (16%) threatened, and 9 (4%) of unknown status. With these numbers, too, the flower strip fauna includes a disproportionate number of non-threatened species (chi-square test with 2 df, $\chi^2 = 12.5$, $P = 0.002$).

Of the 68 species found on the strips, 63% (n = 43) are polylectic and 15% (n = 10) oligolectic. Some 22% (n = 15) parasitize other bee species (Suppl. material 2, Table S2). The respective percentages for the 324 species pool are 51% (n = 165) polylectic, 22% (n = 72) oligolectic, and 27% (n = 87) parasitic (Hofmann and Renner, in review), while in the 232 species pool of the last 20 years, 50% (n = 118) of species are polylectic, 25% (n = 59) oligolectic, and 24% (n = 55) parasitic. Of the oligolectic flower strip visitors, seven specialized on Asteraceae, two on *Campanula* (Campanulaceae), one on *Echium* (Boraginaceae), and one on Fabaceae. There is thus no significant difference in the frequencies of polylectic, oligolectic, or parasitic species among the flower strips and the remainder of Munich either for the larger pool (chi-square test with 2 df, $\chi^2 = 3.62$, $P = 0.164$) or the smaller 1997–2017 pool (2df, $\chi^2 = 4.19$, $P = 0.123$).

‘Catchment areas’ of the flower strips

Our quantification of species recorded between 1997 and 2017 within a radius of 500, 1000, or 1500 m around each of the nine flower strips revealed that the strips at Altostraße (400 records of 105 different species) and Pasinger Stadtpark (329 records of 156 species) were richest in bees within a radius of 1500 m around them, while Weitlstraße and Willy-Brandt-Allee (19 records of 15 species each) have the fewest records within 1500/1600 m around them (Fig. 3; Suppl. material 3, Table S3).

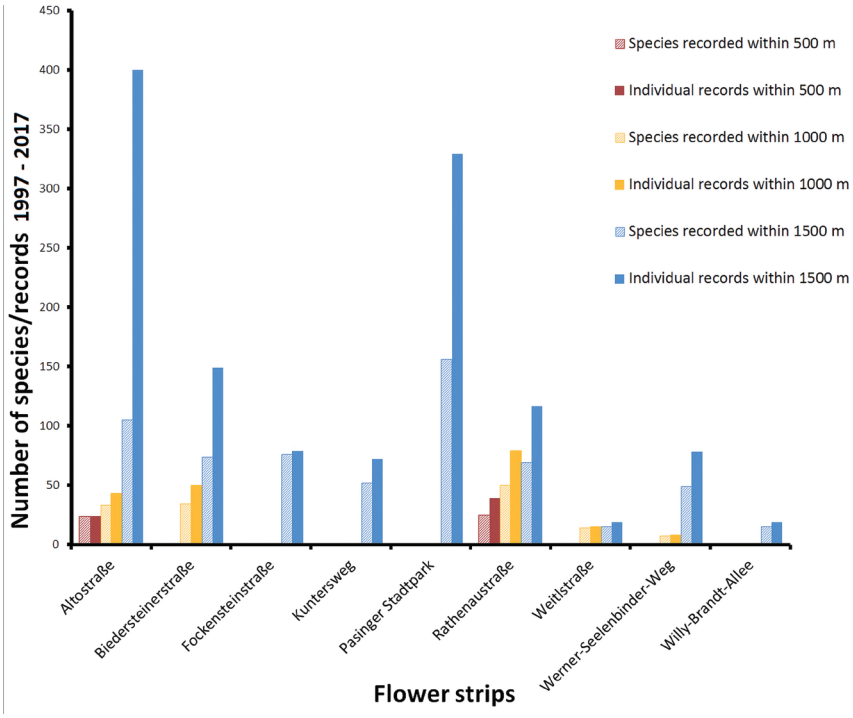

Figure 3. Numbers of species and individuals recorded between 1997 and 2017 within a radius of 500, 1000, and 1500 m from the centre of the respective flower strip (compare Fig. 1). For details of how past recordings were made see Materials and Methods.

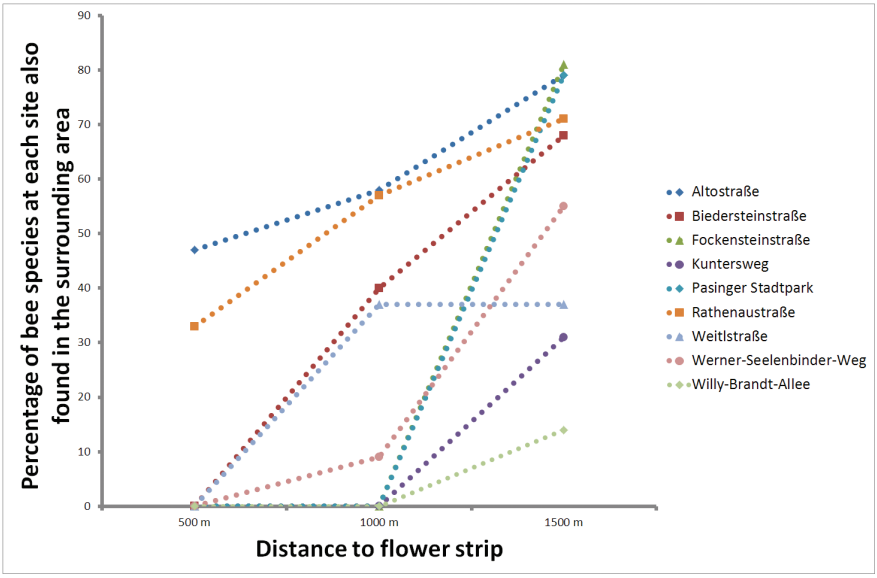

Figure 4. The percentage of bee species recorded at each flower strip that is also found in the surrounding area at distances of 500, 1000, and 1500 m.

Discussion

Bees need time to discover newly created habitat, but Munich's common species did so in just one year, so that the 1000 m^2-small and young flower strips studied here attracted 68 (21%) of the 324 species ever recorded for Munich and 29% of the 232 species recorded during 1997–2017. These percentages are similar to those found for much larger protected sites in Munich. Thus, 105 species (32% of the 324 species pool) were recorded in 2017/2018 in the 21 ha-large Munich botanical garden and 44 species (14% of 324) in a 20 ha-large protected city biotope called 'Virginia Depot' (Hofmann & Renner, in review). Surprisingly, the flower strips attracted a random subset of Munich's bee species in terms of pollen specialization, although as expected, the first-year flower-strip visitors mostly belong to common, non-threatened species. To demonstrate positive effects of flower strips on pollinator populations it would be necessary to show increased abundances of pollinators at the urban landscape scale, which was not part of this study. Still, our data strongly support that flower strip planting in cities helps ensure the availability of foraging resources for pollinators and that this simple conservation measure is effective. We therefore agree with Buhk et al.'s (2018) call that flower strip networks should be implemented much more in the upcoming Common Agricultural Policy (CAP) reform in the European Union.

Acknowledgements

We thank the biology students Pia Schumann, Nadine Dasch, and Thomas Greindl for support with field work, Markus Bräu, Munich city Department of Health and Environment, for sharing bee occurrence data for Munich, and Jack Neff and an anonymous reviewer for their comments on the manuscript.

References

Buhk C, Oppermann R, Schanowski A, Bleil R, Lüdemann J,Maus C (2018) Flower strip networks offer promising long-term effects on pollinator species richness in intensively cultivated agricultural areas. BMC Ecology 18: 55. https://doi.org/10.1186/s12898-018-0210-z

Dicks LV, Ashpole JE, Dänhardt J, James K, Jönsson A, Randall N, Showler D, Smith RK, Turpie S, Williams DR, Sutherland WJ (2017) Farmland Conservation. In: Sutherland WJ, Dicks LV, Ockendon N, Smith RK (Eds) What Works in Conservation 2017. Open Book Publishers, Cambridge, 245–284 . https://doi.org/10.11647/OBP.0131.04

European Commission (2011) CAP Reform – an explanation of the main elements MEMO/11/685. http://www.ala.org.uk/sites/default/files/ExplanatoryMemo.pdf

Hofmann MM, Fleischmann A, Renner SS (2018) Changes in the bee fauna of a German botanical garden between 1997 and 2017, attributable to climate warming, not other parameters. Oecologia 187: 701–706. https://doi.org/10.1007/s00442-018-4110-x

Hofmann MM, Renner SS (in review) Bee species persistence and increase in urban protected sites between 1990 and 2018. Journal of Insect Conservation.

Jönsson AM, Ekroos J, Dänhardt J, Andersson GK, Olsson O, Smith HG (2015) Sown flower strips in southern Sweden increase abundances of wild bees and hoverflies in the wider landscape. Biological Conservation 184: 51–58. https://doi.org/10.1016/j.biocon.2014.12.027

Mandery K, Voith J, Kraus M, Weber K, Wickl K (2003) Rote Liste gefährdeter Bienen (Hymenoptera: Apidae) Bayerns. Bayerisches Landesamt für Umweltschutz 166: 198–207.

Potts SG, Biesmeijer JC, Kremen C, Neumann P, Schweiger O, Kunin WE (2010) Global pollinator declines: trends, impacts and drivers. Trends in Ecology & Evolution 25: 345–353. https://doi.org/10.1016/j.tree.2010.01.007

QGIS Development Team (2019) QGIS Geographic Information System. Open Source Geospatial Foundation Project. http://qgis.osgeo.org

Scheper J, Bommarco R, Holzschuh A, Potts SG, Riedinger V, Roberts SP, Rundlöf M, Smith HG, Steffan-Dewenter I, Wickens JB, Wickens VJ (2015) Local and landscape-level floral resources explain effects of wildflower strips on wild bees across four European countries. Journal of Applied Ecology 52: 1165–1175. https://doi.org/10.1111/1365-2664.12479

Scheuchl E, Willner W (2016) Taschenlexikon der Wildbienen Mitteleuropas: Alle Arten im Porträt. Quelle et Meyer Verlag. Wiebelsheim, 917 pp.

Statistisches Bundesamt (2019) Statistisches Bundesamt. https://www.destatis.de/DE/Themen/Branchen-Unternehmen/Landwirtschaft-Forstwirtschaft-Fischerei/Feldfruechte-Gruenland/Tabellen/zeitreihe-dauergruenland-nach-nutzung.html

Westrich P, Frommer U, Mandery K, Riemann H, Ruhnke H, Saure C, Voith J (2011) Rote Liste und Gesamtartenliste der Bienen (Hymenoptera, Apidae) Deutschlands. In: Binot-Hafke M, Balzer S, Becker N, Gruttke H, Haupt H, Hofbauer N, Ludwig G, Matzke-Hajek G, Strauch M (Eds) Rote Liste gefährdeter Tiere, Pflanzen und Pilze Deutschlands. Band 3: Wirbellose Tiere (Teil 1). – Münster (Landwirtschaftsverlag). Naturschutz und Biologische Vielfalt 70: 373–416. https://www.wildbienen.info/downloads/rote_liste_bienen_fassung_5.pdf

Supplementary material 1

Table S1. Lists of plant species and voucher specimens for the nine flower strips

Authors: Michaela M. Hofmann, Susanne S. Renner

Data type: species data

Link: https://doi.org/10.3897/jhr.75.47507.suppl1

Supplementary material 2

Table S2. GenBank and Diversity Workbench accession numbers of the bee voucher specimens

Authors: Michaela M. Hofmann, Susanne S. Renner

Data type: accession numbers

Explanation note: GenBank (https://www.ncbi.nlm.nih.gov/genbank) and Diversity Workbench (https://diversityworkbench.net/Portal/Diversity_Workbench) accession numbers of the bee voucher specimens. Diversity Work Bench accession numbers start with three letters referring to the respective flower strip site. The remaining numbers are GenBank accession numbers for the DNA barcode sequences. Physical vouchers have been deposited in the Zoologische Staatssammlung München.

Link: https://doi.org/10.3897/jhr.75.47507.suppl2

Supplementary material 3

Table S3. List of bee species records at different radii around the nine flower strips (1997–2017)

Authors: Michaela M. Hofmann, Susanne S. Renner

Data type: species data

Explanation note: Species recorded within the last twenty years at 500, 1000, and 1500 m distance from the respective flower strip

Link: https://doi.org/10.3897/jhr.75.47507.suppl3

JHR 75: 97–108 (2020)
doi: 10.3897/jhr.75.47828
http://jhr.pensoft.net

SHORT COMMUNICATION

JOURNAL OF Hymenoptera RESEARCH
A peer-reviewed open-access journal
The International Society of Hymenopterists

The first gynandromorph of the Neotropical bee *Megalopta amoena* (Spinola, 1853) (Halictidae) with notes on its circadian rhythm

Erin Krichilsky[1], Álvaro Vega-Hidalgo[2], Kate Hunter[3], Callum Kingwell[4], Chelsey Ritner[3], William Wcislo[5], Adam Smith[6]

1 *Department of Entomology, Cornell University, Ithaca, New York, USA* **2** *Escuela de Ciencias Biológicas, Universidad Nacional de Costa Rica, Heredia, Costa Rica* **3** *Biology Department, Utah State University, Logan, Utah, USA* **4** *Department of Neurobiology and Behavior, Cornell University, Ithaca, New York, USA* **5** *Instituto Smithsonian de Investigaciones Tropicales, Balboa, Panamá* **6** *Department of Biological Sciences, George Washington University, Washington DC, USA*

Corresponding author: Erin Krichilsky (ek525@cornell.edu); Adam Smith (adam_smith@gwu.edu)

Academic editor: Jack Neff | Received 30 October 2019 | Accepted 31 December 2019 | Published 27 February 2020

http://zoobank.org/01FF1CE8-64F8-42D1-B9EA-EBB89DBBC70A

Citation: Krichilsky E, Vega-Hidalgo Á, Hunter K, Kingwell C, Ritner C, Wcislo W, Smith A (2020) The first gynandromorph of the Neotropical bee *Megalopta amoena* (Spinola, 1853) (Halictidae) with notes on its circadian rhythm. Journal of Hymenoptera Research 75: 97–108. https://doi.org/10.3897/jhr.75.47828

Abstract

Gynandromorphy is an anomaly that results in an organism phenotypically expressing both male and female characteristics. Here we describe the first gynandromorph of the bee species *Megalopta amoena* (Spinola, 1853) (Halictidae, Augochlorini) and the second record of this anomaly within the genus *Megalopta*. Additionally, we analyzed the bee's circadian rhythm, which has never before been quantified for a gynandromorph. The gynandromorph showed a deviant activity pattern; it was intermediate between that of the male and female *M. amoena*. Our results imply that the brains of bilateral gynandromorphs may have mixed sex-specific signaling. Based on four days of recording, the gynandromorph circadian rhythm was shifted earlier in the day relative to the male and female *M. amoena*, and it exhibited intensity similar to the female.

Keywords

Sweat bee, development, morphology, Augochlorini, gynandromorph, circadian rhythm

Introduction

Gynandromorphy is a rare occurrence in which an organism presents both male and female phenotypes (Wcislo et al. 2004a). Gynandromorphs have been reported in at least 140 bee species, which is only 0.7% of all bee species (Alvarez et al. 2019, Prashantha et al. 2019, reviewed by Wcislo et al. 2004a, Michez et al. 2009, Hinojosa-Díaz et al. 2012). This phenomenon may offer insight into the evolution of specialized morphological traits, such as male-like morphology of female brood-parasitic bee lineages (Wcislo et al. 2004a), the modified morphology of social insect castes (Yang and Abouheif 2011), and novel methods of reproduction (Aamidor et al. 2018). Gynandromorphs are usually unnoticed until specimens are in museum collections, meaning that the behavior and physiology of these bees are seldom studied (Michez et al. 2009, Sampson et al. 2010, Ugajin et al. 2016, Matsuo et al. 2018). Here we report the first gynandromorph discovered in the bee species *Megalopta amoena* (Halictidae, Augochlorini); only one has been previously reported from the genus *Megalopta* (*M. genalis* Meade-Waldo, 1916; Wcislo et al. 2004a).

When the gynandromorph was discovered as a newly eclosed adult, we were engaged in a separate study of the circadian rhythms of *Megalopta* bees (Krichilsky and Vega-Hidalgo et al. unpublished data). We tested the circadian rhythm of this individual using an automated activity monitoring system (Giannoni-Guzmán et al. 2014). The few previous studies of live gynandromorphs have reported data on nesting behavior (Michez et al. 2009), courtship (Michez et al. 2009, Sampson et al. 2010, Matsuo et al. 2018), and gene expression (Ugajin et al. 2016, Matsuo et al. 2018). This is the first report of circadian activity monitoring in a gynandromorph.

Circadian rhythms are ubiquitous in animals and serve to synchronize behavior, physiology, and ecological interactions with the external environment (Dunlap et al. 2004). In bees and other pollinators, modifications of circadian rhythms may allow insects to coordinate their foraging with the timing of floral resource availability (Bloch et al. 2017). The genus *Megalopta* has a bimodal foraging period, occurring in two narrow temporal windows of approximately 90 minutes after sunset and before sunrise, when it is nearly dark (Kelber et al. 2006, Smith et al. 2017).

Methods

Gynandromorph collection

The nest containing the gynandromorph was collected midday GMT-5 on April 24th, 2018 by KH on the Drayton trail in the neotropical forest of Barro Colorado Island, Panamá (BCI; 9°09'N, 79°51'W). The nest was collected by plugging the entrance with cotton wool, placing the nest in a bag, and opening the nest in the lab under a mesh tent. Then unrecognized as a gynandromorph, the individual was in a closed brood cell. Based on the time between discovery and emergence (26 days) and the development time of the congener *M. genalis* (Smith et al 2009, Kapheim et al 2011), it was likely at the

larval stage when collected. The brood cell containing the gynandromorph was put in an incubator to develop until adult emergence with other brood from the nest at 25 C with 70% humidity, which approximates ambient conditions in the forest understory (Windsor 1990). The adults found in the nest were released. The individual was not monitored during development and not noticed as a gynandromorph until the adult stage. Upon eclosion, we weighed the gynandromorph and measured its intertegular and interoccular distances using calipers. The bee was identified as *M. amoena* based on the lack of longitudinal rugulosities on the basal area of the metapostnotum, also known as the basal area of the propodeum (Engel 2006, Santos and Melo 2015). See Wcislo et al. (2004b) for a description of the nesting biology of *M. amoena*, then classified as *M. ecuadoria*; the species has also been previously classified with nine other names (Santos and Melo 2015).

Circadian rhythm

The circadian rhythm was quantified using a Locomotor Activity Monitor (LAM), modified from the *Drosophila* Activity Monitor system (DAM) (Trikinetics Inc., Waltman, MA, USA), following Giannoni-Guzmán et al. (2014). After being weighed and measured, the gynandromorph, an adult female, and a male of *M. amoena* were each placed in a modified 15ml centrifuge tube on May 20th, 2018 and put inside of the LAM and fed with a 50:50 honey:water solution with activity automatically recorded until the gynandromorph's death on May 24th, 2018. The activity monitor measured the number of times, per 15 minute interval, that each bee crossed the laser located in the middle of their tube. The LAM was housed in constant darkness (dark-dark cycle), to test the endogenous circadian rhythm, in an incubator with the same conditions as outlined above. We used the packages *damr v*0.3.4 and *ggetho v0.3.4* of the rethomics workflow (Geissmann et al. 2019) to calculate the actograms in R v3.6.1 (R core team 2019).

We calculated activity percentage and intensity measures. The activity percentage was calculated as the percentage of activity across a day in the 15 minute intervals. If a bee did not cross the laser during an interval, it was recorded as nonactive, whereas if the bee did cross the laser at least one time, it was taken as an active interval. The activity percentage was the percentage of active intervals in a day, this measure did not take into account the intensity of the activity at each interval. The intensity was calculated by taking the highest number of laser crossings per interval in a given day. We report the average and standard deviation of the activity percentage and intensity across days. For the activity percentage and intensity measurements, we included only the second and third days to account for habituation in the first day and for the male and gynandromorph's early death.

Morphology

The terminology for external morphology follows Eickwort (1969) and Michener (2007), with modifications by Santos and Melo (2015).

Photography

A Keyence VHX-5000 digital microscope was used at 100–200× magnification to take images of the specimen. Images were edited and plates were prepared using Adobe Photoshop CC 2017.

Material deposited

The gynandromorph is now deposited at the Instituto Smithsonian de Investigaciones Tropicales (Smithsonian Tropical Research Institute) – Synoptic Insect Collection (STRI-ENTO) in Balboa, Ancón, Panamá. The *M. genalis* gynandromorph found by Wcislo et al. (2004a) was deposited in that same collection.

Results

Nest collection

The gynandromorph eclosed on 19 May, 2018. Its weight upon eclosion was 46.8 mg, the interocular distance was 1.35 mm, the intertegular distance was 1.10 mm, the metasoma was 1.6 mm long, and the overall body length was 4.03 mm. Upon collection, the nest contained two adult females, and three immature individuals, one of which was female, one male, and one gynandromorph (Table 1). The sex of the immature individuals was determined upon eclosion, as they were in an incubator in the sealed brood cells in which they were found. The presence of two adult females indicates a social nest where one was the queen and the other a daughter (Wcislo 2004b, Smith et al. 2019), but we did not dissect ovaries to confirm this. The other two immature individuals eclosed on 26 April, 2018 (male) and 3 May, 2018 (female).

Morphology

The phenotype expressed in the head has a distinct bilateral split of male and female characters (Figure 1A). The side with male characters is on the left, and the side with female characters is on the right, hereinafter referred to as the male side and the female side. The antenna on the male side has 11 flagellomeres, each with a length of 0.34 mm and a scape length of 0.71 mm. The antenna on the female side has 10 flagellomeres, each with a length of 0.23 mm and a scape length of 1.33 mm (Figure 1A). The mandible on the male side is weak, whereas the mandible on the female side is strong and bidentate with supplementary teeth (Figure 1B). The gena is not enlarged on the male side, but is on the female side in order to accommodate the larger mandibular muscu-

Table 1. Information on the contents of the nest collected by Kate Hunter (KH) from Drayton trail, BCI.

Species	Nest	Date Nest Collected	Location	Sex	Status	Eclosion Date
	375	April 24th, 2018	Drayton trail, BCI	Female	Adult	N/A
	375	April 24th, 2018	Drayton trail, BCI	Female	Adult	N/A
M. amoena	375	April 24th, 2018	Drayton trail, BCI	Male	In cell- immature	April 26th, 2018
	375	April 24th, 2018	Drayton trail, BCI	Female	In cell- immature	May 3rd, 2018
	375	April 24th, 2018	Drayton trail, BCI	Gynandromorph	In cell- immature	May 19th, 2018

lature characteristic of females (Figure 1C, D). The clypeal punctures are continuous, moderately dense, and separated by approximately one puncture width (Figure 1B). Ridges are not well defined on the right side of the head.

The posterior upper margin of the metepisternum was modified into a conspicuously large process covered with velvety pilosity (Santos and Melo 2015), it appeared similar on both sides. The hindleg on the female side is more hairy with a more robust femur and tibia, and curved apical spines on the femur (Figure 1G). The hindleg on the male side is less hairy with a more slender femur and tibia, and straight apical spines on the femur (Figure 1F).

The metasoma has bilateral asymmetry, split between male and female characters. This split was visible on the sterna, with the female side showing the metasomal scopa hairs on three fourths of the surface, used for pollen collection (Figure 1I). The male side showed few ventral abdominal hairs and S3 is mostly flat and lacking a mid longitudinal sulcus as in Santos and Melo 2015 (Figure 1E, I). There was no obviously visible asymmetry on the terga. The gynandromorph had a sting on the terminus of the metasoma, pointed outward from the female side of the body (Figure 1H). We did not dissect the specimen to observe internal anatomy, however the position of the sting indicates a mixed arrangement of both sexes.

Circadian rhythm

We compared activity of the 3 specimens in 24 hour darkness (dark:dark) for four days. The male and female activity rhythms are more similar to each other than they are to the gynandromorph (Fig. 2). The gynandromorph was active from 00 to 06 hours during days two to four, whereas the male and female of *M. amoena* showed almost no activity during that time. The gynandromorph's highest activity peak occurred in the interval from 06 to 12 hours. The female's highest activity peak was also from 06 to 12 hours. The male showed lower activity peaks than the other two bees, with the highest peak during the first day between 18 and 24 hours. The gynandromorph's activity percentage was 34 ± 4% per day, the female was 32 ± 3%, and the male was 39 ± 2%. Concerning the activity intensity, the gynandromorph averaged 91 ± 19.80, the male 31.00 ± 2.83, and the female 101.50 ± 43.13.

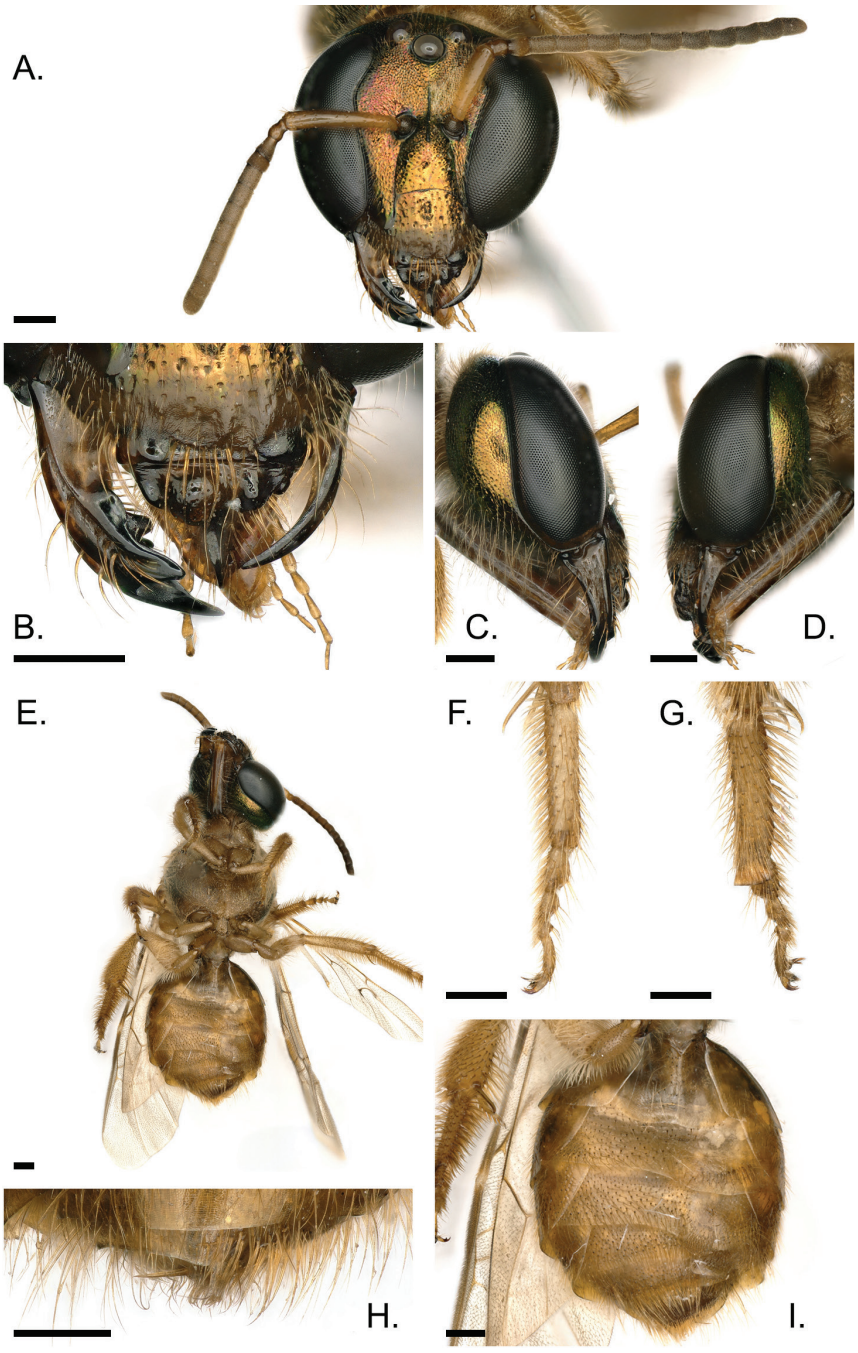

Figure 1. A Frontal view of the head showing the bilateral split between sexes (female left side of image, male right side) **B** detail of female (left) and male (right) mandibles and labrum, frontal view. Lateral view of the **C** male and **D** female genae and mandibles **E** ventral view of gynandromorph (female left side of image, male right side). Femur, apical spines, and tibia of **F** male and **G** female hindlegs **H** dorsal view of stinger **I** ventral view of metasoma (female left side of image, male right side). Scale bars: 500 μm.

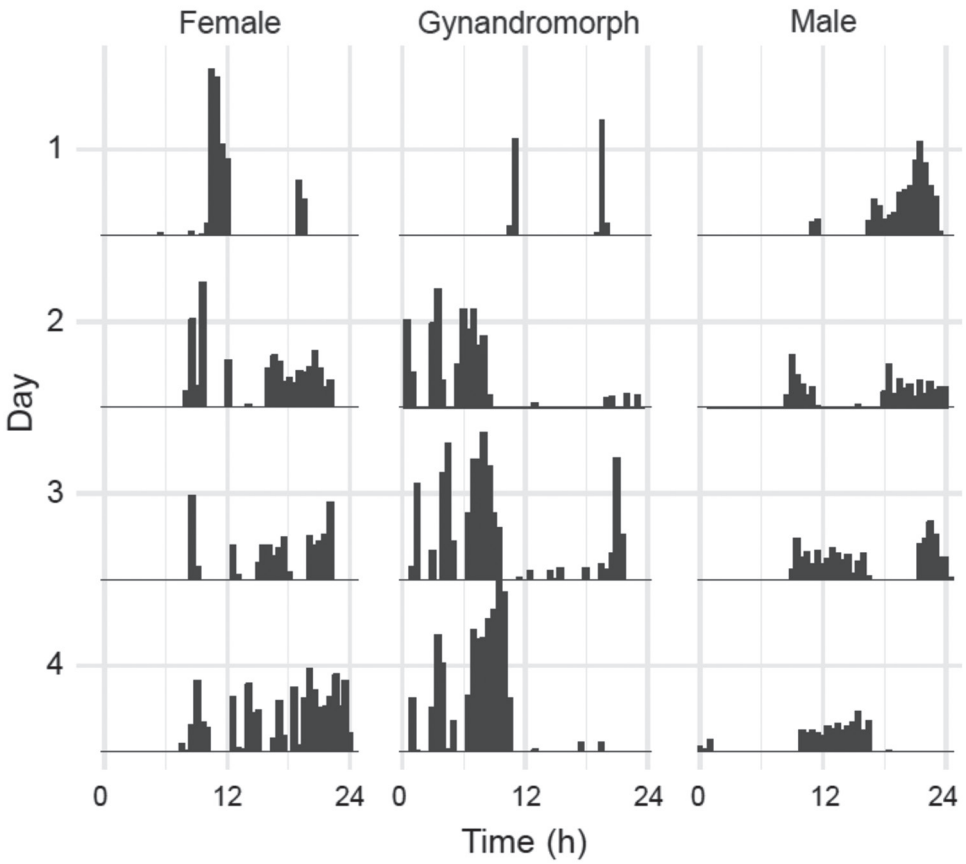

Figure 2. Single-plot actogram of four days of activity in dark-dark conditions showing a female, the gynandromorph, and a male *M. amoena.* Each bar represents the amount of times that the bee crossed the laser in a 15 minute interval. White space indicates lack of activity.

Discussion

Morphology

The gynandromorph of *M. amoena* reported here and that of *M. genalis* (Wcislo et al. 2004a), are the only two discovered for the genus, which occurs throughout the neotropics (Engel 2006, Santos and Melo 2015). Both gynandromorphs were discovered in the course of approximately 20 years of intensive field collections of *Megalopta* bees on BCI, Panamá (e.g. Wcislo et al. 2004b, Smith et al. 2019). This suggests that gynandromorphy is quite rare in the genus. Additionally, this finding is the fourth species of the tribe Augochlorini with a recorded gynandromorph (Alvarez et al. 2014, Engel and Hinojosa-Díaz 2011, Wcislo et al. 2004a). All four Augochlorini gynandromorphs were bilaterally split in the head; the two *Megalopta* gynandromorphs had

male characters on the left side and female on the right (Wcislo et al. 2004a), whereas the *Thectochlora alaris* (Vachal 1904) and *Auglochlora amphitrite* (Schrottky 1909) were the opposite with male characters on the right side and female characters on the left (Alvarez et al. 2014, Engel and Hinojosa-Díaz 2011). Most other recorded gynandromorphs from the family Halictidae are partially bilateral, with male and female expression on the heads and variable phenotypic expression in the mesosoma and metasoma (Wcislo et al. 2004a, Michez et al. 2009, Hinojosa-Díaz et al. 2012).

The gynandromorph of *M. amoena* is of the bilateral type (Michez et al. 2009). The head is approximately equal with respect to the bilateral split. We determined a bilateral split of the mesosoma based on leg morphology but not the metepisternum. The metasoma is majority female, based on the distribution of metasomal scopa hairs. Cockerell (1911) when describing a new genus, then *Androgynella*, hypothesized that a reduced scopa might be a predisposition to cleptoparasitism, as the females are collecting pollen with reduced efficiency. This links back to the discussion brought forth in the review by Wcislo et al. (2004b) that proposes gynandromorphy as a potential evolutionary pathway to cleptoparasitism, more on this in the circadian rhythm section below. The relatively greater proportion of the sterna covered with female-typical hairs suggests that bilateral gynandromorphy need not be symmetrical. The asymmetric sterna and sting suggest that the internal anatomy of our specimen may also be of mixed sex, but we did not dissect it. Furthermore, external and internal anatomy do not always correspond in gynandromorphs (Ugajin et al. 2016).

Hinojosa-Díaz et al. (2012) showed that there is a Holarctic bias in gynandromorph collection, but our study and other recent works (Alvarez et al. 2014, 2019, Prashantha 2019) show that increased research attention in other parts of the world is leading to further discovery of gynandromorphs. Our study highlights a new occurrence of this rare phenomenon and calls for continuously close examination of the morphology of specimens to determine the frequency and distribution of gynandromorphs globally.

Circadian rhythm

This is the first time circadian rhythm was quantified in a gynandromorph and in any species of *Megalopta*. Both male and female *Megalopta* have a bimodal foraging period, with flight occurring approximately 90 minutes before sunrise and after sunset (Kelber et al. 2006). All three specimens used in this study were newly emerged with no prior exposure to natural light conditions, their activity over four days in darkness shows their endogenous circadian rhythm. It appears that the gynandromorph activity rhythm was shifted significantly earlier in the day compared to the male and female of *M. amoena*. In terms of the percentage of activity across the day, the gynandromorph was intermediate between the male and female. In terms of activity intensity, the gynandromorph was more similar to the female than the male. It is possible that its high intensity was due to the gynandromorph trying to express an activity typical of a female *Megalopta*, like foraging for pollen. However, the time shift was atypical and it

seems that though the gynandromorph may have presented an intact neurological circuit for foraging, it also had a delay in conducting that activity. We are referring to this anomalous activity of the gynandromorph as a deviant activity pattern. The name deviant activity pattern is based on the term pheno-deviant used by Wcislo et al. (2004b) to describe deviant phenotypes such as bilateral gynandromorphy. This pattern could result from having a split-sex brain (Matsuo et al. 2018). Future studies of organisms with deviant phenotypes may find this pattern consistent.

To derive meaning from the deviant activity pattern in the gynandromorph we revisit the hypothesis that gynandromorph's could be a potential evolutionary precursor to cleptoparasitism; see Wcislo et al. (2004b) for a review on this hypothesis. In an observational study of *Neopasites cressoni* Crawford 1916, a cleptoparasite of ground nesting bees, the cleptoparasite began flying as early as their hosts and continued after the host ceased (Torchio et al. 1967). Similarly, the gynandromorph *M. amoena* is active when the female has ceased. Our data is not sufficient enough to support that gynandromorphs are the ancestral state of cleptoparasites, rather the deviant activity pattern reported here suggests that there may be a mechanism related to gynandromorphy that might help explain that evolutionary path.

Previous behavioral observations of gynandromorph bees include some instances of individuals conducting behavior characteristic of one sex despite their mixed phenotype, such as excavating a nest or collecting pollen, both female traits (Michez et al. 2009). However, in other cases gynandromorphs expressed novel behaviors. For instance, a gynandromorph of *Bombus ignitus* (Smith, 1869) with a bilaterally split head and male genitalia approached virgin females in a lab assay but took much longer than male bees to attempt copulation, and never successfully copulated (Matsuo et al. 2018). A different gynandromorph of *B. ignitus* also showed non-functional courtship behavior and different levels of expression of the gene *doublesex* between male and female tissue (Ugajin et al. 2016). A gynandromorph of *Osmia ribifloris biedermannii* Michener 1936 with a male head and female body attracted male bees that attempted to mate with it, but none were able to copulate (Sampson et al. 2010).

Although we did not measure gene expression or dissect the brain, our circadian rhythm results suggest a situation potentially similar to the gynandromorph *B. ignitus* described by Matsuo et al. (2018): a bilaterally split brain unable to integrate conflicting sex-specific signaling. However, it should be noted that ours was only a single sample. More studies need to be done to better understand if there is a difference in circadian rhythm based on sex in this species, and to distinguish what the deviant activity pattern of the gynandromorph results from.

Acknowledgements

Thank you to the 2018 Wcislo *Megalopta* lab members Janitce Harwood, Luis Felipe Estrada, and Ana Guiterrez for their feedback, brilliant minds, and for making science fun. We extend our gratitude to the administrators, forest guards, and staff at BCI for

making science possible. And of course, many thanks to STRI for their support. We appreciate Terry Griswold and Michael Branstetter at the USDA-ARS Pollinating Insects Research Unit for allowing us to use the Keyence camera for this project. Adam Smith and William Wcislo are supported by NSF grant #17-1028536545. William Wcislo was supported by general research funds from STRI. Callum Kingwell is supported by fellowships from STRI, Cornell University, and the Natural Sciences and Engineering Research Council of Canada (NSERC). The export of this specimen from the Republic of Panamá was conducted in accordance with local laws under export permit no. SEX/A-73-18 granted by the Ministerio de Ambiente.

References

Aamidor SE, Yagound B, Ronai I, Oldroyd BP (2018) Sex mosaics in the honeybee: how haplodiploidy makes possible the evolution of novel forms of reproduction in social Hymenoptera. Biology Letters 14: 20180670. https://doi.org/10.1098/rsbl.2018.0670

Alvarez LJ, Silva WP, Lucia M, Aguiar AJC (2019) The first cases of gynandromorphism in oil-collecting bees (Hymenoptera, Apidae: Centridini, Tapinotaspidini). Papéis Avulsos de Zoologia 59: e20195936. https://doi.org/10.11606/1807-0205/2019.59.36

Alvarez LJ, Lucia M, Ramello PJ, Abrahamovich AH (2014) Description of two new cases of gynandromorphism in *Paratrigona* Schwarz and *Augochlora* Smith (Hymenoptera: Apidae and Halictidae). Zootaxa 3889: 447–450. https://doi.org/10.11646/zootaxa.3889.3.7

Bloch G, Bar-Shai N, Cytter Y, Green R (2017) Time is honey: circadian clocks of bees and flowers and how their interactions may influence ecological communities. Philosophical Transactions of the Royal Society B: Biological Sciences 372: 20160256. https://doi.org/10.1098/rstb.2016.0256

Cockerell TDA (1911): Descriptions and records of bees. XXXV, Androgynella detersa. Annals of the Magazine of Natural History. 7: 310–319. https://doi.org/10.1080/00222931108692943

Dunlap JC, Loros JJ, DeCoursey PJ (2004) Chronobiology: biological timekeeping. Sinauer Associates.

Eickwort GC (1969) Tribal positions of Western Hemisphere green sweat bees, with comments on their nest architecture (Hymenoptera: Halictidae). Annals of the Entomological Society of America 62: 652–660. https://doi.org/10.1093/aesa/62.3.652

Engel MS, Hinojosa-Díaz IA (2011) A remarkable gynandromorph of *Thectochlora alaris* (Vachal 1904)(Hymenoptera: Halictidae). Entomofauna 32: 241–248.

Engel MS (2006) A new nocturnal bee of the genus *Megalopta*, with notes on other Central American species. Mitteilungen des Internationalen Entomologischen Vereins E V Frankfurt 31: 37–49.

Geissmann Q, Rodriguez LG, Beckwith EJ, Gilestro GF (2019) Rethomics: An R framework to analyse high-throughput behavioural data. PloS one 14: e0209331. https://doi.org/10.1371/journal.pone.0209331

Giannoni-Guzmán MA, Avalos A, Perez JM, Loperena EJO, Kayım M, Medina JA, Massey SE, Kence M, Kence A, Giray T (2014) Measuring individual locomotor rhythms in honey

bees, paper wasps and other similar-sized insects. Journal of Experimental Biology 217: 1307–1315. https://doi.org/10.1242/jeb.096180

Hinojosa-Díaz IA, Gonzalez VH, Ayala R, Mérida J, Sagot P, Engel MS (2012) New orchid and leaf-cutter bee gynandromorphs, with an updated review (Hymenoptera, Apoidea). Zoosystematics and Evolution 88: 205–214. https://doi.org/10.1002/zoos.201200017

Kapheim KM, Bernal SP, Smith AR, Nonacs P, Wcislo WT (2011) Support for maternal manipulation of developmental nutrition in a facultatively eusocial bee, *Megalopta genalis* (Halictidae). Behavioral Ecology and Sociobiolgy 65: 1179–1190. https://doi.org/10.1007/s00265-010-1131-9

Kelber A, Warrant EJ, Pfaff M, Wallén R, Theobald JC, Wcislo WT, Raguso RA (2006) Light intensity limits foraging activity in nocturnal and crepuscular bees. Behavioral Ecology 17: 63–72. https://doi.org/10.1093/beheco/arj001

Matsuo K, Kubo R, Sasaki T, Ono M, Ugajin A (2018) Scientific note on interrupted sexual behavior to virgin queens and expression of male courtship-related gene fruitless in a gynandromorph of bumblebee, *Bombus ignitus*. Apidologie 49: 411–414. https://doi.org/10.1007/s13592-018-0568-0

Michez D, Rasmont P, Terzo M, Vereecken NJ (2009) A synthesis of gynandromorphy among wild bees (Hymenoptera: Apoidea), with an annotated description of several new cases Annales de la Société Entomologique de France 45: 365–375. https://doi.org/10.1080/00379271.2009.10697621

Michener CD (2007) The Bees of the World. 2nd edn. Johns Hopkins, Baltimore.

Prashantha C, Lucia M, Belavadi VV (2019) Two new cases of gynandromorphism in Xylocopinae bees (Hymenoptera: Apidae) from India. Oriental Insects 53: 291–297. https://doi.org/10.1080/00305316.2018.1508522

R Core Team (2019) R: A language and environment for statistical computing. R Foundation for Statistical Computing, Vienna, Austria. https://www.R-project.org/

Sampson B, Kirker G, Werle C (2010) Morphology, courtship and mating of a mixed bilateral Gynander of *Osmia ribifloris biedermannii* Michener (Hymenoptera: Megachilidae). Journal of the Kansas Entomological Society 83: 347–352. https://doi.org/10.2317/JKES0910.28.1

Santos L, Melo G (2015) Updating the taxonomy of the bee genus *Megalopta* (Hymenoptera: Apidae, Augochlorini) including revision of the Brazilian species. Journal of Natural History 49: 575–674. https://doi.org/10.1080/00222933.2014.946106

Smith AR, Kapheim KM, O'Donnell S, Wcislo WT (2009) Social competition but not subfertility leads to a division of labour in the facultatively social sweat bee *Megalopta genalis* (Hymenoptera: Halictidae). Animal Behavior 78: 1043–1050. https://doi.org/10.1016/j.anbehav.2009.06.032

Smith AR, Kitchen SM, Toney RM, Ziegler C (2017) Is nocturnal foraging in a tropical bee an escape from interference competition? Journal of Insect Science 17(2): 1–7. https://doi.org/10.1093/jisesa/iex030

Smith AR, Kapheim KM, Wcislo WT (2019) Survival and productivity benefits of sociality vary seasonally in the tropical, facultatively eusocial bee *Megalopta genalis*. Insectes Sociaux. 66: 555–568. https://doi.org/10.1007/s00040-019-00713-z

Torchio PF, Rozen Jr. JG, Bohart GE, and Favreau MS (1967) Journal of the New York Entomological Society 75(3): 132–146.

Ugajin A, Matsuo K, Kubo R, Sasaki T, Ono M (2016) Expression profile of the sex determination gene doublesex in a gynandromorph of bumblebee, *Bombus ignitus*. The Science of Nature 103: 17. https://doi.org/10.1007/s00114-016-1342-7

Wcislo WT, Gonzalez VH, Arneson L (2004a) A review of deviant phenotypes in bees in relation to brood parasitism, and a gynandromorph of *Megalopta genalis* (Hymenoptera: Halictidae). Journal of Natural History 38: 1443–1457. https://doi.org/10.1080/0022293031000155322

Wcislo WT, Arneson L, Roesch K, Gonzalez V, Smith A, Fernández H (2004b) The evolution of nocturnal behaviour in sweat bees, *Megalopta genalis* and *M. ecuadoria* (Hymenoptera: Halictidae): an escape from competitors and enemies? Biological Journal of the Linnean Society 83: 377–387. https://doi.org/10.1111/j.1095-8312.2004.00399.x

Windsor DM (1990) Climate and moisture variability in a tropical forest: long-term records from Barro Colorado Island, Panama. Smithsonian Contributions to the Earth Sciences 29: 1–148. https://doi.org/10.5479/si.00810274.29.1

Yang AS, Abouheif E (2011) Gynandromorphs as indicators of modularity and evolvability in ants. Journal of Experimental Zoology Part B: Molecular and Developmental Evolution 316: 313–318. https://doi.org/10.1002/jez.b.21407